University of Alberta

CHITOSAN IN DIFFERENTIAL FLOTATION OF BASE METAL SULFIDES

by

Peng Huang

A thesis submitted to the Faculty of Graduate Studies and Research
in partial fulfillment of the requirements for the degree of

Doctor of Philosophy

in
Materials Engineering

Department of Chemical and Materials Engineering

Fall 2013
Edmonton, Alberta

ABSTRACT

Chitosan, a naturally occurring polymer, was studied as a potential selective depressant in the differential flotation of sulfide minerals. In single mineral flotation tests, chalcopyrite, galena, sphalerite and pyrite were depressed to different extents. However, in the differential flotation of the sulfide mineral mixtures (Cu-Pb, Zn-Pb and Fe-Pb), chitosan selectively depressed chalcopyrite, sphalerite or pyrite while galena was selectively floated using xanthate as a collector.

To delineate the adsorption mechanisms of chitosan on the sulfide minerals, several surface analysis techniques were applied. Time-of-flight secondary ion mass spectrometric (ToF-SIMS) measurements were conducted to map chitosan distribution on the different mineral surfaces within a mineral mixture. The ToF-SIMS measurements showed that chitosan preferentially adsorbed on chalcopyrite, sphalerite or pyrite but not on galena in the chalcopyrite-galena, sphalerite-galena and pyrite-galena mixtures.

X-ray photoelectron spectroscopic (XPS) analyses were performed to study the adsorption mechanisms between chitosan and the sulphide minerals. High resolution binding energy spectra of N 1s and O 1s electrons were obtained for chitosan-treated chalcopyrite, sphalerite, pyrite, and galena. The spectra showed chemical shifts of the N 1s electrons of the protonated amine groups and the O 1s electrons of the hydroxyl groups from chitosan. Therefore it was concluded that the selective adsorption of chitosan on chalcopyrite, sphalerite and pyrite was due

to a strong chemical interaction between the surface copper, zinc or iron atoms and the amine and the hydroxyl groups on chitosan. No such a strong interaction was observed between galena and chitosan. The competitive adsorption was attributed to the differences in the electron affinity of the lattice metal ions. Chitosan was found to bind strongly with metal ions with a high electron affinity.

ACKNOWLEDGEMENT

I would like to express my deepest gratitude to Professor Qi Liu for his guidance in my academic career in the past four years. It was a delightful experience working under his instruction because he always granted priority to students' interests. It has been my great honour to be his student.

I am very indebted to my supervising committee members: Professor Hongbo Zeng and Professor Phillip Choi. Their suggestions provide valuable information for this research.

I would like to thank all the colleagues from Mineral Processing Group for all the support and discussions and I enjoyed working in this group.

I appreciate the help from Dr. Mingli Cao and Dr. Jihua Gong in training me with the instrument operation and giving suggestions on this work.

My thanks are also extended to Yang Pan, Wenbo Xie and all the other friends in Chemical and Material Department for their friendship and support.

I want to thank financial support from both the Natural Sciences and Engineering Research Council of Canada (NSERC) through a Discovery Grant and the Alberta Innovates through funding to the Canadian Centre for Clean Coal/Carbon and Mineral Processing Technologies (C^5MPT).

Finally, I am grateful to fiancee Jing Wang for her love, encouragement and inspiration in the last four years. She was, and will always be the source of power driving me to complete the work.

TABLE OF CONTENTS

CHAPTER 1 Introduction....1
1.1 Froth Flotation....1
1.2 Depressant....2
1.3 Chitosan....5
1.3.1 The structure and characteristics of chitosan....5
1.3.2 Applications of chitosan....10
1.3.3 Adsorption isotherms....13
1.3.4 Complex formation with metal ions....16
1.4 Objectives....24
1.5 Organization of the Thesis....25
1.6 References....27
CHAPTER 2 Using Chitosan as a Selective Depressant in the Differential Flotation of Cu-Pb Sulfides....35
2.1 Introduction....35
2.2 Materials and Methods....38
2.2.1 Materials....38
2.2.2 Experimental methods....39
2.3 Results and Discussion....42
2.3.1 Flotation of single minerals....42
2.3.2 Flotation of chalcopyrite-galena mixtures....44
2.3.3 Adsorption of metal Ions on chitosan....48
2.3.4 ToF-SIMS images of chalcopyrite-galena mixtures treated with chitosan....50
2.3.5 N 1s binding energy spectra of the sulfide minerals after treatment with chitosan....51
2.4 Conclusions....55
2.5 References....57
CHAPTER 3 Adsorption Mechanisms of Chitosan on Chalcopyrite and Galena in Aqueous Suspensions....62
3.1 Introduction....62
3.2 Materials and Methods....65
3.2.1 Materials....65
3.2.2 ATR-FTIR measurements....66
3.2.3 ToF-SIMS measurements....67
3.2.4 XPS measurements....67
3.2.5 Flotation and contact angle measurement....68
3.3 Results and Discussion....69

3.3.1 ATR-FTIR spectra of sulfide minerals after treatment with chitosan ..69
3.3.2 ToF-SIMS analyses of sulfide minerals after treatment with chitosan.73
3.3.3 XPS analyses of sulfide minerals after treatment with chitosan.....78
3.3.4 Chitosan with different degrees of deacetylation as flotation depressants 86
3.4 Conclusions.....90
3.5 References.....91
CHAPTER 4 Selective Depression of Sphalerite by Chitosan in Differential Pb-Zn Flotation.....97
4.1 Introduction.....97
4.2 Materials and Methods.....99
4.2.1 Materials 99
4.2.2 Experimental methods 100
4.3 Results and Discussion 103
4.3.1 Flotation of sphalerite-galena mixtures 103
4.3.2 ToF-SIMS analyses of sphalerite after treatment with chitosan.....107
4.3.3 XPS analyses of sphalerite and copper-coated sphalerite after treatment with chitosan 110
4.4. Conclusions.....118
4.5 References.....119
CHAPER 5 Selective Depression of Pyrite with Chitosan in Pb-Fe Sulfide Flotation.....123
5.1 Introduction.....123
5.2 Experimental 125
5.2.1 Materials 125
5.2.2 Flotation 126
5.2.3 ToF-SIMS analysis 126
5.2.4 XPS measurements 127
5.2.5 Adsorption study.....128
5.3 Results and Discussion 129
5.3.1 Flotation tests 129
5.3.2 Surface characterization.....132
5.3.3 Possible mechanisms for the selective adsorption 140
5.4 Conclusions.....144
5.5 References.....145
CHAPTER 6 Conclusions and Recommendations 148
6.1 General Conclusions 148
6.2 Claims of Originality 150
6.3 Suggestions for Future Work.....152
Appendices.....153

LIST OF TABLES

Table 1.1 Typical depressants used in differential sulfide mineral flotation 3

Table 2.1 Binding energy (eV) for N 1s peaks of chitosan, galena and chalcopyrite.....55

Table 3.1 FTIR bands of chitosan with assignments.....71

LIST OF FIGURES

Figure 1. 1 Structures of chitosan and chitin 7
Figure 1. 2 The five types of adsorption isotherm 13
Figure 1. 3 Adsorption isotherms for copper onto chitosan at pH 4.5: (a) Langmuir isotherm, (b) Freundlich isotherm 15
Figure 1.4 Effect of lysozyme initial concentration on lysozyme adsorption on the dye-ligand, dye-ligand-Fe(III) and dye-ligand-Cu(II) immobilized IPNs membrane. Procion Brown MX 5BR loading: 0:361 μmol ml-1 IPNs membrane; pH: 6.0; temperature: 25 ℃.....17
Figure 1.5 Comparison of different models for fitting of experimental Cd-sorption by Ascophyllum nodosum #5. ▲, Freundlich; ■, Langmuir; ●, Dubinin-Radushkevic 18
Figure 1.6 Adsorption isotherms for copper onto chitosan at pH 4.5: Redlich-Peterson isotherm 19
Figure 1.7 Formation of chitosan chelates with one copper ion bond to two amino groups (Bridge Model) 23
Figure 1.8 Formation of chitosan chelates with one copper ion bond to one hydroxyl, one amino and two water molecules (left), and with two hydroxyl and two amino groups (Pendant Model) 24
Figure 2.1 Structures of chitosan and chitin 37
Figure 2.2 Flotation of single minerals of chalcopyrite and galena as a function of pH in the presence and absence of chitosan as a depressant. (KEX: 1.25×10^{-4} mol/L; Chitosan: 0.67 mg/L; Condition time: 3 min; Flotation time: 3 min) 43
Figure 2.3 Flotation of mixtures of chalcopyrite and galena (weight ratio 1:1) as a function of pH. (a). Metal grade in froth products; (b). Metal recovery in froth products. (KEX: 1.25×10^{-4} mol/L; Chitosan: 0.67 mg/L; Condition time: 3 min; Flotation time: 3 min) 45
Figure 2.4 Flotation of mixtures of chalcopyrite and galena as a function of the weight ratio of chalcopyrite to galena. (a). Metal grade in froth products;

(b). Metal recovery in froth products. (pH = 4; KEX: 1.25 × 10^{-4} mol/L; Chitosan: 0.67 g/L; Condition time: 3 min) 47

Figure 2.5 Adsorption density of metal ions on chitosan as a function of the equilibrium concentration of metal ions in aqueous solution. Initial solution including: (a). Cu^{2+} or Pb^{2+}; (b). Cu^{2+} and Pb^{2+}. 49

Figure 2.6 Positive-ion images of 64 µm × 64 µm region of the surface of a mixture of chalcopyrite and galena (weight ratio 1:1) after chitosan (0.3 mg) adsorption. (a) image of chalcopyrite (Cu^{+}); (b) image of galena (Pb^{+}); (c) image of chitosan ($C_6H_{11}O_4N^{+}$).....51

Figure 3.1 Structures of chitosan and chitin 63

Figure 3.2 ATR-FTIR spectra of (a) chitosan on galena surface, (b) chitosan on chalcopyrite surface and (c) chitosan. 71

Figure 3.3 Positive-ion images of a 64 µm × 64 µm region from the surface of a mixture of chalcopyrite and galena (weight ratio 1:1) after chitosan adsorption. (a) image of Cu^{+}; (b) image of Pb^{+}; (c) image of $C_6H_{11}O_4N^{+}$.....75

Figure 3.4 Part of the positive ion ToF-SIMS spectra of a 64 µm × 64 µm region from the surface of (a) chitosan (CT), (b) chitosan (CT) at pH 4 and (c) a mixture of chalcopyrite alena (1:1) after chitosan adsorption. 77

Figure 3.5 Positive-ion images of a 64 µm × 64 µm region from the surface of a mixture of chalcopyrite and galena (weight ratio 1:1) after chitosan adsorption. (a) image of NH_4^{+}; (b) image of $CuNH_4^{+}$; (c) image of $PbNH_4^{+}$. 77

Figure 3.6 XPS peak fitting for narrow scan spectra of chitosan, (a) N 1s spectrum (b) O 1s spectrum. 82

Figure 3.7 XPS narrow scan spectra with the curve fitting of chalcopyrite, (a) N 1s spectrum (b) O 1s spectrum, and chalcopyrite adsorbed with chitosan (CT), (c) N 1s spectrum (d) O 1s spectrum. 84

Figure 3.8 XPS N 1s peak fitting of galena before (a) and after (b) chitosan (CT) adsorption. 85

Figure 3.9 Flotation of single minerals of chalcopyrite and galena as a function of pH with chitosan (CT or HCT) as a depressant. (KEX: 1.25×10^{-4} mol/L; CT or HCT: 0.67 mg/L; Condition time: 3 min; Flotation time: 3 min)..... 88

Figure 3.10 Flotation of mixtures of chalcopyrite and galena as a function of pH. (a). Metal grade in froth products; (b). Metal recovery in froth products. (KEX: 1.25×10^{-4} mol/L; CT or HCT: 0.67 mg/L; Condition time: 3 min; Flotation time: 3 min).....89

Figure 4.1 Structures of chitosan and chitin 99

Figure 4.2 Flotation recovery of sphalerite and galena from their mixtures as a function of EDTA concentration. KEX: 1.25×10^{-4} mol/L; Chitosan: 0.67 mg/L when used; Condition time: 3 min; Flotation time: 3 min.105

Figure 4.3 Flotation recovery of galena and copper-coated sphalerite from their mixtures as a function of pH. KEX: 1.25×10-4 mol/L; Chitosan: 0.67 mg/L; Condition time: 3 min; Flotation time: 3 min.....107

Figure 4.4 Part of the positive ion ToF-SIMS spectra of 171 μm × 171 μm region from the surface of (a) sphalerite-chitosan; (b) copper-coated sphalerite-chitosan.....109

Figure 4.5 Positive-ion images of 171 μm × 171 μm region from the surface of copper-coated sphalerite after chitosan adsorption. (a) image of sphalerite (Zn^+); (b) image of Cu^+; (c) image of chitosan ($C_6H_{11}O_4N^+$).....110

Figure 4.6 XPS narrow scan spectra with deconvoluted peaks for sphalerite: (a) N 1s spectrum, (b) O 1s spectrum; and chitosan-treated sphalerite: (c) N 1s spectrum, (d) O 1s spectrum. 115

Figure 4.7 XPS narrow scan spectra with deconvoluted peaks for copper-coated sphalerite (a) N 1s spectrum (b) O 1s spectrum, and chitosan treated copper-coated sphalerite (c) N 1s spectrum (d) O 1s spectrum. 117

Figure 5.1 Flotation of single minerals of pyrite and galena as a function of pH in the presence and absence of chitosan as a depressant. (KEX: 1.25×10^{-4}

mol/L; Chitosan: 0.67 mg/L; Condition time: 3 min; Flotation time: 3 min) 130

Figure 5.2 Flotation of mixtures of pyrite and galena (weight ratio 1:1) as a function of pH. (a). Metal grade in froth products; (b). Metal recovery in froth products. (KEX: 1.25×10^{-4} mol/L; Chitosan: 0.67 mg/L; Condition time: 3 min; Flotation time: 3 min) 131

Figure 5.3 Positive-ion images of an 177 μm ×177 μm area from the surface of a mixture of pyrite and galena (weight ratio 1:1) after chitosan adsorption at pH 4. (a) image of Fe^+; (b) image of $C_6H_{11}O_4N^+$; (c) image of Pb^+.....133

Figure 5.4 Positive-ion images of an 177 μm ×177 μm area from the surface of a mixture of pyrite and galena (weight ratio 1:1) after chitosan adsorption at pH 6. (a) image of Fe^+; (b) image of $C_6H_{11}O_4N^+$; (c) image of Pb^+.....134

Figure 5.5 N 1s high resolution spectra with deconvoluted peaks: (a) pyrite at pH 4, (b) chitosan-treated pyrite at pH 4: (c) pyrite at pH 6, (d) chitosan-treated pyrite at pH 6. 137

Figure 5.6 O 1s high resolution spectra with deconvoluted peaks: (a) pyrite at pH 4, (b) chitosan-treated pyrite at pH 4: (c) pyrite at pH 6, (d) chitosan-treated pyrite at pH 6. 139

Figure 5.7 Adsorption density as a function of equilibrium concentration of metal ions in aqueous solution. (a). Cu^{2+} and Ca^{2+}; (b). Cu^{2+} and Mn^{2+}. (Temperature: 25 ℃ Adsorption time: 30 min) 143

CHAPTER 1

INTRODUCTION

Sulfide minerals are the major sources of base metals such as copper, zinc, nickel and lead. A significant amount of precious metals (gold, silver and platinum group metals) as well as rare earth metals are also produced from sulfide minerals. For economic and technological reasons, the mineral feed to the metal smelters must meet stringent high- grade and low-impurity requirements, i.e., the feed must contain a certain minimum concentrations of the sulfide mineral, and does not exceed the maximum allowed impurity concentrations. However, in nature, a sulfide mineral is always inter-grown with other sulfide and non-sulfide minerals. In order to meet the smelter requirements, mineral separation technologies, froth flotation in particular, are used to improve the concentration of a specific sulfide mineral in an ore and to remove deleterious impurities.

1.1 Froth Flotation

Froth flotation, which was introduced in minerals industry around 1905, utilizes the interfacial properties of mineral particles, more specifically the surface wettability, to separate different minerals. Typically, a valuable mineral that is to be recovered is made hydrophobic, while the gangue minerals (waste rock particles) are made hydrophilic, through the use of various flotation reagents. The hydrophobicized mineral particles attach to injected gas bubbles, float to pulp surface and form a stable froth layer which is continuously removed to form the “flotation concentrate”, while the gangue minerals are left in the flotation cell, forming the “flotation tailings”, thus achieving the separation. In a so-called “reverse flotation” process, the gangue minerals are made hydrophobic while the value minerals are kept hydrophilic. The chemical and electrochemical properties

as well as the sequence of reagent addition control the surface properties in the flotation process. Although the flotation process has been studied intensively in the past century, flotation phenomena are still not fully understood (Bulatovic, 2007; Fuerstenau, 2003; Fuerstenau et al., 2007) and the mineral flotation operation is still largely considered an art rather than science.

As stated earlier, in froth flotation, flotation reagents are introduced to mineral slurry to modify the surface properties of mineral particles. According to their functions, the reagents are divided into collectors, frothers, activators and depressants. Collectors are organic chemicals that make mineral surface hydrophobic and thus assist in the attachment of the particles to gas bubbles, which allows the particles to be recovered in the froth product. Frothers, compounds containing hydrophilic and hydrophobic chains, are used to produce stable froth in flotation system when the collector itself is insufficient to act as a frother. Both activators and depressants, which are often referred to as flotation regulators, are added to modify the actions of collectors on desired mineral surfaces. Activators normally adsorb on mineral surfaces and produce sites to facilitate the interaction between mineral surface and the collector. A depressant is a chemical that can either prevent a collector from adsorbing onto the minerals, or make the surface of a given mineral hydrophilic (Bulatovic, 2007) irrespective of the collectors.

1.2 Depressant

At present, inorganic reagents have been routinely used as selective sulfide mineral flotation depressants. For example, to separate copper sulfide minerals (such as chalcopyrite, $CuFeS_2$) from lead sulfide minerals (such as galena, PbS), either sodium cyanide is used to depress the copper sulfide minerals while the lead sulfide minerals are floated by thiol collectors (such as xanthate or dithiophosphate), or sodium dichromate, sodium sulfide, or sulphur dioxide is used to depress the lead sulfide minerals while the copper sulfide minerals are

floated by a thiol collector. Clearly, the aforementioned inorganic depressants are highly toxic or hazardous (Liu and Laskowski, 2006). Other instances of the use of inorganic depressants are shown in Table 1.1. Due to the increasingly stringent environmental pollution control regulations, the use of such toxic or hazardous depressants is under increasing pressure and it is imperative that they be replaced by more environmentally friendly chemicals.

Table 1.1 Typical depressants used in differential sulfide mineral flotation (Bulatovic, 2007)

Differential flotation of sulfide minerals of	Typical depressants used in separation
Cu-Zn	$ZnSO_4$ and NaCN to depress zinc sulfide
Cu-Pb	Dichromate, soda ash-SO_2, SO_2-dextrin or guar gum to depress lead sulfide
Cu-Fe	Lime with cyanide, Na_2SO_3, $Na_2S_2O_5$ or SO_2, A3-3 (a mixture of Na_2SiO_3: $Na_2S_2O_5$: $Al_2(SO_3)_3$), oxalic acid-NH_4Cl mixture, etc., to depress iron sulfide
Cu-Mo	Na_2S/NaHS, and arsenic Nokes reagent to depress copper sulfide
Pb-Zn	$ZnSO_4$ and NaCN, lime-NaCN/HQS (modified dextrin) mixture-SO_2, complexed cyanide with modified starches or dextrins to depress zinc sulfide

A significant amount of research has been undertaken to study potential non-toxic replacements for the toxic inorganic depressants. Naturally occurring polymers of carbohydrates (i.e., polysaccharides), such as starch, dextrin, cellulose, and guar gum, have been tested or used as selective depressants. The earliest use of polysaccharide as a depressant in the differential Cu-Pb sulfide separation was reported by Dolivo-Dobrovoskii and Rogachevskaya (1957). In their study, they used a water-soluble starch to depress chalcopyrite and separate it from chalcopyrite-galena mixture at natural pH. In 1978, Schnarr (1978) and Allan and Bourke (1978) reported the application of polysaccharides combined with sulfur

dioxide as depressants in commercial Cu-Pb sulfide flotation separation circuits. To understand the adsorption mechanism of polysaccharides on mineral surfaces, Liu and Laskowski (1989) investigated the interaction between dextrin and sulfide mineral surface. Their research result shows that the mineral surface metal ionic species and thus pulp pH played a primary role in the adsorption of dextrin. Selective separation was achieved in the tests on artificial mixtures of galena and chalcopyrite when xanthate and dextrin were used at proper pH values. The results of dextrin adsorption on chalcopyrite and galena indicated that at neutral pH, chalcopyrite was depressed while galena was floated while in alkaline solution galena was depressed and chalcopyrite was floated. To apply the conclusions obtained in the laboratory study, dextrin was tested to depress Pb at pH 12 in a commercial Cu-Pb sulfide separation circuit of a pilot plant and full plant (Bolin and Laskowski, 1991). In the pilot plant tests, the results of separation process were consistent with the ones observed in the laboratory. Meanwhile, the results indicated that the flotation tests were sensitive to the addition of dextrin. When dextrin was used in the full plant tests, neither the Cu concentrate nor the Pb concentrate was as good as that produced when dichromate was used as the depressant for galena in the original commercial circuit. Bolin and Laskowski (1991) attributed this to the inappropriate dextrin dosage and pulp pH in the plant tests.

In 1997, Bogusz et al. (1997) suggested that metal ions originating from other minerals or process water promoted the adsorption of polysaccharides (e.g., dextrin) on all sulfide minerals and thus led to their non-selective adsorption in commercial differential sulfide flotation circuits. Liu and Zhang (2000) studied the selectivity of dextrin in the Cu-Pb sulfide (chalcopyrite-galena) system in the presence and absence of calcium ions. The results confirmed the conclusions from Bogusz et al. (1997). It was found that calcium ions significantly deteriorated the flotation recovery of chalcopyrite during chalcopyrite-galena differential flotation using dextrin and xanthate. This was attributed to the adsorption of calcium ionic species on the chalcopyrite surface, making it indistinguishable from that of

galena in terms of dextrin adsorption. The addition of sodium citrate removed the calcium ionic species from the chalcopyrite surfaces and restored the flotation selectivity.

The adsorption behaviour of dextrin on nickel sulfide is similar to that on galena. Selective separation of Cu-Ni sulfide can be achieved by depressing nickel sulfide (Nyamekye and Laskowski, 1994) using dextrin. Nyamekye and Laskowski (1991) studied the interaction between various dextrin and chalcocite (Cu_2S) or heazlewoodite (Ni_3S_2) through adsorption tests. The results from adsorption density and flotation tests indicated that the added dextrin enhanced the selective flotation separation of Cu-Ni sulfide minerals. Laskowski and Nyamekye (1994) also indicated that dextrin was applied as a depressant for Ni sulfide in the commercial flotation separation of a Cu-Ni bulk concentrate at Kotalahti Mine in Finland until the plant shut down in 1987.

1.3 Chitosan

1.3.1 The structure and characteristics of chitosan

Motivated by the applications of polysaccharides in minerals industry, chitosan, as one of the derivative polysaccharides, was chosen to be studied in this PhD dissertation research. Chitosan is a deacetylated product from chitin, the second most abundant natural biopolymers in the world next to cellulose. It is widely found to build with various proteins as supporting materials of a multitude of natural organisms to form their exoskeletons. The main commercial chitin product is from the shells of marine crustaceans which are disposed of as wastes of seafood production processes for lobsters, prawns, crabs and shrimps (Gerente et al., 2007; Hirano, 1989). Due to the uncertain variations in the physicochemical properties of chitin products from crustacean, the chitin products with pure and uniform structure are typically obtained from microbial sources such as fungi,

yeasts and molds, and are applied in pharmaceutical and biomedical fields (Zorica et al., 2010).

The basic structure unit of chitin is β-(1-4)-linked N-acetyl-D-glucosamine, a derivative of β-D-glucose (Figure 1.1). The mono unit of chitin may be regarded as an acetamido group replacing the hydroxyl at C-2 position. With the unique structure, chitin is insoluble in water and most organic solvents. In the presence of mineral acids in aqueous solutions, it can be dissolved in hexafluoroisopropanol, hexafluoroacetone and chloroalcohols. It is also soluble in dimethylacetamide with 5% lithium chloride (Ravi Kumar, 2000). Chitosan is a copolymer with β-(1-4)-linked D-glucosamine and β-(1-4)-linked N-acetyl-D-glucosamine (Figure 1.1), produced from the partial deacetylation of chitin in hot alkaline solution. The term "chitosan" usually refers to the product from chitin having a degree of deacetylation (DA) of greater than 50%. As a derivative of β-D-glucose, chitosan contains either the amine groups (D-glucosamine) or the acetamido groups (N-acetyl-D-glucosamine) at the C-2 positions. In acidic media, the amine groups can be protonated, which converts the polymer solution to a weak polyelectrolyte and makes chitosan soluble. The protonation reaction can be represented by the following scheme:

$$RNH_2 + H^+ \longrightarrow RNH_3^+$$

The equilibrium constant for the above reaction is in the range of 6.3-7.2 (Stöhr et al., 2001). Due to the protonation reaction, chitosan becomes a cationic polymer in aqueous solutions. The properties of chitosan are significantly affected by DA and molecular weights, which will be discussed later.

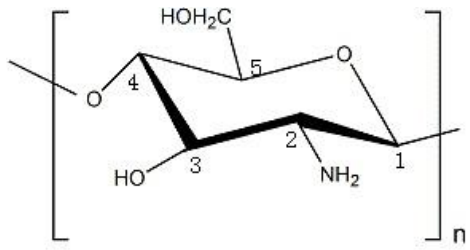

(a) chitosan

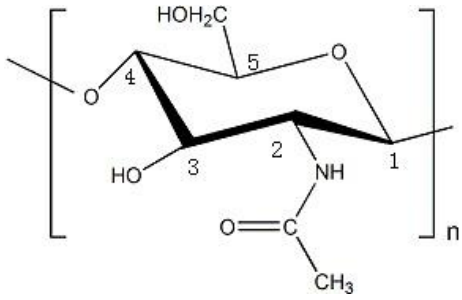

(b) chitin

Figure 1. 1 Structures of chitosan and chitin (Rinaudo, 2006).

After deacetylation treatment, the obtained chitosan product may be the fully or partially *N*-deacetylated derivative from chitin. Various analytical techniques, such as infrared spectroscopy (IR), X-ray photoelectron spectroscopy (XPS), elemental analysis, enzymatic reactions, ultraviolet (UV) spectroscopy, ^{1}H liquid-state nuclear magnetic resonance (NMR) and solid-state ^{13}C NMR, have been conducted to determine the DA of a chitosan sample, i.e., the fraction of $–NH_2$ groups in the structural unit (Rinaudo, 2006). In the XPS method, the high resolution N 1s binding energy spectrum is resolved to three peaks. The peak at 399.5 eV is attributed to $–NH_2$ (amine) in the basic structural unit of chitosan (Amaral et al., 2005; Lawrie et al., 2007) and this peak is used to calibrate the entire XPS spectrum of chitosan. The peak at 400.5 eV is caused by O=C–NH– (amide) (Lawrie et al., 2007) which is from the residual acetyl unit. The third peak at 401.9 eV corresponds to protonated amine (ammonium). Therefore, the combined percentages of the relative intensities of amine ($–NH_2$) and ammonium ($–NH_3^+$) indicates the degree of deacetylation of the chitosan sample (Lawrie et al., 2007). In addition to the aforementioned traditional methods, Rusu-Balaita (2003) investigated the titration method for the determination of DA. Their procedure involved dissolving the chitosan in a small excess of HCl solution followed by the addition of NaOH to neutralize the protonated $–NH_2$ using conductivity measurements. ^{1}H liquid-state NMR, considered by some as one of the most convenient techniques (Rinaudo, 2006), is used to characterize the acetyl content of soluble chitosan sample (Hirai et al., 1991; Sorlier et al., 2001) dissolved in a DCl/D_2O solvent. The acetyl content is measured in reference to the ratio of the areas of the methyl protons of the N-acetylglucosamine residues ($–NH_3^+$) to that of the sum of all the H_2 to H_6 protons of both glucosamine and N-acetylglucosamine residues (Hirai et al., 1991).

$$DA(\%) = \{1 - (\tfrac{1}{3} I_{CH3} / \tfrac{1}{6} I_{H2\text{-}H6})\} \times 100 \qquad (1.1)$$

Currently, for solid chitosan samples, ^{13}C and ^{15}N solid-state NMR is considered as the most reliable technique to evaluate the DA (Rinaudo, 2006). By the ^{13}C

NMR spectra, the DA was measured by the ratio of the integrated areas of the carbonyl or methyl group to that of all the carbon atoms in the structural unit (Heux et al., 2000; Raymond et al., 1993). In the ^{15}N NMR measurement, as the ^{15}N is only present in the signals of acetyl and *N*-deacetylated groups, DA was calculated by identifying the two groups in the ^{15}N NMR spectra (Yu et al., 1999) and taking their ratios.

Another important characteristic of chitosan is the molecular weight. High-performance liquid chromatography (HPLC) can be used to determine the molecular weight distributions of chitosan, according to a set of combination of glass pore sizes and column lengths used in the chromatographical columns (Wu et al., 1976). To measure the weight-average molecular weights, laser light-scattering spectrometry is used with the advantages of being rapid, non-destructive and high precision (Muzzarelli et al., 1987). It is also well established that viscometry is a simple and rapid method to measure molecular weight by studying the intrinsic viscosity [η]. Molecular weight of chitosan sample in solvents is related to the intrinsic viscosity by the Mark-Houwink equation:

$$\eta = KM^{\alpha} \qquad (1.2)$$

where *K* and *a* are constants depending on the solvent and solution temperature.

During viscosity measurements, the solvent for chitosan is usually a dilute acid solution. As aggregation may occur when chitosan is dissolved in an acid solution, attentions should be paid when apply the values of parameters of K and α to measure molecular weight of chitosan samples. Rinaudo (2006) compared the previous studies with respect to the molecular weight characterization in different proposed solvents and showed that the solvent may promote aggregation to overestimate the molecular weight. To eliminate the interference of aggregation, Rinaudo et al. (1993) proposed a solvent which was made of 0.3 M acetic acid and 0.2 M sodium acetate at pH 4.5 where no chitosan aggregation was detected. A valid molecular weight was obtained by size exclusion chromatography (SEC),

viscometer and multi-angle light scattering detectors to calculate the Mark-Houwink parameters (Rinaudo, 2006).

1.3.2 Applications of chitosan

Chitosan is produced by the deacetylation of chitin, a main component in the supporting material of living organisms. The presence of amino and hydroxyl functional groups make chitosan to possess highly advantageous properties of biodegradability, biocompatibility, non-toxicity and strong metal ion chelation ability (Ngah et al., 2010; Se-Kwon, 2010b). In the past decades, these properties have been exploited in multiple research areas and commercial applications including wastewater treatment (Boddu et al., 2003; Burke et al., 2002; Ravi Kumar, 2000), paper and textile industry (Choy et al., 2001; Chung et al., 1998; Houshyar and Amirshahi, 2002; Jocić et al., 1997; Shin and Yoo, 1998; Struszczyk, 1987), agriculture and food industry (Crini and Badot, 2008; Egger et al., 1999; Gerente et al., 2007; Srinivasa et al., 2002; Teixeira et al., 1990).

Due to the unique molecular structure, chitosan has been used in environmental engineering for wastewater treatment including metal ion sequestration, dyes removal, polychlorinated biphenyl removal, chemical waste detoxification and desalination. Metal ion sequestration, dyes removal and food applications will be discussed in the following sections.

1.3.2.1 Metal capture from wastewater

The amino groups on chitosan structural unit, derived from deacetylation of chitin, have strong complexing ability with metal ions. Chitosan has been shown to adsorb large amounts of metal ions and form metal ionic complexes. Such properties have generated interest in its use in the recovery of heavy metal ions from a wide range of effluent systems in the last decade (Boddu et al., 2003; Burke et al., 2002; Peniche-Covas et al., 2003; Ravi Kumar, 2000). Gernente et al. (2007) conducted a comprehensive review of the current studies of isothermal

adsorption capacities of metal ions on chitosan in various systems. The review shows that the Langmuir adsorption isotherm provides a good fitting of the equilibrium adsorption data in most chitosan-metal ion equilibrium systems. After studying the equilibrium isotherm equations and the established equilibrium models, Gernente et al. (2007) were able to provide a better understanding of the adsorption mechanism and the surface properties of chitosan. A large amount of information has been reported with regard to the adsorption capacities of chitosan for metal ions. As the specific adsorption capacity for each type of metal ion was affected by various factors such as the suspension pH, the physical form of chitosan (flakes, beads, etc.), the initial metal ion concentration, and the method of chitosan preparation (such as degree of agitation, contact method, etc.), it is difficult to make generalizations for the specific metal adsorption capacity of chitosan. For instance, in Gernente's study, the maximum reported adsorption capacity of copper ions ranged from 5 to 500 mg Cu/g for chitosan flakes, from 60 to 1100 mg Cu/g for chitosan beads, and close to 170 mg Cu/g for a chitosan membrane.

1.3.2.2 Dyes removal

Various kinds of dyestuffs are often discharged in effluents of wastewater from textile industries, which are highly visible and toxic to the environment. It is well known that the dyes are recalcitrant molecules, resistant to aerobic digestion, and resistant to oxidizing agents. Therefore, it is difficult to find an effective method to treat these dyes with favourable economy. As a low cost adsorbent, chitosan has a high affinity to dyestuffs and easy to recover in concentrated form (Choy et al., 2001; Crini and Badot, 2008; Houshyar and Amirshahi, 2002; Jocić et al., 1997; Shin and Yoo, 1998; Wu et al., 2000, 2001; Yoshida et al., 1993). Currently, the mainly used chitosan in practice is raw chitosan (unmodified) due to its economic advantage. Chitosan derivatives, such as cross-linked chitosan, chitosan-based composites, modified polymer and membranes, have been exploited. The modification has made chitosan a more effective adsorbent (Crini

and Badot, 2008). For instance, raw chitosan has a low adsorption capacity to the basic dyes (water-soluble cationic dyes). After derivatization, the adsorption capacity of the modified chitosan was enhanced significantly (Ravi Kumar, 2000). Currently, the abundant literature which covers the adsorption performances of chitosan in dye solution has confirmed the extremely high affinity of chitosan to many classes of dyes, including disperse, direct, reactive, acid, vat, sulfur and naphthol dyes (Ravi Kumar, 2000). In particular, due to the polycationic structure of chitosan in aqueous solutions, chitosan possesses outstanding removal capacities to anionic dyes.

1.3.2.3 Food applications

The unusual antimicrobial properties make chitosan and its derivatives important additives in food industry (Crini and Badot, 2008; Egger et al., 1999; Gerente et al., 2007; Shahidi et al., 1999; Srinivasa et al., 2002; Teixeira et al., 1990). Studies show that chitosan possesses strong antimicrobial property against a wide range of micro-organisms including bacteria, yeast and fungi (Rabea et al., 2003). Because of the ability of chitosan to chelate with metal ions, the toxins and microbial productions are inhibited by chitosan. Thereby, chitosan and its derivatives have been applied in the production of value-added food products with such functions as the preservation of foods from microbial deterioration, the formation of biodegradable films, and the recovery of waste material from processing food rejects, purification of water, clarification and deacidification of fruit juices and so on (Shahidi et al., 1999).

As chitosan is derived from exoskeleton of natural organisms, it has the potential to be exploited in medicine, such as in biomedical engineering (Koide, 1998; Loke et al., 2000; Struszczyk, 2002; Wang et al., 2002), and healthcare (Gonz á lez Siso et al., 1997; Ilium, 1998; Martino et al., 1996; Muzzarelli, 1989). Many researchers are developing and identifying other potential applications of chitosan, such as the recent study of using chitosan as a gene vehicle (Lai and Lin, 2009; Mumper et al., 1995).

1.3.3 Adsorption isotherms

The systems involving the adsorption of a single metal ion on chitosan were extensively studied to investigate the adsorption capacity of chitosan to the metal ions. The adsorption data are usually fitted by equilibrium isotherm equations for commercial design purpose.

In general, adsorption isotherms can be classified into two broad categories: physical and chemical adsorption. The classification is dependent upon the interaction forces between adsorbate molecules and adsorbent. Brunauer et al. (1994) proposed five physical adsorption isotherm types (Figure 1.2). Various studies have been taken to look for model expressions to describe the types of isotherms. The typical adsorption isotherm models which have been tested in the chitosan studies include the followings.

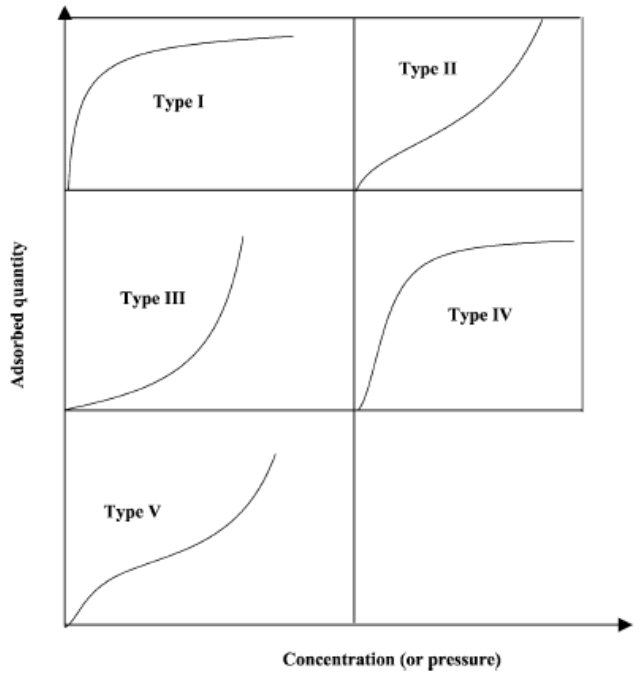

Figure 1. 2 The five types of adsorption isotherm (Brunauer et al., 1994)

1.3.3.1 The Langmuir isotherm

In 1906, Irving Langmuir proposed a model isotherm to describe the adsorption of gas on a solid surface at a fixed temperature. It is the most common model to study adsorption equilibrium. The Langmuir adsorption isotherm (Figure 1.3a) is based on three assumptions:

1. The surface of the adsorbent is homogeneous and all the adsorption sites are equivalent to each other.
2. The adsorbed molecules do not interact on adjunction location, i.e., there is no lateral interaction.
3. Only a monolayer is formed on the adsorbent surface.

The Langmuir adsorption isotherm for the case of metal ion adsorption on chitosan can be expressed by the following equation (Gerente et al., 2007):

$$q_e = \frac{q_m a_l C_e}{1+a_l C_e} \qquad (1.3)$$

where q_e is the equilibrium metal ions adsorption density on a substrate, mmol/g
C_e is the equilibrium metal ions concentration in the solution, mg/dm^3
q_m is the maximum amount of metal ions that could be adsorbed on the substrate, mmol/g
a_l is a constant of the Langmuir model, dm^3/mg

1.3.3.2 The Freundlich isotherm

In 1909, Herbert F. Freundlich proposed an empirical model to describe the adsorption isotherm. In comparison with the Langmuir model, the Freundlich isotherm can be applied to multilayer adsorption on heterogeneous surfaces. For metal ion adsorption on chitosan, the Freundlich isotherm (Figure 1.3b) can be written as follows (Gerente et al., 2007):

$$q_e = K_F C_e^{b_F} \qquad (1.4)$$

where q_e is the equilibrium metal ions adsorption density on a substrate, mmol/g

C_e is the equilibrium metal ions concentrations in the solution, mg/dm^3

K_F is Freundlich isotherm constant, dm^3/g

b_F is Freundlich isotherm exponent constant, dimensionless.

By comparing Figures 1.3a and 1.3b, it can be seen that Langmuir equation is a better equilibrium model for the adsorption of copper ions onto chitosan at pH 4.5 (Ng. et al., 2002).

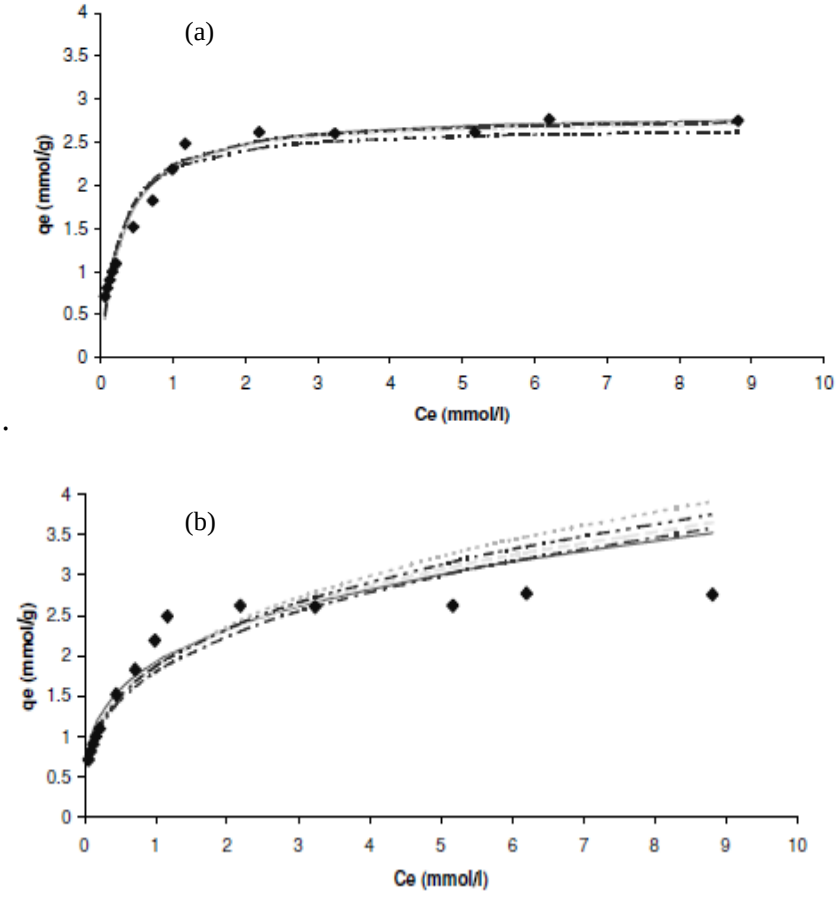

Figure 1. 3 Adsorption isotherms for copper onto chitosan at pH 4.5: (a) Langmuir isotherm, (b) Freundlich isotherm (Ng et al., 2002).

1.3.3.3 The Temkin Isotherm

Temkin isotherm takes into account of adsorbent-adsorbate interactions. It assumes that the heat of adsorption of all molecules in the layer would decrease linearly rather than logarithmically with coverage (Aharoni and Ungarish, 1977). The Temkin isotherm has been applied to study the adsorption of enzyme onto modified chitosan membranes which are heterogeneous surfaces. The isotherm model is given by the following equation:

$$q_e = \frac{RT}{b} \ln (A_T C_e) \qquad (1.5)$$

where q_e is the equilibrium metal ions adsorption density on a substrate, mmol/g

C_e is the equilibrium metal ions concentrations in the solution, mg/dm^3

A_T is Temkin isotherm equilibrium binding constant, mL/mg

b is Temkin isotherm constant, dimensionless.

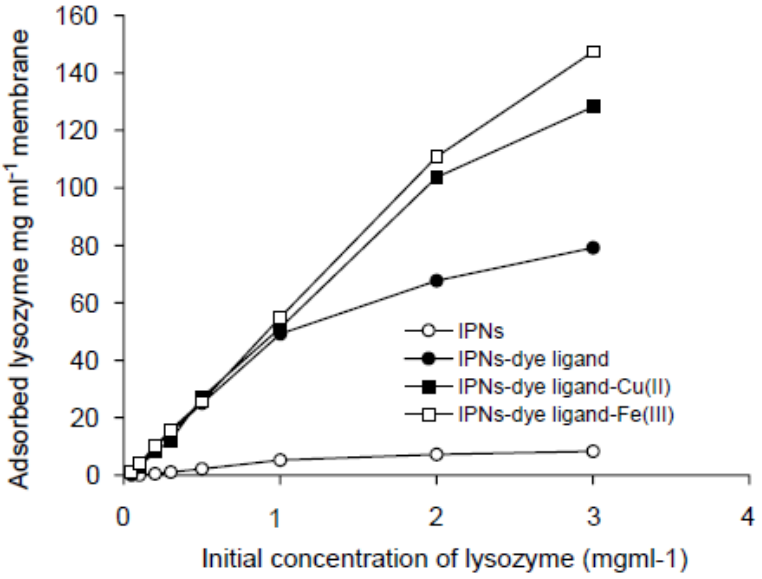

Figure 1.4 Effect of lysozyme initial concentration on lysozyme adsorption on the dye-ligand, dye-ligand-Fe(III) and dye-ligand-Cu(II) immobilized IPNs membrane. Procion Brown MX 5BR loading: 0:361 μmol ml-1 IPNs membrane; pH: 6.0; temperature: 25℃ (Bayramoglu et al., 2002).

1.3.3.4 The Dubinin-Radushkevich Isotherm

Dubinin-Radushkevich isotherm is described as the adsorption mechanism with a Gaussian energy distribution onto a heterogeneous surface. It has been tested for the adsorption of copper onto chitosan with a porous structure. The isotherm is an empirical model and generally expressed as the following equation (Dubinin, 1960, Radushkevich, 1949):

$$q_e = q_D \exp\left(-B_D \left[RT ln\left(1 + \frac{1}{C_e}\right)\right]^2\right) \qquad (1.6)$$

where q_e is the equilibrium metal ions adsorption density on an substrate, mmol/g

q_D is the theoretical isotherm saturation capacity, mmol/g

C_e is the equilibrium metal ions concentrations in the solution, mg/dm^3

B_D is the constant for the mean free energy of adsorption per mole of the adsorbate as it is transferred to the surface of the solid from infinite distance in the solution.

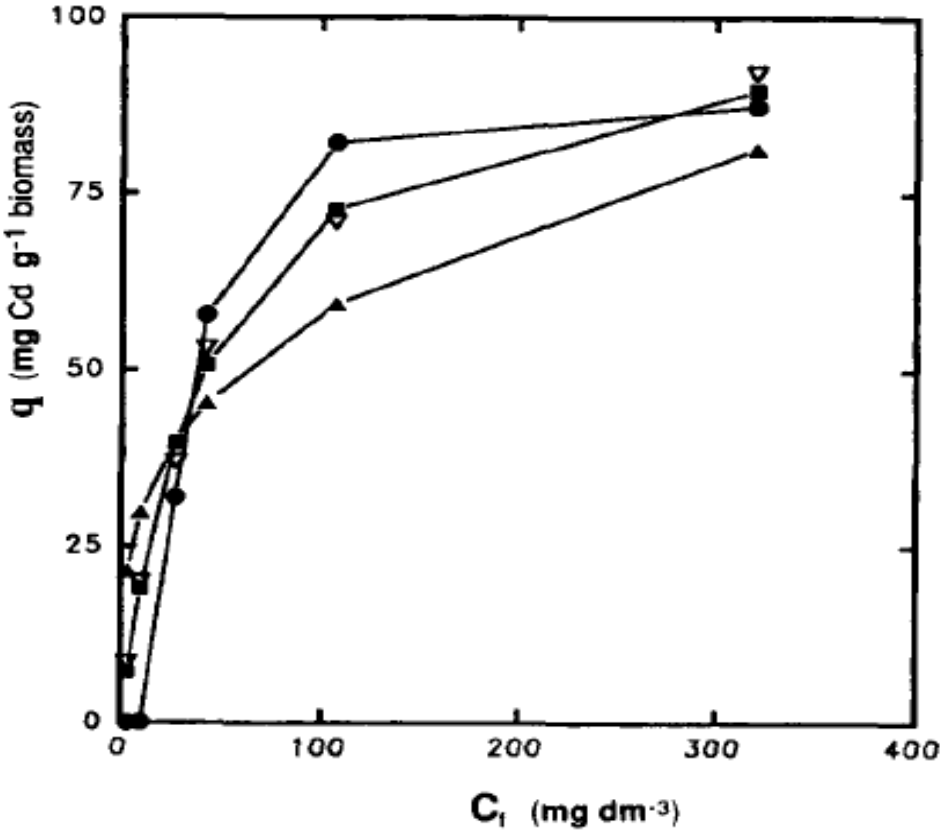

Figure 1.5 Comparison of different models for fitting of experimental Cd-sorption by Ascophyllum nodosum #5. ▲, Freundlich; ■, Langmuir; ●, Dubinin-Radushkevich (Leusch et al., 1995).

1.3.3.5 The Redlich-Peterson Isotherm

Redlich-Peterson isotherm incorporates three parameters and is a hybrid isotherm which combines both the Langmuir and Freundlich equations (Redlich and Peterson, 1959). It can be used to represent adsorption equilibrium over a wide concentration rage because of its dual features. It has been applied particularly to adsorbents that are heterogeneous. The isothermal model approaches Freundlich

isotherm model at high concentration and is in accordance with the low concentration limit of the Langmuir model. It can be described as follows:

$$q_e = \frac{K_R C_e}{1 + a_R C_e^{b_R}} \qquad (1.7)$$

where q_e is the equilibrium metal ions adsorption density on an subtrate, mmol/g

C_e is the equilibrium metal ions concentrations in the solution, mg/dm^3

K_R is Redlich-Peterson isotherm constant, ml/mg

a_R is Redlich-Peterson isotherm constant, 1/mg

b_R is Redlich-Peterson isotherm exponent, dimensionless.

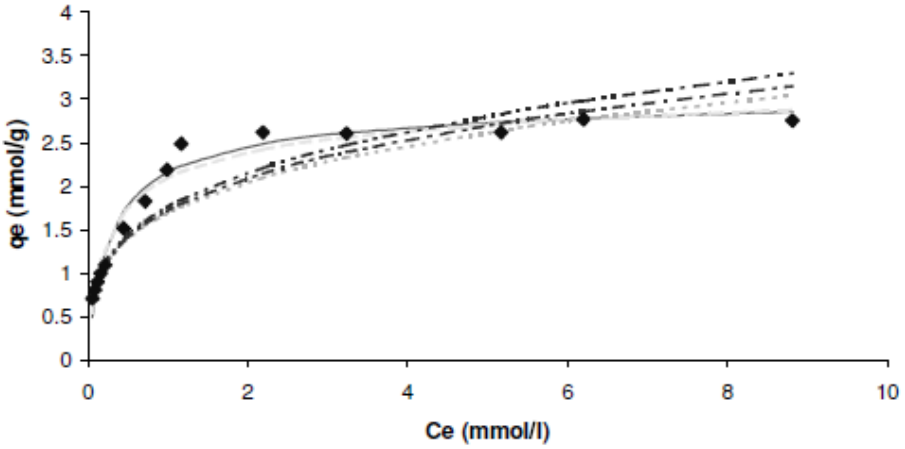

Figure 1.6 Adsorption isotherms for copper onto chitosan at pH 4.5: Redlich-Peterson isotherm (Ng et al., 2002).

1.3.4 Complex formation with metal ions

It has been shown that chitosan has good complexing ability with metal ions in aqueous solutions (Boddu et al., 2003; Burke et al., 2002; Gerente et al., 2007; Lasko and Hurst, 1999; Muzzarelli, 1977; Ngah et al., 2010; Nomanbhay and Palanisamy, 2005; Onsosyen and Skaugrud, 1990). The amino groups (Chui et al., 1996; Stöhr et al., 2001; Vold et al., 2003), together with the hydroxyl groups (Deans and Dixon, 1992; Kamiński and Modrzejewska, 1997; Lerivrey et al.,

1986; Monteiro and Airoldi, 1999; Sun and Wang, 2006; Wang et al., 2004), were considered as the major binding sites for the uptake of metal ions in aqueous solutions by chitosan. Therefore, the degree of deacetylation and the molar density of amino and hydroxyl groups on chitosan surface are the key factors to consider for the ability of chitosan to adsorb metal ions.

In addition to the chitosan composition (i.e., the degree of deacetylation), four main categories of factors were identified by Gerente et al. (2007) as the primary factors affecting the metal ion adsorption performance of chitosan. These are: physical type, source, process application factors, and physical properties. The physical type of chitosan was considered the most important factor affecting metal ion adsorption in terms of capacity and adsorption rate. To enhance the adsorption capacity, large amount of research has been dedicated to shape chitosan to different physical types such as beads, gels, swollen beads, powder, nanoparticles, solid fibers, hollow fibers, membranes, and spongelike or honeycomb structures. All these modifications are intended to increase the surface area and porosity of chitosan to meet the requirements of chitosan application. Chitosan sources (potential sources: squid, crab, shrimp, fungi, etc.) have the influence on the physicochemical characteristics of the chitosan such as molecular weight, degree of acetylation, etc. The process application factors, such as the solution pH and temperature, also have a great effect on the adsorption rate and capacity.

Many research publications are aimed at delineating the mechanisms of complex formation, but the conclusions on the formation of chitosan-metal complex are still contradictory. Different models were proposed concerning the structure of the complexes, including the bridge model (Blair and Ho, 1981; Schlick, 1986) and the pendant model (Domard, 1987; Piron and Domard, 1998; Roberts et al., 1992). The major differences for the formation models were the bonding structure of nitrogen atoms and metal ions in space. The bridge model, as shown in Figure 1.7, illustrates that at least two amino groups from one chitosan chain share the same

metal ions. In the pendant model (Domard, 1987; Piron and Domard, 1998; Roberts et al., 1992), it was proposed that some hydroxyl groups of the intra and inter chitosan chains were involved in the coordination in addition to the amino groups. Figure 1.8 shows a structure which was proposed by Monterio and Airoldi (Monteiro and Airoldi, 1999). As can be seen, the hydroxyl and amino groups in chitosan and water were bound to form chitosan-metal ion complex. More recently, the complexation of copper ion by chitosan was investigated by the complementary potentiometric and spectrophotometric techniques. It was suggested that two structures, $\{[Cu(NH_2)]^{2+}, 2OH^-, H_2O\}$ and $\{[Cu(NH_2)_2]^{2+}, 2OH^-\}$, existed as the complexes between chitosan and Cu^{2+} ions. The first structure is more stable at pH 5-5.8 while the second one is predominant above pH 5.8, showing that the complexes were dependent on pH. In another study, the chitosan-Fe^{3+} complexes were characterized by IR spectroscopy and the study showed that the ferric ion was coordinated with two glucosamine monomers in chitosan, three molecular water and one chloride ion. The general formula is proposed by the authors as $\{[Fe(H_2O)_3(Glu)_2Cl]Cl_2 \cdot H_2O\}$ (Nieto et al., 1992), where Glu represents a glucosamine residue.

Despite the large amount of work on the adsorption capacities of metal ions on chitosan, only limited studies were reported with respect to the selective adsorption of metal ions on chitosan from mixed metal ion solutions. Vold et al (2003) studied the adsorption of chitosan in binary metal ion system. The adsorption performance showed that chitosan displayed selectivity in the adsorption of Cu^{2+} over Ni^{2+}, Zn^{2+} and Cd^{2+} in the binary mixtures at pH lower than 4.7. Rinaudo (2006) listed the selective adsorption order of chitosan in divalent cation mixtures as Cu^{2+} » $Hg^{2+} > Zn^{2+} > Cd^{2+} > Ni^{2+} > Co^{2+} \sim Ca^{2+}$. Furthermore, other adsorbents with nitrogen-based functional groups, such as DETA (diethylenetriamine)-functionalized polymeric adsorbent (P-DETA) and amine functionalized fine-grained activated carbon (NH_2-AC), were found to have the selective adsorption behaviors in aqueous solutions (Lam et al., 2006; Liu et al., 2008; Yantasee et al., 2004). Liu et al. (2008) reported that both copper and

lead ions were significantly adsorbed on P-DETA in the single metal species system (only copper or lead ions). According to FTIR and XPS results, they suggested that the nitrogen atoms in the amine groups of DETA in P-DETA formed coordination bonds with copper and lead ions in single metal species system. In contrast, in the binary Cu-Pb metal ionic species systems, P-DETA adsorbed a considerable amount of copper ions with little lead ions being adsorbed. The adsorption tests showed P-DETA has selective adsorption on copper ions over lead ions in binary metal species system. To illustrate the selective adsorption of P-DETA, XPS measurement was made and the results suggested that an adsorbed copper ion coordinated with more nitrogen atoms than an adsorbed lead ion on P-DETA. Furthermore, Liu et al. (2008) proposed that much of the lead ions was weakly bound or physically adsorbed on P-DETA while copper ions formed stable complexes with P-DETA. Yanasee et al. (2004) measured the competitive adsorption of Cu^{2+} on NH_2-AC. They found that the affinity of NH_2-AC toward metal ions follows the decreasing order of Cu^{2+}, Pb^{2+}, Ni^{2+}, and Cd^{2+}.

Even though there has been an increasing interest in the selective adsorption behaviors of chitosan towards different metal ionic species, the adsorption mechanisms were still not elucidated clearly at present. A number of characteristic properties of metal ions, including hydrated radius, hardness, and electronegativity, have been examined to explain the selective adsorption mechanisms. In terms of hardness, Pearson's hard-soft acids-bases (HSAB) principle is widely used to enhance the understanding of reaction mechanism of transition metals and coordination ligands (Lam et al., 2006b; Parr and Pearson, 1983; Pearson, 1963). According to the HSAB theory, hard acids and hard bases prefer to bind together to form ionic complexes and soft acids and soft bases prefer to bind together to form covalent complexes (Klopman, 1968; Pearson, 1963). For instance, Yantasee et al. (2004) applied the HSAB theory to explain the selective adsorption of metal ions on NH_2-AC. The copper ion, as a borderline cation, has the tendency to react with aniline nitrogen which was soft base. By

following the HSAB theory, Lam et al. (2006) designed an adsorbent containing NH_2 groups to selectively remove Cu^{2+} from the binary solution of Cu-Ag. However, the HSAB theory is used to provide a qualitative rather than quantitative explanation for the coordination reactions. It does not show the reaction intensity order of metal ions which are borderline cations with certain coordination ligands.

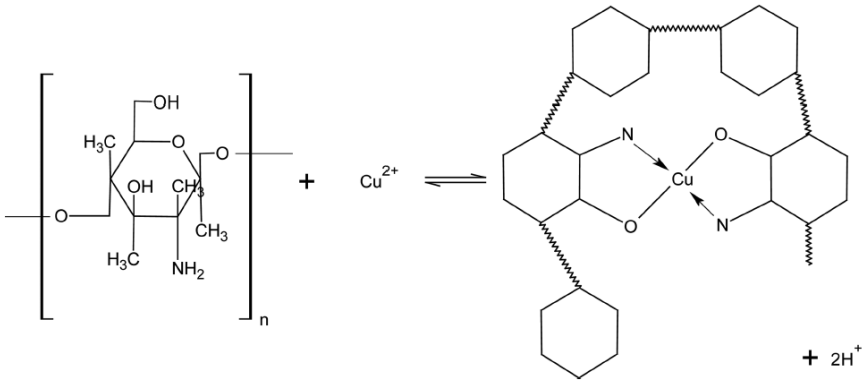

Figure 1.7 Formation of chitosan chelates with one copper ion bond to two amino groups (Bridge Model) (Gerente et al., 2007; Kamiński and Modrzejewska, 1997).

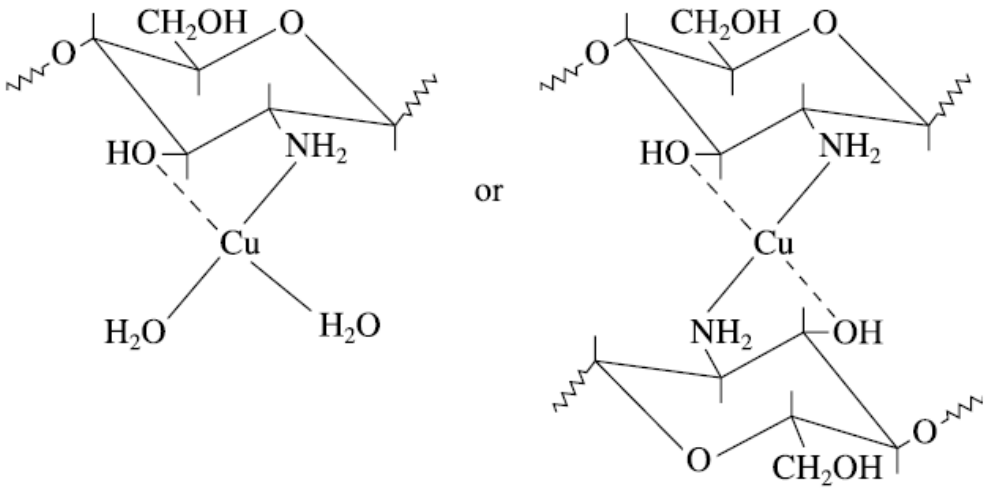

Figure 1.8 Formation of chitosan chelates with one copper ion bond to one hydroxyl, one amino and two water molecules (left), and with two hydroxyl and two amino groups (Pendant Model) (Monteiro and Airoldi, 1999).

1.4 Objectives

The objective of this dissertation research is to investigate the use of chitosan as a possible novel selective depressant which assists in the flotation separation of different sulfide minerals, and to study the adsorption mechanisms of chitosan on the sulfide mineral surfaces to understand the possible selective depressive functions. Specific experimental studies include:

- Flotation separation of Cu-Pb, Zn-Pb and Fe-Pb sulfide minerals using chitosan as a depressant in the presence of a thiol collector such as xanthate.
- The effect of solution pH, chitosan concentration, and degree of deacetylation on the flotation separation performance.

- The surface chemistry of sulfide minerals after chitosan adsorption. Such studies will provide information on the selective adsorption of chitosan on the different sulfide minerals, and the mechanisms of the chitosan-mineral interactions.

It is expected that the dissertation research will provide useful information to guide the development of environmentally benign non-toxic flotation depressants in the differential sulfide mineral flotation.

1.5 Organization of the Thesis

This thesis is organized in manuscript-based style. It includes four main chapters (Chapters 2, 3, 4 and 5) for the study of chitosan as a novel depressant in the differential flotation of sulfide minerals of Cu-Pb (Chapters 2 and 3), Pb-Zn (Chapter 4) and Pb-Fe (Chapter 5).

Chapter 1 gives a general introduction to the status of sulfide mineral flotation and the types of depressants used in the differential sulfide flotation. It also includes a comprehensive review of literature information on the structure, properties and applications of chitosan.

Chapter 2 presents the study of using chitosan as a selective depressant in the differential flotation of Cu-Pb sulfides. The flotation results of chalcopyrite ($CuFeS_2$) and galena (PbS) and their mixtures will be presented.

Chapter 3 concerns the adsorption mechanism of chitosan on chalcopyrite and galena from aqueous suspensions. The selective adsorption of chitosan in the chalcopyrite-galena system was investigated by the surface analysis techniques including attenuated total reflection Fourier transform infrared spectroscopy (ATR-FTIR), time-of-flight secondary ion mass spectrometry (ToF-SIMS) and X-ray photoelectron spectroscopy (XPS).

Chapter 4 focuses on the selective adsorption of chitosan on Zn and Pb sulfide minerals. The flotation tests of sphalerite (ZnS) and galena and their mixtures were conducted. The adsorption mechanism of chitosan on sphalerite was studied and contrasted with the adsorption of chitosan on galena to explain the observed selective flotation behavior.

Chapter 5 presents the investigation of the selective adsorption of chitosan in Fe and Pb sulfide minerals. Flotation tests were carried out on pyrite and galena and their mixtures, and the adsorption mechanisms of chitosan on pyrite were studied and compared with galena. In addition, the competitive adsorption mechanisms of chitosan in all the three studied sulfide mineral systems, Cu-Pb, Zn-Pb and Fe-Pb sulfides, were discussed to attempt to give a unified view of the adsorption mechanisms of chitosan on the studied sulfide minerals.

Chapter 6 presents general conclusions resulting from this dissertation research, claim of the originality and suggestions for future research work.

1.6 References

Allan, W., Bourke, R.D., 1978. Mattabi Mines Ltd. Milling Practice in Canada, 16,175-176.

Aharoni, C., and Ungarish, M., 1977. Kinetics of activated chemisorption. Part 2. Theoretical models, Journal of the Chemical Society, Faraday Transactions 73, 456.

Amaral, I., Granja, P., Barbosa, M., 2005. Chemical modification of chitosan by phosphorylation: an XPS, FT-IR and SEM study. Journal of Biomaterials Science, Polymer Edition 16, 1575-1593.

Bayramoglu, G., Kaya, B., and Arica, M.Y., 2002. Procion brown MX-5BR attached and Lewis metals ion-immobilized poly(hydroxyethyl methacrylate)/chitosan IPNs membranes: Their lysozyme adsorption equilibria and kinetics characterization, Chemical Engineering Science 57, 2323.

Blair, H.S., Ho, T.C., 1981. Studies in the adsorption and diffusion of ions in chitosan. Journal of Chemical Technology and Biotechnology 31, 6-10.

Boddu, V.M., Abburi, K., Talbott, J.L., Smith, E.D., 2003. Removal of hexavalent chromium from wastewater using a new composite chitosan biosorbent. Environmental science & technology 37, 4449-4456.

Bogusz, E., Brienne, S.R., Butler, I., Rao, S.R., Finch, J.A., 1997. Metal ions and dextrin adsorption on pyrite. Minerals Engineering 10, 441-445.

Bolin, N.J., Laskowski, J.S., 1991. Polysaccharides in flotation of sulfides. Part II. Copper/lead separation with dextrin and sodium hydroxide. International Journal of Mineral Processing 33, 235-241.

Bulatovic, S., 2007. Handbook of Flotation Reagents: Chemistry, Theory and Practice: Flotation of Sulfide Ores. Elsevier Science Ltd.

Bulatovic, S.M., Wyslouzil, D.M., 1985. Selection of reagent scheme to treat massive sulfide ores. In Complex Sulfide. Proceedings of a Symposium Sponsored by TMS of AIME and CIM; AIME, Inc.: San Diego, California, 10-13, 101-137.

Burke, A., Yilmaz, E., Hasirci, N., Yilmaz, O., 2002. Iron (III) ion removal from solution through adsorption on chitosan. Journal of applied polymer science 84, 1185-1192.

Choy, K.K.H., Porter, J.F., Mckay, G., 2001. A film-pore-surface diffusion model for the adsorption of acid dyes on activated carbon. Adsorption 7, 231-247.

Chui, V., Mok, K., Ng, C., Luong, B., Ma, K., 1996. Removal and recovery of copper (II), chromium (III), and nickel (II) from solutions using crude shrimp chitin packed in small columns. Environment international 22, 463-468.

Chung, Y.S., Lee, K.K., Kim, J.W., 1998. Durable press and antimicrobial finishing of cotton fabrics with a citric acid and chitosan treatment. Textile research journal 68, 772.

Crini, G., Badot, P.M., 2008. Application of chitosan, a natural aminopolysaccharide, for dye removal from aqueous solutions by adsorption processes using batch studies: A review of recent literature. Progress in Polymer Science 33, 399-447.

Deans, J.R., Dixon, B.G., 1992. Uptake of Pb^{2+} and Cu^{2+} by novel biopolymers. Water Research 26, 469-472.

Dolivo-Dobrovoskii, V.V., Rogachevskaya, T.A., 1957. Depression action of some high-molecular organic compounds on sulfide minerals. Obogashch. Rud 1, 30-40.

Domard, A., 1987. pH and cd measurements on a fully deacetylated chitosan: application to Cu(II)--polymer interactions. International journal of biological macromolecules 9, 98-104.

Dubinin, M.M., 1960. The potential theory of adsorption of gases and vapors for adsorbents with energetically non-uniform surface, Chemical Reviews 60, 235.

Egger, G., Cameron-Smith, D., Stanton, R., 1999. The effectiveness of popular, non-prescription weight loss supplements. Med J Aust 171, 604-608.

Fuerstenau, M.C., 2003. Principles of mineral processing. The Society for Mining, Metallurgy and Exploration.

Fuerstenau, M.C., Jameson, G.J., Yoon, R.H., 2007. Froth flotation: a century of innovation. Society for Mining Metallurgy.

Gerente, C., Lee, V., Cloirec, P.L., McKay, G., 2007. Application of chitosan for the removal of metals from wastewaters by adsorption-mechanisms and models review. Critical reviews in environmental science and technology 37, 41-127.

González Siso, M., Lang, E., Carreno-Gomez, B., Becerra, M., Otero Espinar, F., Blanco Mendez, J., 1997. Enzyme encapsulation on chitosan microbeads. Process Biochemistry 32, 211-216.

Heux, L., Brugnerotto, J., Desbrieres, J., Versali, M.F., Rinaudo, M., 2000. Solid state NMR for determination of degree of acetylation of chitin and chitosan. Biomacromolecules 1, 746-751.

Hirai, A., Odani, H., Nakajima, A., 1991. Determination of degree of deacetylation of chitosan by 1 H NMR spectroscopy. Polymer Bulletin 26, 87-94.

Hirano, S., 1989. Production and application of chitin and chitosan in Japan. Elsevier, London, England, pp. 37-43.

Houshyar, S., Amirshahi, S.H., 2002. Treatment of cotton with chitosan and its effect on dyeability with reactive dyes. Iranian Polymer Journal 11, 295-302.

Huang, P., Cao, M., Liu, Q., 2012. Using chitosan as a selective depressant in the differential flotation of Cu–Pb sulfides. International Journal of Mineral Processing 106–109, 8-15.

Ilium, L., 1998. Chitosan and its use as a pharmaceutical excipient. Pharmaceutical Research 15, 1326-1331.

Jocić, D., Julia, M., Erra, P., 1997. Application of a chitosan/nonionic surfactant mixture to wool assessed by dyeing with a reactive dye. Journal of the Society of Dyers and Colourists 113, 25-31.

Kamiński, W., Modrzejewska, Z., 1997. Application of chitosan membranes in separation of heavy metal ions. Separation Science and Technology 32, 2659-2668.

Klopman, G., 1968. Chemical reactivity and the concept of charge-and frontier-controlled reactions. Journal of the American Chemical Society 90, 223-234.

Koide, S., 1998. Chitin-chitosan: properties, benefits and risks. Nutrition research 18, 1091-1101.

Lai, W.F., Lin, M.C.M., 2009. Nucleic acid delivery with chitosan and its derivatives. Journal of controlled release 134, 158-168.

Lam, K.F., Yeung, K.L., McKay, G., 2006. A rational approach in the design of selective mesoporous adsorbents. Langmuir 22, 9632-9641.

Lasko, C.L., Hurst, M.P., 1999. An investigation into the use of chitosan for the removal of soluble silver from industrial wastewater. Environmental science & technology 33, 3622-3626.

Laskowski, J.S., Nyamekye, G.A., 1994. Adsorption studies in flotation research: differential flotation of Cu-Ni sulfides using dextrin. Castro, S. and Alvarez, J., Editors, 15-18.

Lawrie, G., Keen, I., Drew, B., Chandler-Temple, A., Rintoul, L., Fredericks, P., Grøndahl, L., 2007. Interactions between alginate and chitosan biopolymers characterized using FTIR and XPS. Biomacromolecules 8, 2533-2541.

Lerivrey, J., Dubois, B., Decock, P., Micera, G., Urbanska, J., Kozlowski, H., 1986. Formation of D-glucosamine complexes with Cu (II), Ni (II) and Co (II) ions. Inorganica chimica acta 125, 187-190.

Leusch, A., Holan, Z.R., and Volesky, B., 1995. Biosorption of heavy-metals (Cd, Cu, Ni, Pb, Zn) by chemically-reinforce biomass of marine-algae, Journal of Chemical Technology and Biotechnology 62, 279-288.

Liu, C., Bai, R., San Ly, Q., 2008. Selective removal of copper and lead ions by diethylenetriamine-functionalized adsorbent: Behaviors and mechanisms. Water Research 42, 1511-1522.

Liu, Q., Laskowski, J.S., 1989. The role of metal hydroxides at mineral surfaces in dextrin adsorption, II. Chalcopyrite-galena separations in the presence of dextrin. International Journal of Mineral Processing 27, 147-155.

Liu, Q., Laskowski, J.S., 2006. Adsorption of polysaccharide onminerals,In: Somasundaran, P. (Ed.), Encyclopedia of Surface and Colloid Science, Second Edition. Taylor & Francis, New York, pp. 649–668.

Liu, Q., Zhang, Y., 2000. Effect of calcium ions and citric acid on the flotation separation of chalcopyrite from galena using dextrin. Minerals Engineering 13, 1405-1416.

Loke, W.K., Lau, S.K., Yong, L.L., Khor, E., Sum, C.K., 2000. Wound dressing with sustained anti ‐ microbial capability. Journal of biomedical materials research, Part A 53, 8-17.

Martino, A., Pifferi, P., Spagna, G., 1996. Immobilization of [beta]-glucosidase from a commercial preparation. Part 2. Optimization of the immobilization process on chitosan. Process Biochemistry 31, 287-293.

Monteiro, O.A.C., Airoldi, C., 1999. Some thermodynamic data on copper-chitin and copper-chitosan biopolymer interactions. Journal of colloid and interface science 212, 212-219.

Mumper, R., Wang, J., Claspell, J., Rolland, A., 1995. Novel polymeric condensing carriers for gene delivery, pp. 178-179.

Muzzarelli, R., 1989. Amphoteric derivatives of chitosan and their biological significance. Chitin and chitosan. New York: Elsevier Applied Science, 87–99.

Muzzarelli, R.A.A., 1977. Chitin. Pergamon Press New York.

Muzzarelli, R.A.A., Lough, C., Emanuelli, M., 1987. The molecular weight of chitosans studied by laser light-scattering. Carbohydrate Research 164, 433-442.

Ngah, W., Teong, L., Hanafiah, M., 2010. Adsorption of dyes and heavy metal ions by chitosan composites: A review, Carbohydrate Polymers. Elsevier, pp. 1446-1456.

Nieto, J., Peniche-Covas, C., Del Bosque, J., 1992. Preparation and characterization of a chitosan-Fe (III) complex. Carbohydrate Polymers 18, 221-224.

Nomanbhay, S.M., Palanisamy, K., 2005. Removal of heavy metal from industrial wastewater using chitosan coated oil palm shell charcoal. Electronic Journal of Biotechnology 8, 43-53.

Nyamekye, G.A., Laskowski, J.S., 1991. The differential flotation of INCO matte with the use of polysaccharides. Proceeding of the Copper '91 International Symposium, Dobby, G.S., Argyropoulos, S.A., Rao, S.R., Eds.; Pergamon Press 2, 231-243.

Onsosyen, E., Skaugrud, O., 1990. Metal recovery using chitosan. Journal of Chemical Technology & Biotechnology 49, 395-404.

Parr, R.G., Pearson, R.G., 1983. Absolute hardness: companion parameter to absolute electronegativity. Journal of the American Chemical Society 105, 7512-7516.

Pearson, R.G., 1963. Hard and soft acids and bases. Journal of the American Chemical Society 85, 3533-3539.

Peniche‐Covas, C., Alvarez, L., Argüelles‐Monal, W., 2003. The adsorption of mercuric ions by chitosan. Journal of applied polymer science 46, 1147-1150.

Piron, E., Domard, A., 1998. Interactions between chitosan and [alpha] emitters: 238Pu and 241Am. International journal of biological macromolecules 23, 121-125.

Rabea, E.I., Badawy, M.E.T., Stevens, C.V., Smagghe, G., Steurbaut, W., 2003. Chitosan as antimicrobial agent: applications and mode of action. Biomacromolecules 4, 1457-1465.

Radushkevich, L.V., 1949. Potential theory of sorption and structure of carbons, Zhurnal Fizicheskoi Khimii 23, 1410.

Ravi Kumar, M.N.V., 2000. A review of chitin and chitosan applications. Reactive and functional polymers 46, 1-27.

Raymond, L., Morin, F.G., Marchessault, R.H., 1993. Degree of deacetylation of chitosan using conductometric titration and solid-state NMR. Carbohydrate Research 246, 331-336.

Redlich, O., and Peterson, D.L., 1959. A useful adsorption isotherm, The Journal of Physical Chemistry 63, 1024.

Rinaudo, M., 2006. Chitin and chitosan: Properties and applications. Progress in Polymer Science 31, 603-632.

Rinaudo, M., Milas, M., Dung, P.L., 1993. Characterization of chitosan. Influence of ionic strength and degree of acetylation on chain expansion. International journal of biological macromolecules 15, 281-285.

Roberts, G., Taylor, K., Brine, C., Sanford, P., Zikakis, J., 1992. Surface activity and foam-enhancing properties of N-(2-hydroxyalkyl) chitosans. Advances in Chitin and Chitosan, Elsevier, Amsterdam (1992), pp. 179-186.

Rusu-Balaita, L., Desbrieres, J., Rinaudo, M., 2003. Formation of a biocompatible polyelectrolyte complex: chitosan-hyaluronan complex stability. Polymer Bulletin 50, 91-98.

Schlick, S., 1986. Binding sites of copper2+ in chitin and chitosan. An electron spin resonance study. Macromolecules 19, 192-195.

Schnarr, J.R., 1978. Brunswick mining and smelting corporation. Milling Practice in Canada, CIM Spec 16, 158-161.

Se-Kwon, K., 2010. Chitin, Chitosan, Oligosaccharides and Their Derivatives : Biological Activities and Applications. 69-70.

Shahidi, F., Arachchi, J.K.V., Jeon, Y.J., 1999. Food applications of chitin and chitosans. Trends in Food Science & Technology 10, 37-51.

Shin, Y., Yoo, D.I., 1998. Use of chitosan to improve dyeability of DP - finished cotton (II). Journal of applied polymer science 67, 1515-1521.

Sorlier, P., Denuzière, A., Viton, C., Domard, A., 2001. Relation between the degree of acetylation and the electrostatic properties of chitin and chitosan. Biomacromolecules 2, 765-772.

Srinivasa, P., Baskaran, R., Ramesh, M., Harish Prashanth, K., Tharanathan, R., 2002. Storage studies of mango packed using biodegradable chitosan film. European Food Research and Technology 215, 504-508.

Stöhr, C., Horst, J., Höll, W.H., 2001. Application of the surface complex formation model to ion exchange equilibria: Part V. Adsorption of heavy metal

salts onto weakly basic anion exchangers. Reactive and functional polymers 49, 117-132.

Struszczyk, H., 1987. Microcrystalline chitosan. I. Preparation and properties of microcrystalline chitosan. Journal of applied polymer science 33, 177-189.

Struszczyk, M., 2002. Chitin and chitosan—Part II. Applications of chitosan. Polimery 47, 396-403.

Sun, S., Wang, A., 2006. Adsorption properties and mechanism of cross-linked carboxymethyl-chitosan resin with Zn (II) as template ion. Reactive and functional polymers 66, 819-826.

Tien, C., 1994. Adsorption Calculation and Modeling, in: Series in Chemical Engineering, Butterworth–Heinemann, London.

Teixeira, M.A., Paterson, W.J., Dunn, E.J., Li, Q., Hunter, B.K., Goosen, M.F.A., 1990. Assessment of chitosan gels for the controlled release of agrochemicals. Industrial & engineering chemistry research 29, 1205-1209.

Vold, I., Varum, K.M., Guibal, E., Smidsrod, O., 2003. Binding of ions to chitosan--selectivity studies. Carbohydrate Polymers 54, 471-477.

Wang, L., Khor, E., Wee, A., Lim, L.Y., 2002. Chitosan ‐ alginate PEC membrane as a wound dressing: Assessment of incisional wound healing. Journal of biomedical materials research, Part A 63, 610-618.

Wang, X., Du, Y., Liu, H., 2004. Preparation, characterization and antimicrobial activity of chitosan-Zn complex. Carbohydrate Polymers 56, 21-26.

Wu, A., Bough, W.A., Conrad, E.C., Alden, K.E., 1976. Determination of molecular-weght distribution of chitosan by high-performance liquid chromatography. Journal of Chromatography A 128, 87-99.

Wu, F.C., Tseng, R.L., Juang, R.S., 2000. Comparative adsorption of metal and dye on flake-and bead-types of chitosans prepared from fishery wastes. Journal of hazardous materials 73, 63-75.

Wu, F.C., Tseng, R.L., Juang, R.S., 2001. Kinetic modeling of liquid-phase adsorption of reactive dyes and metal ions on chitosan. Water Research 35, 613-618.

Yantasee, W., Lin, Y., Fryxell, G.E., Alford, K.L., Busche, B.J., Johnson, C.D., 2004. Selective removal of copper (II) from aqueous solutions using fine-grained activated carbon functionalized with amine. Industrial & engineering chemistry research 43, 2759-2764.

Yoshida, H., Okamoto, A., Kataoka, T., 1993. Adsorption of acid dye on cross-linked chitosan fibers: equilibria. Chemical engineering science 48, 2267-2272.

Yu, G., Morin, F.G., Nobes, G.A.R., Marchessault, R.H., 1999. Degree of acetylation of chitin and extent of grafting PHB on chitosan determined by solid state N-15 MMR. Macromolecules 32, 518-520.

Zorica, K.-J., Zivomir, P., Andrija, S., 2010. Chitin and Chitosan from Microorganisms, Chitin, Chitosan, Oligosaccharides and Their Derivatives. CRC Press, pp. 25-36.

CHAPTER 2

USING CHITOSAN AS A SELECTIVE DEPRESSANT IN THE DIFFERENTIAL FLOTATION OF Cu-Pb SULFIDES*

2.1. Introduction

Copper and lead sulfide minerals such as chalcopyrite and galena are separated by froth flotation using a thiol collector and appropriate depressants. At present, inorganic depressants are routinely used as the selective depressants. For example, sodium cyanide is used to depress copper sulfide minerals while lead sulfides are floated. Conversely, sodium dichromate, sodium sulfide, or a combination of sulfur dioxide and dextrin (starch) is used to depress lead sulfides while copper sulfides are floated (King, 1982; Liu and Laskowski, 2006). These inorganic depressants are toxic and hazardous, and also lack the ability to lower the mechanical entrainment of the depressed minerals (King, 1982; Liu and Laskowski, 2006). In other words, while the depressants may be able to selectively render the mineral surface hydrophilic, they cannot prevent the mineral to enter the flotation froth product when its particle size is ultrafine (less than 10 μm or so). With the increasingly rigid environmental pollution control regulations, and the increasing need of fine grinding to liberate minerals from the lower grade finely disseminated ores, the use of such toxic inorganic depressants is under increasing pressure. It is imperative that they be replaced by environmentally friendly chemicals, especially the environmentally friendly chemicals that may also selectively flocculate the minerals to be depressed in order to lower their entrainment. Motivated by such requirements, chitosan, a

* This paper was published in International Journal of Mineral Processing: P. Huang, M. Cao and Qi Liu, 2012. Using chitosan as a selective depressant in the differential flotation of Cu-Pb sulfides. International Journal of Mineral Processing, Vol. 106-109, 8-15. http://dx.doi.org/10.1016/j.minpro.2012.01.001.

non-toxic natural polymer, is tested in this study as a potential depressant in the differential flotation separation of Cu-Pb sulfides.

Chitosan is a natural polyaminosaccharide (Ngah et al., 2010) produced from the deacetylation of chitin, the main component of the crustaceans shells (Muzzarelli, 1973b; Se-Kwon, 2010a). The basic structure units of chitosan and chitin are β-(1-4)-linked D-glucosamine and β-(1-4)-linked N-acetyl-D-glucosamine, respectively, as shown in Figure 2.1 (Gerente et al., 2007). Chitin is the second most abundant natural polysaccharide in the world next to cellulose. Most of the chitin and chitosan are commercially produced from the shells of marine crustaceans, particularly lobsters and prawns (Gerente et al., 2007; Hirano, 1989). Recently, chitosan from other origins, such as mushrooms, honeybees, and silkworms, etc., have also been exploited to meet the specific requirements for human use on industrial scales (Wu et al., 2004; Yen and Mau, 2007a, b; Zhang et al., 2000).

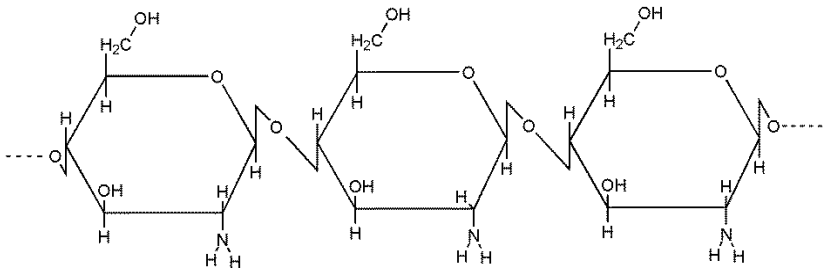

(a) chitosan

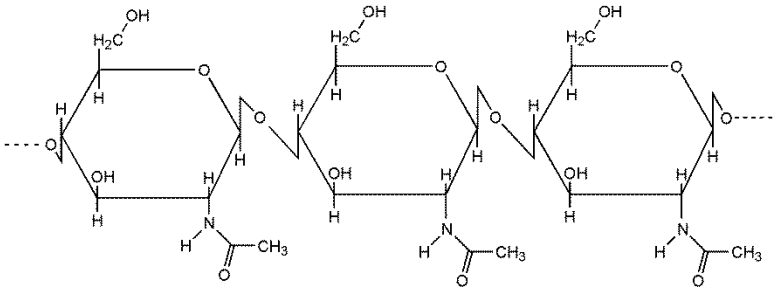

(b) chitin

Figure 2.1 Structures of chitosan and chitin (Gerente et al., 2007).

Chitosan has been studied and exploited in a number of areas due to its abundant resources, biodegradability, biocompatibility and film-forming ability. It has been commercially applied in a wide range of industrial sectors, such as wastewater treatment (Boddu et al., 2003; Burke et al., 2002; Ravi Kumar, 2000), paper and textile industry (Choy et al., 2001; Chung et al., 1998; Houshyar and Amirshahi, 2002; Jocić et al., 1997; Shin and Yoo, 1998; Struszczyk, 1987), biomedical engineering (Koide, 1998; Loke et al., 2000; Struszczyk, 2002; Wang et al., 2002), healthcare (González Siso et al., 1997; Ilium, 1998; Martino et al., 1996; Muzzarelli, 1989), agriculture and food industry (Crini and Badot, 2008; Egger et al., 1999; Gerente et al., 2007; Srinivasa et al., 2002; Teixeira et al., 1990). However, no attempt has been reported concerning the application of chitosan in mineral flotation. As can be seen from Figure 2.1, chitosan contains amino and hydroxyl groups. These functional groups can promote chitosan to interact (Bassi et al., 2000; Blair and Ho, 1981; Deans and Dixon, 1992; Domard, 1987; Findon et al., 1993; Lerivrey et al., 1986; Monteiro and Airoldi, 1999; Rhazi et al., 2002;

Schlick, 1986) and form stable complexes and chelates with heavy metal ions to different extents (Boddu et al., 2003; Burke et al., 2002; Gerente et al., 2007; Lasko and Hurst, 1999; Ngah et al., 2010; Nomanbhay and Palanisamy, 2005; Onsosyen and Skaugrud, 1990). It is expected that chitosan could potentially form metal complex on mineral surfaces and make the surface hydrophilic, thus depressing the flotation of specific minerals in a flotation separation process. Motivated by such an idea, the differential flotation separation of Cu-Pb sulfide minerals with the use of chitosan was studied to find out whether chitosan could act as an effective selective depressant. It was observed that chitosan selectively depressed copper sulfide while lead sulfide could be floated by a thiol collector such as xanthate. The result is reported in the following together with a study on the adsorption mechanism of the chitosan on the copper and lead sulfide minerals.

2.2 Materials and Methods

2.2.1 Materials

Chitosan, with a reported molecular weight ranging from 190,000 to 310,000 and a degree of deacetylation of 75% - 85% (85.7% based on the XPS results of this work), was obtained from Sigma-Aldrich. The chitosan was dissolved by diluted hydrochloric acid (0.2 mol/L) before using. High purity chalcopyrite and galena were purchased from Ward's Scientific Establishment and used as the copper and lead sulfide minerals in the experiments. The lumps of the chalcopyrite and galena were separately crushed (Retsch jaw crusher, USA) and hand-picked to obtain high purity samples, and then further crushed and pulverized with a Pulverisette 2 mechanized agate mortar/pestle grinder (Fritsch, Germany). The -75+38 μm size fractions were screened out for use in the flotation tests. The finer, -20 μm, fractions were utilized for surface analysis, including ToF-SIMS and XPS. In order to minimize oxidation, the mineral samples were sealed in plastic bottles and stored in a freezer at -10 ℃.

X-ray diffraction measurements on the chalcopyrite and galena samples showed that there were no impurities except for a minor amount of quartz in chalcopyrite. Chemical analysis of the samples showed that the chalcopyrite sample contained 29.26% Cu, indicating a purity of 84.5% chalcopyrite, and that galena contained 84.00% Pb, representing a purity of 97.0% galena.

The specific surface areas of both chalcopyrite and galena were determined by Quantachrome Autosorb 1MP (Quantachrome Instruments, USA) based on BET Theory, using N_2 (g) as the adsorbate. The specific surface area was 0.38 m^2/g for the -75+38 μm chalcopyrite, 1.19 m^2/g for the -20 μm chalcopyrite, 0.15 m^2/g for the -75+38 μm galena, and 0.5 m^2/g for the -20 μm galena.

Hydrochloric acid and sodium hydroxide, purchased from Fisher Scientific Canada, were used to adjust pH. Potassium ethyl xanthate (KEX) was obtained from Prospec Chemicals Ltd, Canada, and used as a collector in the flotation tests. It was purified by washing with ethyl ether anhydrous and acetone (Fisher Scientific, Canada) following the protocol of Foster (1928) before use. $CuCl_2 \cdot 2H_2O$ (Fisher Scientific, Canada) and $Pb(NO_3)_2$ (Merck, Canada) were used as the sources of Cu^{2+} and Pb^{2+} ions in the solution to study their adsorption on chitosan. Distilled water was used in t all the tests.

2.2.2 Experimental methods

2.2.2.1 Flotation

The flotation tests were conducted in a flotation tube, the construction of which was described in detail by Cao and Liu (2006). Briefly, a sintered glass frit, which had a pore size of 1.6 μm, was fitted at the base of the flotation tube. On the top of the frit, a magnetic stirring bar was used to agitate the flotation pulp. A narrow throat was constructed to connect the flotation tube to a collection bulb. Such a narrow throat could allow only one bubble to pass at a time when no frother was used, thus minimizing mechanical entrainment.

In a typical test, 1.5 g of the -75+38 μm samples (single mineral or mineral mixtures with certain weight ratio) were mixed with 150 mL distilled water in a beaker for 3 min during which the solution pH was adjusted using either hydrochloric acid or sodium hydroxide. An appropriate amount of chitosan and KEX were added sequentially into the pulp and conditioned for 3 min each. The conditioned slurry was transferred to the flotation tube, and floated for 3 min using high purity nitrogen gas. After the flotation was finished, both the froth product and tailings were collected and dried to calculate mineral recovery. In the mineral mixture flotation tests, the metal contents of Cu and Pb in the froth and tailings were determined by dissolving the dried samples with aqua regia and analyzing the solutions using a Varian SpectrAA-220FS (Varian, USA) atomic absorption spectrometer (AAS).

2.2.2.2 Adsorption of metal ions by chitosan

The adsorption tests were conducted in a SI-600 shaking incubator (Jeio Tech, USA) with a shaking rate of 250 rpm at 25°C. Chitosan was mixed with 50 mL distilled water in a conical flask, and this was followed by the addition of a given amount of solutions with known metal ion (Cu^{2+} or Pb^{2+}) concentration, either alone or pre-mixed together. The flask was stoppered and placed in the shaking incubator and shaken for 30 min. The suspension was then filtered and the supernatant was used to determine the equilibrium concentrations of the metal ions using the Varian AAS. The adsorption density of the metal ions on chitosan was calculated by the difference between the initial concentration and the equilibrium concentration.

2.2.2.3 ToF-SIMS measurements

ToF-SIMS images and element maps of the chalcopyrite-galena mixture after treating with chitosan were obtained on a ToF-SIMS IV spectrometer (ION-TOF GmbH). For spectra acquisition, a high energy beam of Bi^{+} ions (25 kV) was focused on the sample surface at an area of 64 μm × 64 μm. The positive ion mass

spectra were obtained and calibrated by the secondary ion peaks for H^+, CH_3^+ and Na^+. Images were then generated by mapping the mass-selected ion intensity in a burst alignment mode with pixels of 128 × 128 per image. The test sample was prepared by mixing 0.5 g chalcopyrite with 0.5 g galena, and 0.3 mg of chitosan in 100 mL distilled water at pH 4. The suspension was conditioned in the incubator for 30 min, and the minerals were filtered, washed with 200 mL distilled water through the filtration funnel and dried in a desiccator in vacuum before ToF-SIMS analysis. To minimize oxidation, the analysis was carried out within 12 hours after sample preparation.

2.2.2.4 XPS measurements

XPS survey scan and high-resolution spectra were acquired on an AXIS 165 X-ray photoelectron spectrometer (Kratos Analytical). Monochromatic Al Kα source (hv = 1486.6 eV) was used at a power of 210 W for all data acquisition. The vacuum pressure inside the analytical chamber was lower than 3×10^{-8} Pa. The analyzed area on the sample surface was 400 μm × 700 μm. The resolution of the instrument is 0.55 eV for Ag 3d and 0.70 eV for Au 4f peaks.

To prepare the mineral sample for the XPS analysis, 1 g chalcopyrite or galena was mixed with 2 mg of chitosan in 100 mL distilled water at pH 4. The suspension was conditioned in the incubator for 30 min, and the mineral solids were filtered, washed with 200 mL distilled water through the filter funnel and dried in a desiccator in vacuum before XPS analysis. To minimize oxidation, the analysis was carried out within 12 hours after sample preparation.

The survey scans were collected for binding energy range from 1100 eV to 0 eV with an analyzer pass energy of 160 eV and a step of 0.4 eV. To collect the high-resolution spectra, the pass-energy was set at 20 eV with a step of 0.1 eV. No charge neutralization was required through the spectra collection. XPS sampling depth for photoelectrons was 3-10 nm, which was more than enough to provide information of the mineral surfaces in this work. CasaXPS Version 2.3.15

instrument software was used to process the XPS data after spectra collection. The Shirley-type background subtraction was chosen to optimize the peak height through the high-resolution spectra analysis. And then, according to previously published data, the processed spectra were calibrated, resolved and refined into individual Gaussian-Lorentzian peaks and imported into a graphic software (Origin, OriginLab Corp) package for displaying the optimized fitting peaks from the high-resolution spectra.

2.3. Results and Discussion

2.3.1 Flotation of single minerals

The recovery of chalcopyrite and galena in single mineral flotation tests with and without chitosan as a depressant is shown in Figure 2.2. The collector used in the tests was potassium ethyl xanthate (KEX). Figure 2.2 shows that both chalcopyrite and galena were floatable with a high recovery of more than 88% at the tested pH range. However, when 0.67 mg/L chitosan was added, the floatability of both chalcopyrite and galena dropped significantly. At pH 3, the flotation recovery of chalcopyrite dropped from over 90% in the absence of chitosan, to about 60% in the presence of the 0.67 mg/L chitosan. Between pH 3 and 5 and in the presence of chitosan, the recovery of chalcopyrite decreased from 60% to about 20%, and stayed there at higher pH's. For galena, its recovery dropped from 91% in the absence of chitosan to 80% in the presence of 0.67 mg/L chitosan at pH 3. Between pH 3 and 5 and in the presence of chitosan, galena recovery dropped from 80% to about 40% and stayed there at higher pH's. The recoveries of both chalcopyrite and galena decreased sharply in the pH range of 3 to 5, which was consistent with the reported results on the adsorption behavior of the metal ions on chitosan as a function of pH (Chu, 2002; Kasgöz et al., 2003; Saucedo et al., 1992; Wan Ngah et al., 2002; Wu et al., 1999). In alkaline solutions, chitosan was not soluble and probably aggregated with the mineral

particles, causing their depression. It is interesting to note that at pH higher than 4.5, galena exhibited higher flotation recovery than chalcopyrite in the presence of 0.67 mg/L chitosan. However, the difference in the recovery was not sufficient for chitosan to be used as a selective depressant in the separation of chalcopyrite and galena. Therefore, it would appear that chitosan would not be a selective depressant in the Cu-Pb separation.

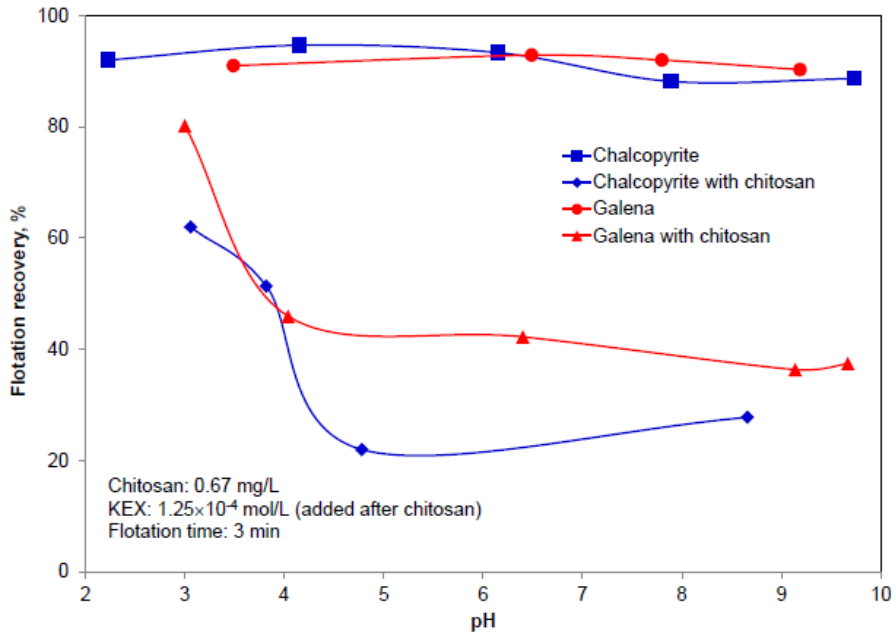

Figure 2.2 Flotation of single minerals of chalcopyrite and galena as a function of pH in the presence and absence of chitosan as a depressant. (KEX: 1.25×10^{-4} mol/L; Chitosan: 0.67 mg/L; Condition time: 3 min; Flotation time: 3 min)

2.3.2 Flotation of chalcopyrite-galena mixtures

Although the single mineral flotation tests in the presence of chitosan did not show any separation window, the flotation tests conducted on the artificial mixtures of chalcopyrite and galena (weight ratio 1:1) did prove the possibility of using chitosan as a selective depressant in the Cu-Pb separation. Figure 2.3a shows the metal grade in the flotation concentrate and Figure 2.3b shows the chalcopyrite and galena recovery in the concentrate floated from the mixtures. The metal grade of the artificial mixtures before flotation is also shown in Figure 2.3a for comparison. As can be seen, galena was separated from chalcopyrite in acidic solutions lower than pH 5 with an optimum separation at pH around 4, where galena was floated and chalcopyrite was depressed. It was interesting to note that the floatability of chalcopyrite and galena in the mineral mixtures was not the same as in single mineral flotation tests. At around pH 4, the flotation recovery of galena in the chalcopyrite-galena mineral mixtures was high at 95% while when it was floated alone its recovery was only 46%. At the same time, at around pH 4, the recovery of chalcopyrite was 20% when it was floated alone, but it was 30% in the mineral mixture flotation tests. This indicated that competitive adsorption of chitosan occurred on the sulfide minerals, with chalcopyrite adsorbing more chitosan than galena.

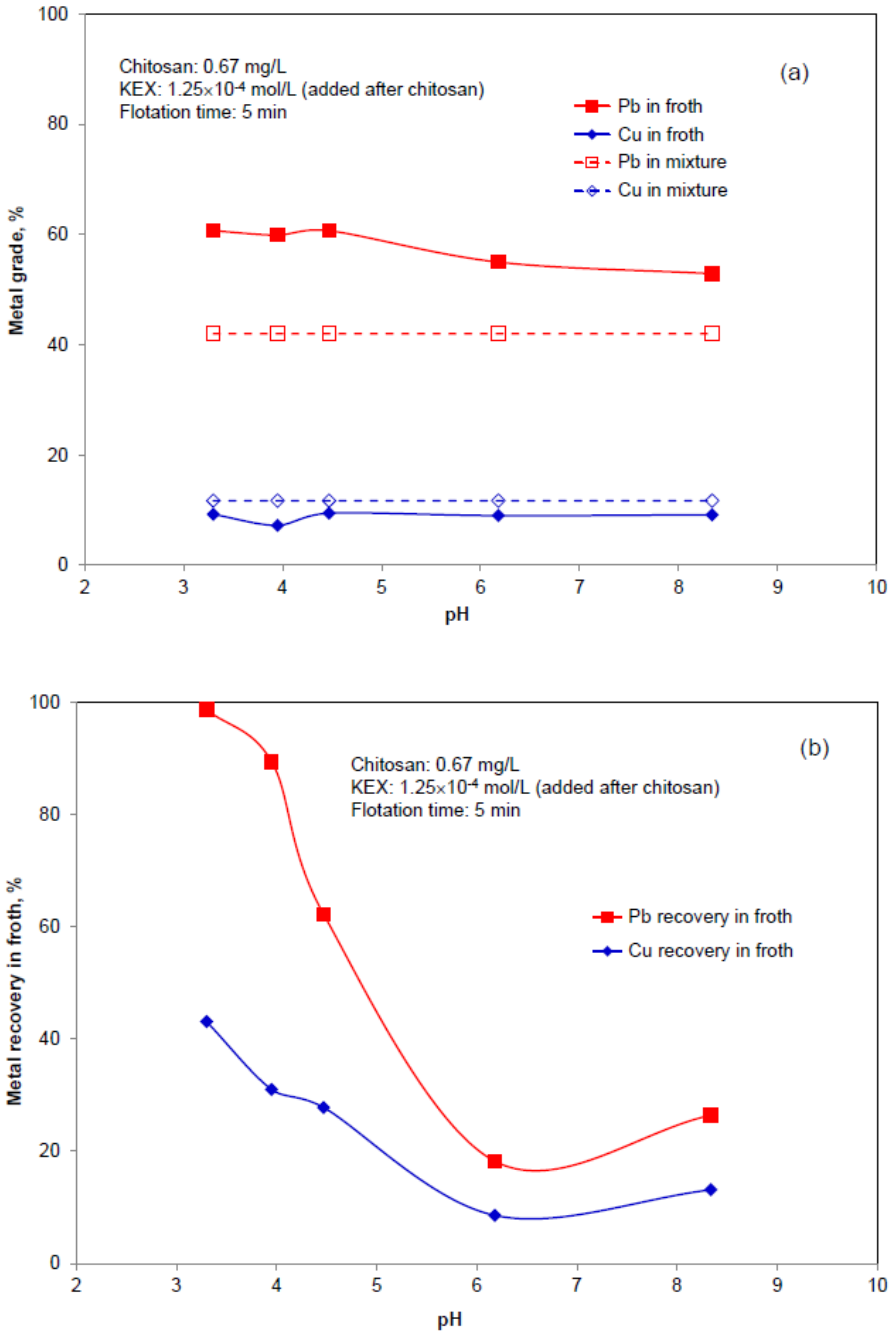

Figure 2.3 Flotation of mixtures of chalcopyrite and galena (weight ratio 1:1) as a function of pH. (a). Metal grade in froth products; (b). Metal recovery in froth products. (KEX: 1.25×10^{-4} mol/L; Chitosan: 0.67 mg/L; Condition time: 3 min; Flotation time: 3 min)

As the mineral mixture was prepared at 1:1 weight ratio, and because the specific surface areas of the -75+38 μm chalcopyrite and galena were 0.38 m^2/g and 0.15 m^2/g, respectively, it may be perceived that the reason that chalcopyrite adsorbed more chitosan was due to its larger surface area. However, flotation tests on mineral mixtures in which the chalcopyrite and galena were mixed at different ratios (Figure 2.4) showed that this was not the case. At a chalcopyrite:galena weight ratio of 0.5:1, the total surface area of chalcopyrite was about the same as that of galena. However, Figure 2.4b shows that the flotation recovery of chalcopyrite was about 40% while that of galena was over 80%. In fact, as can be seen from Figure 2.4a, after flotation separation, the lead content in the concentrate increased while that of copper decreased at all chalcopyrite:galena weight ratios tested (from 0.25 to 2). The results indicated that chitosan preferentially adsorbed on chalcopyrite surface when both chalcopyrite and galena were present in the suspension, and it could be used as a potential depressant to selectively separate galena from chalcopyrite in acidic suspensions.

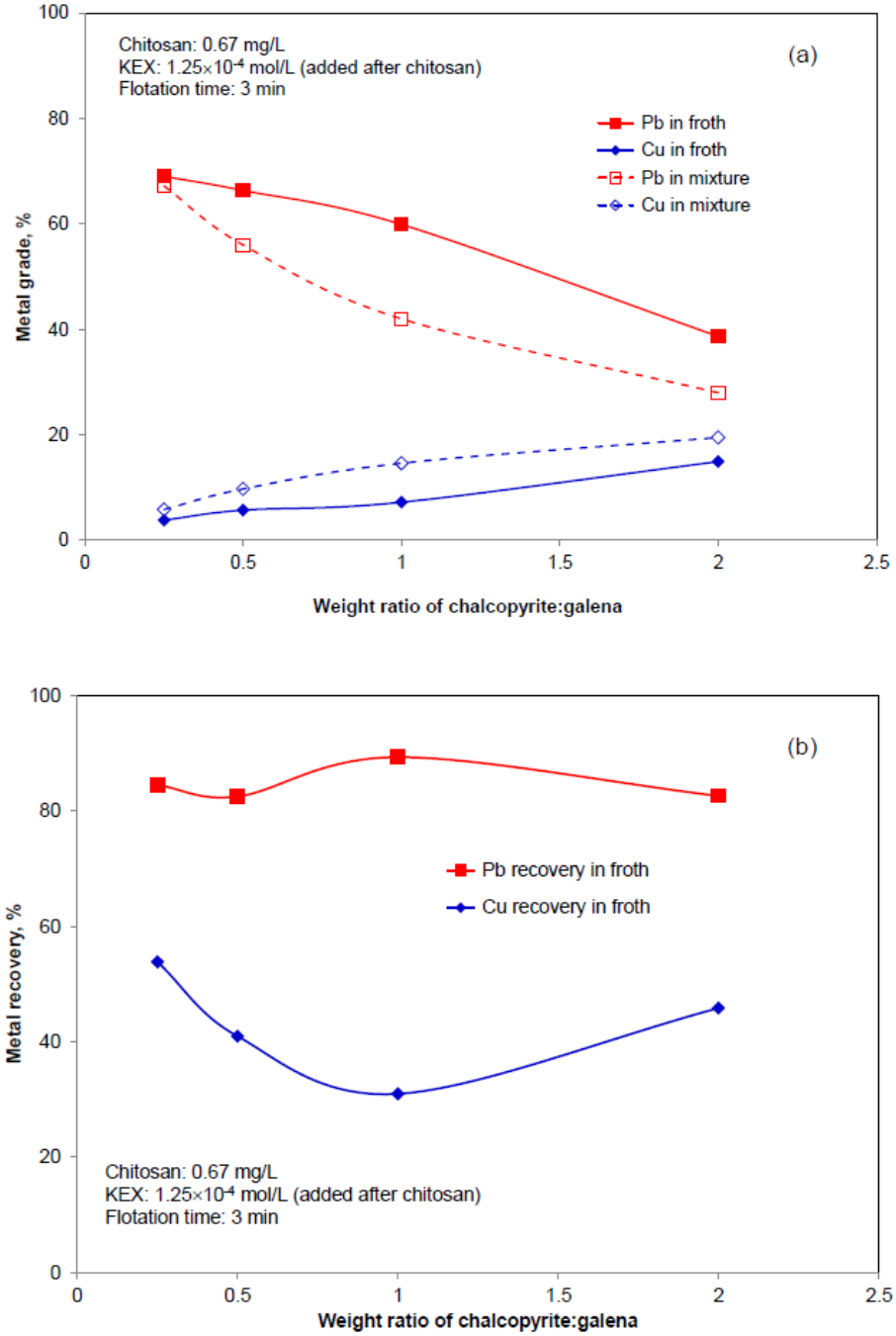

Figure 2.4 Flotation of mixtures of chalcopyrite and galena as a function of the weight ratio of chalcopyrite to galena. (a). Metal grade in froth products; (b). Metal recovery in froth products. (pH = 4; KEX: 1.25 × 10^{-4} mol/L; Chitosan: 0.67 g/L; Condition time: 3 min)

2.3.3 Adsorption of metal ions on chitosan

Metal ion adsorption on solid chitosan has been used as a way to assess the affinity of chitosan to different metal ions (Genç et al., 2003; González-Dávila et al., 1990; Ng et al., 2002; Wan Ngah et al., 2002; Wu et al., 2000, 2001). To study the observed competitive adsorption of chitosan in chalcopyrite and galena mixed mineral flotation, chitosan was used to adsorb Cu^{2+} and Pb^{2+} ions in acidic solutions where either a single metal ion or a mixture of both Cu^{2+} and Pb^{2+} ions were used. Figure 2.5a shows the adsorption isotherm (type I adsorption isotherm) of Cu^{2+} or Pb^{2+} ions on chitosan. As can be seen, Cu^{2+} and Pb^{2+} ions can both adsorb on chitosan. At low equilibrium concentrations, the adsorption density of Cu^{2+} ions on chitosan was slightly higher than that of Pb^{2+} ions. The adsorption data was consistent with the single mineral flotation results, where chalcopyrite was found to be depressed more severely than galena by chitosan, leading to its lower recovery.

Figure 2.5b shows the adsorption isotherms of Cu^{2+} and Pb^{2+} ions on chitosan when both metal ions were present in the solution. The curves typically fit type II adsorption isotherm. A significant adsorption density difference between Cu^{2+} and Pb^{2+} ions was observed when the equilibrium concentration C_e was over 1 mmol/L. Although the concentrations of chitosan used in the flotation tests were much lower than 1 mmol/L, the results indicated the higher affinities of chitosan to Cu^{2+} ions. In fact, by comparing the adsorption density at the same equilibrium concentration in Figure 2.5a and Figure 2.5b, it can be seen that the adsorption density of Cu^{2+} from Cu^{2+}-Pb^{2+} mixture was significantly higher than that from Cu^{2+}-only solution.

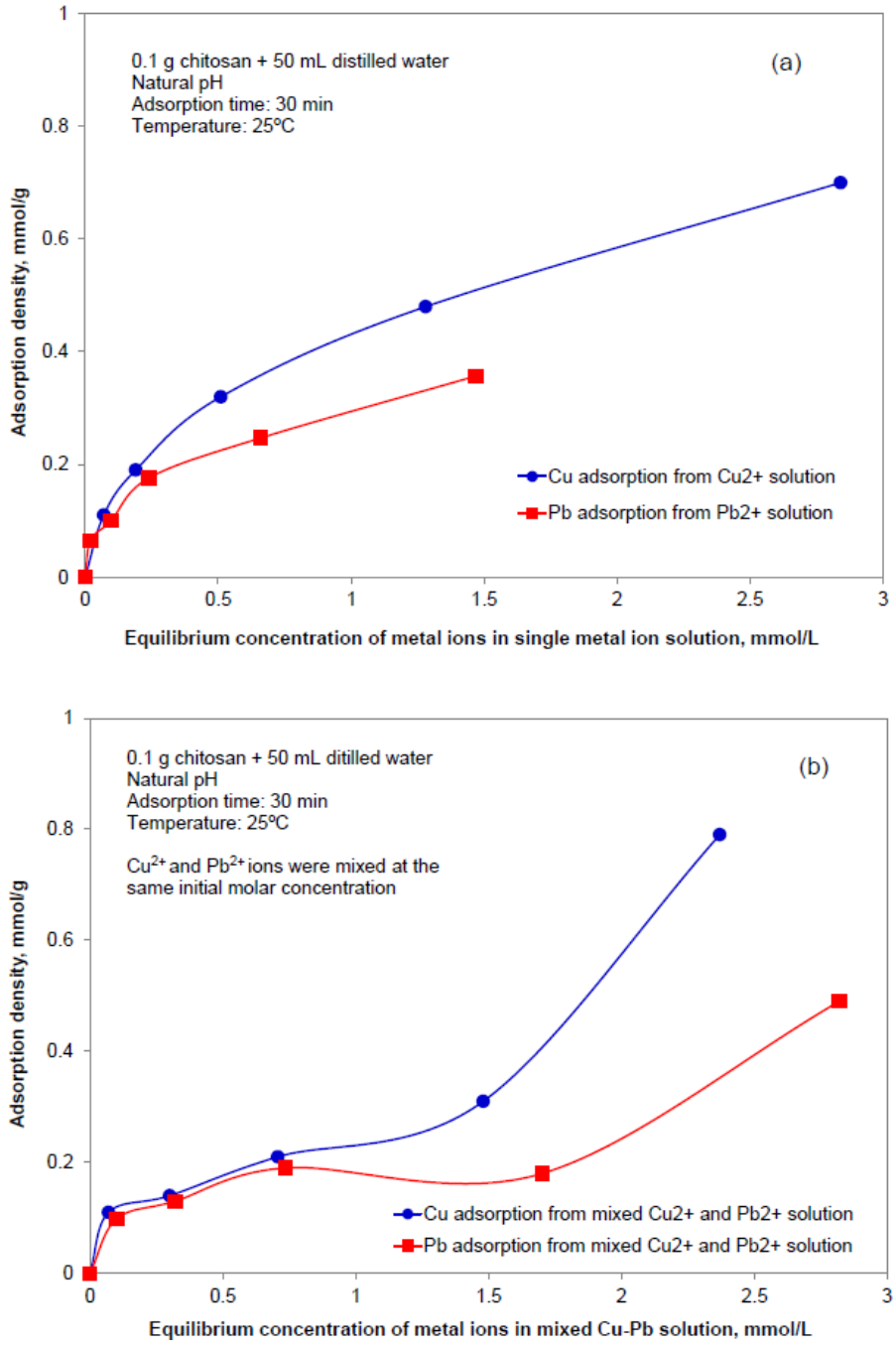

Figure 2.5 Adsorption density of metal ions on chitosan as a function of the equilibrium concentration of metal ions in aqueous solution. Initial solution including: (a). Cu^{2+} or Pb^{2+}; (b). Cu^{2+} and Pb^{2+}.

2.3.4 ToF-SIMS images of chalcopyrite-galena mixtures treated with chitosan

ToF-SIMS was employed to determine metal ion and chitosan distribution on the mineral surface, to illustrate the selective adsorption of chitosan on chalcopyrite and galena surfaces. On the surface of the mixture of chalcopyrite and galena after treatment with chitosan, the positive ion of Cu^+ selected by the identified mass from the spectra was used to represent the chalcopyrite distribution since chalcopyrite was the only source of Cu^+. Similarly, the positive ion of Pb^+ was used to determine the distribution of galena in the mixture. The fragment of $C_6H_{11}O_4N^+$, as the monomeric unit of chitosan, was used to detect the distribution of chitosan on the mineral mixture surface. Figures 2.6a, b and c show the distribution of chalcopyrite, galena, and chitosan in the mineral mixture on a sample area of 64 μm × 64 μm. Figures 2.6a and b show that chalcopyrite and galena had similar particle sizes (~20 μm) and complemented to each other on the sampled area. Figure 2.6c shows the distribution of chitosan. Due to the low dosage of chitosan in the solution, the intensity of chitosan was lower than those of chalcopyrite and galena. However, the distribution of chitosan can still be observed in the image. By comparing these three images, it can be seen that chitosan distribution matches exactly with the pattern of chalcopyrite distribution, indicating that the added chitosan has mostly adsorbed on chalcopyrite with very little on galena, i.e., its adsorption was selective.

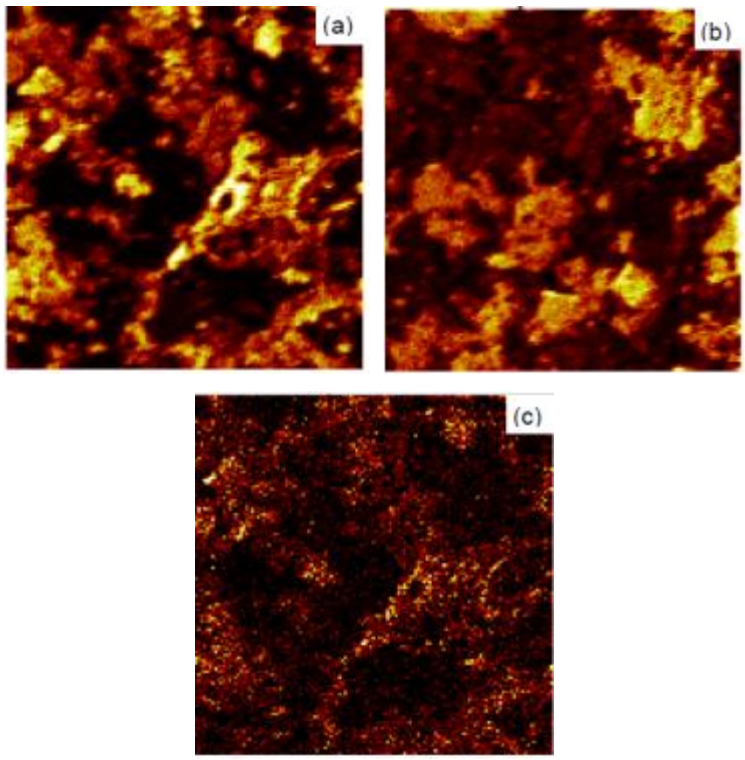

Figure 2.6 Positive-ion images of 64 μm × 64 μm region of the surface of a mixture of chalcopyrite and galena (weight ratio 1:1) after chitosan (0.3 mg) adsorption. (a) image of chalcopyrite (Cu^+); (b) image of galena (Pb^+); (c) image of chitosan ($C_6H_{11}O_4N^+$).

2.3.5 N 1s binding energy spectra of the sulfide minerals after treatment with chitosan

X-ray photoelectron spectroscopic (XPS) technique was employed to provide an understanding of the selective adsorption of chitosan on chalcopyrite from the chalcopyrite-galena mixtures. The XPS survey scan and the narrow scan of N 1s spectra were first performed on chitosan. The observed N 1s binding energies shifted slightly from literature data (Amaral et al., 2005; Dambies et al., 2000; Lawrie et al., 2007), probably caused by charging effect. As the typical calibration bands representing carbon and oxygen were linked to other components, making them difficult to distinguish, the N 1s (BE = 399.5 eV) component was used as an

internal standard to correct the shift. After calibration, the resolved N 1s spectra of chitosan are shown in Figure 2.7a. As can be seen, three peaks were required to fit the curve. The peak at 399.5 eV (Amaral et al., 2005; Lawrie et al., 2007) originates from $-NH_2$ (amine) in the basic structural unit of chitosan and this peak is used to calibrate the entire XPS spectrum. The peak at 400.5 eV (Lawrie et al., 2007) is caused by O=C-NH- (amide) which is from the original chitin. The third peak at 401.9 eV corresponds to protonated amine (ammonium).

The XPS survey scans were also performed on chalcopyrite and galena, with narrow scans of N 1s spectra performed on both minerals after chitosan treatment. The N 1s spectra are shown in Figure 2.7b and Figure 2.7c, respectively. Two peaks originating from Cu $2p^{3/2}$ at 932.0 eV on the chalcopyrite spectrum (not shown) and Pb $4f^{7/2}$ at 137.5 eV on the galena spectrum (not shown) were used to calibrate the entire XPS spectrum of chalcopyrite and galena, respectively. No peak corresponding to N species was found near 400 eV, which is the binding energy of N 1s (Amaral et al., 2005; Dambies et al., 2000; Lawrie et al., 2007; Ramanathan et al., 2005), during the XPS survey scan of chalcopyrite and galena before chitosan treatment. However, the N 1s peaks were observed from the XPS survey scans on both chalcopyrite and galena after chitosan adsorption, suggesting the presence of chitosan on the mineral surfaces. In order to identify the species of nitrogen on the mineral surfaces, narrow scans of N 1s were carried out, the spectra deconvoluted, and the results shown in Figures 2.7b and c. On the N 1s spectrum on galena (Figure 2.7c), the peaks at 399.4 eV and 400.5 eV are attributed to amine and amide groups, respectively, while no peak corresponding to ammonium was observed. For chalcopyrite (Figure 2.7b), all the three species with their binding energy peaks at 399.6 eV, 400.9 eV and 401.5 eV were detected. It is observed that the binding energy shifts of amine (-0.1 eV) and amide (0.0 eV) on galena are very small, compared to the obvious binding energy shifts of amide (+0.4 eV) and the appearance of ammonium (401.5 eV) on chalcopyrite. The relatively large binding energy shifts of amide and the existence of ammonium on chalcopyrite suggests a chemical adsorption mechanism of

chitosan on chalcopyrite. Therefore, the adsorption of chitosan on chalcopyrite is likely through chelation and the formation of chitosan-metal ion complexes that were described by Boddu et al. (2003), Burke et al. (2002), Gerente et al. (2007), Lasko and Hurst (1999), Ngah et al. (2010), Nomanbhay and Palanisamy (2005), and Onsosyen and Skaugrud (1990).

The positions of the N 1s binding energies and the relative intensities (RI) of the peaks on galena and chalcopyrite are summarized in Table 2.1. As can be seen, the total percentage of amine ($–NH_2$) and ammonium ($–NH_3^+$) was 85.7%, indicating that the degree of deacetylation of the chitosan was 85.7%. Correspondingly the chitosan contained about 14.3% amide groups (from the original chitin). However, Table 2.1 shows that 69% of the nitrogen species adsorbed on galena surfaces were amide and only 31% were amine, indicating that most of the species adsorbed on galena surfaces were in fact un-deacetylated chitin instead of chitosan. On the other hand, only 23% of the nitrogen species adsorbed on chalcopyrite was amide groups, and the remaining 77% were chitosan. It seems that chitin adsorbed more strongly on galena while chitosan adsorbed more strongly on chalcopyrite. This will be further illustrated in the next chapter.

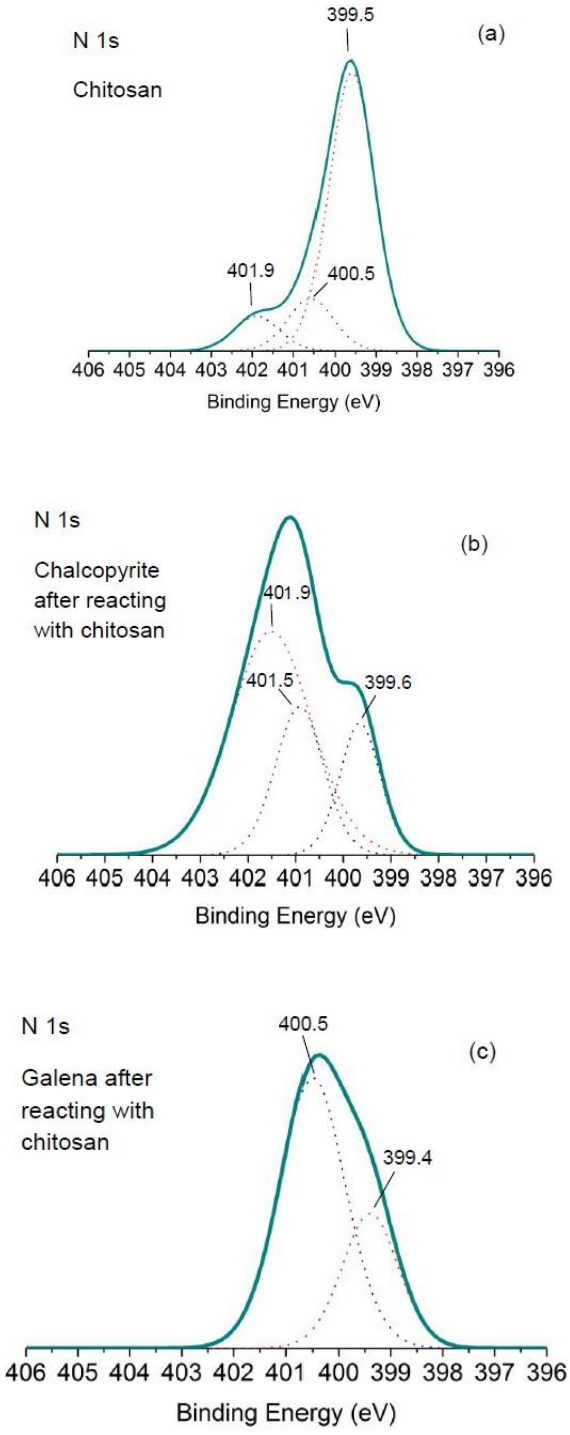

Figure 2.7 N 1s spectra of (a) chitosan, (b) chalcopyrite and (c) galena after chitosan adsorption.

Table 2.1 Binding energy (eV) for N 1s peaks of chitosan, galena and chalcopyrite

Species	Chitosan*	Galena-chitosan[#]		Chalcopyrite-chitosan[&]	
	BE (eV)	BE (eV)	RI (%)	BE (eV)	RI (%)
Amine (-NH_2)	399.5	399.4	30.96	399.6	17.33
Amide (-NH-C=O)	400.5	400.5	69.04	400.9	23.48
Ammonium (protonated –NH_2)	401.9			401.5	59.19

* Chitosan spectra calibrated by N 1s 399.5 eV.
[#] Galena spectra calibrated by Pb 4f 137.5 eV.
[&] Chalcopyrite spectra calibrated by Cu 2p 932.0 eV.

2.4 Conclusions

Chitosan, a naturally occurring polymer, was exploited in the differential flotation separation of Cu-Pb sulfide minerals (chalcopyrite and galena). In single mineral flotation of chalcopyrite and galena, both minerals were depressed by chitosan without any noteworthy difference. However, in the flotation of mixed mineral systems of chalcopyrite and galena (at different weight ratio), galena was floatable while chalcopyrite was depressed by chitosan in acidic solution between pH 3 and 5. The best results were observed at pH 4, where the recovery of galena was as high as 95% while chalcopyrite was depressed with low recovery (30%).

Measurement of the adsorption density of Cu^{2+} and Pb^{2+} ions on solid chitosan, from both single ionic solutions and mixed ionic (Cu^{2+} and Pb^{2+}) solutions, showed that Cu^{2+} ions had higher affinity to chitosan than Pb^{2+} ions. ToF-SIMS images taken from mixed mineral systems after chitosan treatment clearly showed that chitosan mainly adsorbed on chalcopyrite surface and not on galena.

The XPS spectra of N 1s electrons in chitosan before and after reacting with chalcopyrite and galena were measured and analyzed. Deconvolution of the N 1s spectra of chitosan showed three nitrogen-bearing groups in chitosan, amine (-NH_2), ammonium (-NH_3^+), and amide (O=C-NH-). The amide group was originated from the un-deacetylated chitin. Integrated areas of the peaks showed that while the chitosan contained about 14.3% amide groups (i.e., a degree of deacetylation of 85.7%), the chitosan adsorbed on galena contained 69% amide groups, and the chitosan adsorbed on chalcopyrite contained only 23% amide groups. The results indicated that chitosan adsorbed more strongly on chalcopyrite, while the undeacetylated chitin may have adsorbed more strongly on galena.

As an abundant natural polymer that is nontoxic and biodegradable, chitosan (and chitin) may potentially be used as a selective depressant to replace the conventional toxic inorganic depressants in Cu-Pb sulfide mineral separation.

2.5 References

Amaral, I., Granja, P. and Barbosa, M., 2005. Chemical modification of chitosan by phosphorylation: an XPS, FT-IR and SEM study. Journal of Biomaterials Science, Polymer Edition, 16(12): 1575-1593.

Bassi, R., Prasher, S.O. and Simpson, B., 2000. Removal of selected metal ions from aqueous solutions using chitosan flakes. Separation Science and Technology, 35(4): 547-560.

Blair, H.S. and Ho, T.C., 1981. Studies in the adsorption and diffusion of ions in chitosan. Journal of Chemical Technology and Biotechnology, 31(1): 6-10.

Boddu, V.M., Abburi, K., Talbott, J.L. and Smith, E.D., 2003. Removal of hexavalent chromium from wastewater using a new composite chitosan biosorbent. Environmental science & technology, 37(19): 4449-4456.

Burke, A., Yilmaz, E., Hasirci, N. and Yilmaz, O., 2002. Iron (III) ion removal from solution through adsorption on chitosan. Journal of applied polymer science, 84(6): 1185-1192.

Cao, M. and Liu, Q., 2006. Reexamining the functions of zinc sulfate as a selective depressant in differential sulfide flotation--The role of coagulation. Journal of colloid and interface science, 301(2): 523-531.

Choy, K.K.H., Porter, J.F. and Mckay, G., 2001. A film-pore-surface diffusion model for the adsorption of acid dyes on activated carbon. Adsorption, 7(3): 231-247.

Chu, K.H., 2002. Removal of copper from aqueous solution by chitosan in prawn shell: adsorption equilibrium and kinetics. Journal of hazardous materials, 90(1): 77-95.

Chung, Y.S., Lee, K.K. and Kim, J.W., 1998. Durable press and antimicrobial finishing of cotton fabrics with a citric acid and chitosan treatment. Textile research journal, 68(10): 772.

Crini, G. and Badot, P.M., 2008. Application of chitosan, a natural aminopolysaccharide, for dye removal from aqueous solutions by adsorption processes using batch studies: A review of recent literature. Progress in Polymer Science, 33(4): 399-447.

Dambies, L., Guimon, C., Yiacoumi, S. and Guibal, E., 2000. Characterization of metal ion interactions with chitosan by X-ray photoelectron spectroscopy. Colloids and Surfaces A: Physicochemical and Engineering Aspects, 177(2-3): 203-214.

Deans, J.R. and Dixon, B.G., 1992. Uptake of Pb2+ and Cu2+ by novel biopolymers. Water Research, 26(4): 469-472.

Domard, A., 1987. pH and cd measurements on a fully deacetylated chitosan: application to Cu(II)--polymer interactions. International journal of biological macromolecules, 9(2): 98-104.

Egger, G., Cameron-Smith, D. and Stanton, R., 1999. The effectiveness of popular, non-prescription weight loss supplements. Med J Aust, 171(11-12): 604-8.

Findon, A., McKay, G. and Blair, H.S., 1993. Transport studies for the sorption of copper ions by chitosan. Journal of Environmental Science & Health Part A, 28(1): 173-185.

Foster, L.S., 1928. Preparation of xanthates and other organic thiocarbonates. Utah Eng. Exp. Sta.

Genç Ö., Soysal, L., Bayramoglu, G., Arica, M. and Bektas, S., 2003. Procion Green H-4G immobilized poly (hydroxyethylmethacrylate/chitosan) composite membranes for heavy metal removal. Journal of hazardous materials, 97(1-3): 111-125.

Gerente, C., Lee, V., Cloirec, P.L. and McKay, G., 2007. Application of chitosan for the removal of metals from wastewaters by adsorption-mechanisms and models review. Critical reviews in environmental science and technology, 37(1): 41-127.

González-Dávila, M., Santana-Casiano, J.M. and Millero, F.J., 1990. The Adsorption of Cd (II) and Pb (II) to chitin in seawater. Journal of colloid and interface science, 137(1): 102-110.

González Siso, M. et al., 1997. Enzyme encapsulation on chitosan microbeads. Process Biochemistry, 32(3): 211-216.

Hirano, S., 1989. Production and application of chitin and chitosan in Japan. Elsevier, London, England, pp. 37-43.

Houshyar, S. and Amirshahi, S.H., 2002. Treatment of cotton with chitosan and its effect on dyeability with reactive dyes. Iranian Polymer Journal, 11: 295-302.

Ilium, L., 1998. Chitosan and its use as a pharmaceutical excipient. Pharmaceutical Research, 15(9): 1326-1331.

Jocić, D., Julia, M. and Erra, P., 1997. Application of a chitosan/nonionic surfactant mixture to wool assessed by dyeing with a reactive dye. Journal of the Society of Dyers and Colourists, 113(1): 25-31.

Kasgöz, H., Özgümüs, S. and Orbay, M., 2003. Modified polyacrylamide hydrogels and their application in removal of heavy metal ions. Polymer, 44(6): 1785-1793.

King, R., 1982. Principles of flotation. South African Institute of Mining and Metallurgy, Kelvin House, 2 Holland St, Johannesburg, South Africa, 1982. 268: 159-182.

Koide, S., 1998. Chitin-chitosan: properties, benefits and risks. Nutrition research, 18(6): 1091-1101.

Lasko, C.L. and Hurst, M.P., 1999. An investigation into the use of chitosan for the removal of soluble silver from industrial wastewater. Environmental science & technology, 33(20): 3622-3626.

Lawrie, G. et al., 2007. Interactions between alginate and chitosan biopolymers characterized using FTIR and XPS. Biomacromolecules, 8(8): 2533-2541.

Lerivrey, J. et al., 1986. Formation of D-glucosamine complexes with Cu (II), Ni (II) and Co (II) ions. Inorganica chimica acta, 125(4): 187-190.

Liu, Q. and Laskowski, J.S., 2006b. Adsorption of polysaccharide onminerals,In: Somasundaran, P. (Ed.), Encyclopedia of Surface and Colloid Science, Second Edition. Taylor & Francis, New York, pp. 649–668.

Loke, W.K., Lau, S.K., Yong, L.L., Khor, E. and Sum, C.K., 2000. Wound dressing with sustained anti-microbial capability. Journal of biomedical materials research, 53(1): 8-17.

Martino, A., Pifferi, P. and Spagna, G., 1996. Immobilization of [beta]-glucosidase from a commercial preparation. Part 2. Optimization of the immobilization process on chitosan. Process Biochemistry, 31(3): 287-293.

Monteiro, O.A.C. and Airoldi, C., 1999. Some thermodynamic data on copper-chitin and copper-chitosan biopolymer interactions. Journal of colloid and interface science, 212(2): 212-219.

Muzzarelli, R., 1989. Amphoteric derivatives of chitosan and their biological significance. Chitin and chitosan. New York: Elsevier Applied Science: 87–99.

Muzzarelli, R.A.A., 1973. Natural chelating polymers; alginic acid, chitin and chitosan. 144-176.

Ng, J., Cheung, W. and McKay, G., 2002. Equilibrium studies of the sorption of Cu (II) ions onto chitosan. Journal of colloid and interface science, 255(1): 64-74.

Ngah, W., Teong, L. and Hanafiah, M., 2010. Adsorption of dyes and heavy metal ions by chitosan composites: A review. Carbohydrate Polymers: 1446-1456.

Nomanbhay, S.M. and Palanisamy, K., 2005. Removal of heavy metal from industrial wastewater using chitosan coated oil palm shell charcoal. Electronic Journal of Biotechnology, 8(1): 43-53.

Onsosyen, E. and Skaugrud, O., 1990. Metal recovery using chitosan. Journal of Chemical Technology & Biotechnology, 49(4): 395-404.

Ramanathan, T., Fisher, F., Ruoff, R. and Brinson, L., 2005. Amino-functionalized carbon nanotubes for binding to polymers and biological systems. Chemistry of materials, 17(6): 1290-1295.

Ravi Kumar, M.N.V., 2000. A review of chitin and chitosan applications. Reactive and functional polymers, 46(1): 1-27.

Rhazi, M. et al., 2002. Contribution to the study of the complexation of copper by chitosan and oligomers. Polymer, 43(4): 1267-1276.

Saucedo, I., Guibal, E., Roulph, C. and Le Cloirec, P., 1992. Sorption of uranyl ions by a modified chitosan: kinetic and equilibrium studies. Environmental technology, 13(12): 1101-1115.

Schlick, S., 1986. Binding sites of copper2+ in chitin and chitosan. An electron spin resonance study. Macromolecules, 19(1): 192-195.

Se-Kwon, K., 2010. Chitin, Chitosan, Oligosaccharides and Their Derivatives : Biological Activities and Applications. 117-118.

Shin, Y. and Yoo, D.I., 1998. Use of chitosan to improve dyeability of DP-finished cotton (II). Journal of applied polymer science, 67(9): 1515-1521.

Srinivasa, P., Baskaran, R., Ramesh, M., Harish Prashanth, K. and Tharanathan, R., 2002. Storage studies of mango packed using biodegradable chitosan film. European Food Research and Technology, 215(6): 504-508.

Struszczyk, H., 1987. Microcrystalline chitosan. I. Preparation and properties of microcrystalline chitosan. Journal of applied polymer science, 33(1): 177-189.

Struszczyk, M., 2002. Chitin and chitosan—Part II. Applications of chitosan. Polimery, 47(6): 396-403.

Teixeira, M.A. et al., 1990. Assessment of chitosan gels for the controlled release of agrochemicals. Industrial & engineering chemistry research, 29(7): 1205-1209.

Wan Ngah, W., Endud, C. and Mayanar, R., 2002. Removal of copper (II) ions from aqueous solution onto chitosan and cross-linked chitosan beads. Reactive and functional polymers, 50(2): 181-190.

Wang, L., Khor, E., Wee, A. and Lim, L.Y., 2002. Chitosan-alginate PEC membrane as a wound dressing: Assessment of incisional wound healing. Journal of biomedical materials research, 63(5): 610-618.

Wu, F.C., Tseng, R.L. and Juang, R.S., 1999. Role of pH in metal adsorption from aqueous solutions containing chelating agents on chitosan. Industrial & engineering chemistry research, 38(1): 270-275.

Wu, F.C., Tseng, R.L. and Juang, R.S., 2000. Comparative adsorption of metal and dye on flake-and bead-types of chitosans prepared from fishery wastes. Journal of hazardous materials, 73(1): 63-75.

Wu, F.C., Tseng, R.L. and Juang, R.S., 2001. Kinetic modeling of liquid-phase adsorption of reactive dyes and metal ions on chitosan. Water Research, 35(3): 613-618.

Wu, T., Zivanovic, S., Draughon, F.A. and Sams, C.E., 2004. Chitin and Chitosan Value-Added Products from Mushroom Waste. Journal of agricultural and food chemistry, 52(26): 7905-7910.

Yen, M.T. and Mau, J.L., 2007a. Physico-chemical characterization of fungal chitosan from shiitake stipes. LWT-Food Science and Technology, 40(3): 472-479.

Yen, M.T. and Mau, J.L., 2007b. Selected physical properties of chitin prepared from shiitake stipes. LWT-Food Science and Technology, 40(3): 558-563.

Zhang, M., Haga, A., Sekiguchi, H. and Hirano, S., 2000. Structure of insect chitin isolated from beetle larva cuticle and silkworm (Bombyx mori) pupa exuvia. International journal of biological macromolecules, 27(1): 99-105.

CHAPTER 3

ADSORPTION MECHANISMS OF CHITOSAN ON CHALCOPYRITE AND GALENA IN AQUEOUS SUSPENSIONS*

3.1 Introduction

As shown in the previous chapter, chitosan, a naturally occurring, biodegradable, and non-toxic polyaminosaccharide (Ngah et al., 2010), was found to be a selective depressant in the differential flotation separation of Cu-Pb sulfides. With the addition of chitosan in a weakly acidic suspension, galena was floated by xanthate while chalcopyrite was depressed. However, in single mineral flotation of chalcopyrite or galena, both minerals were depressed albeit to different degrees. The observed flotation selectivity was attributed to the competitive adsorption of chitosan on chalcopyrite in preference to galena, although the mechanisms of such competitive adsorption were unclear.

The main component of chitosan is a linear structure of β-(1-4)-linked D-glucosamine, partially deacetylated from the β-(1-4)-linked N-acetyl-D-glucosamine, the basic structure unit of chitin. The chemical structures of chitosan and chitin were shown in Figure 3.1 (Gerente et al., 2007). Due to the outstanding properties such as biodegradability, biocompatibility, non-toxicity and strong metal ion chelation ability (Ngah et al., 2010; Se-Kwon, 2010), chitosan and its derivatives attracted considerable interest by researchers in the past several decades. Today, chitosan has been studied and applied in a wide range of industrial sectors, such as environmental engineering (Boddu et al., 2003; Burke et al., 2002; Choy et al., 2001; Chung et al., 1998; Jocić et al., 1997; Onsosyen

* This paper was published in Colloids and Surfaces A: Physicochemical and Engineering Aspects: P. Huang, M. Cao and Qi Liu, 2012. Adsorption of chitosan on chalcopyrite and galena in aqueous suspensions. Colloids and Surfaces A: Physicochemical and Engineering Aspects, Vol. 409, 167-175. http://dx.doi.org/10.1016/j.colsurfa.2012.06.016.

and Skaugrud, 1990; Ravi Kumar, 2000; Shin and Yoo, 1998), biomedicine (Kim and Rajapakse, 2005; Koide, 1998; Loke et al., 2000; Mourya and Inamdar, 2008; Struszczyk, 2002; Wang et al., 2002), healthcare (González Siso et al., 1997; Ilium, 1998; Martino et al., 1996; Muzzarelli, 1989), food industry (Aider, 2010; Crini and Badot, 2008; Egger et al., 1999; Gerente et al., 2007; Shahidi et al., 1999; Srinivasa et al., 2002; Teixeira et al., 1990), etc. Meanwhile, fundamental studies on chitosan have been moving along in support of the exploitations and the applications (Blair and Ho, 1981; Boddu et al., 2003; Burke et al., 2002; Domard, 1987; Gerente et al., 2007; Lasko and Hurst, 1999; Muzzarelli, 1977; Ngah et al., 2010; Nomanbhay and Palanisamy, 2005; Onsosyen and Skaugrud, 1990; Piron and Domard, 1998; Roberts et al., 1992; Schlick, 1986).

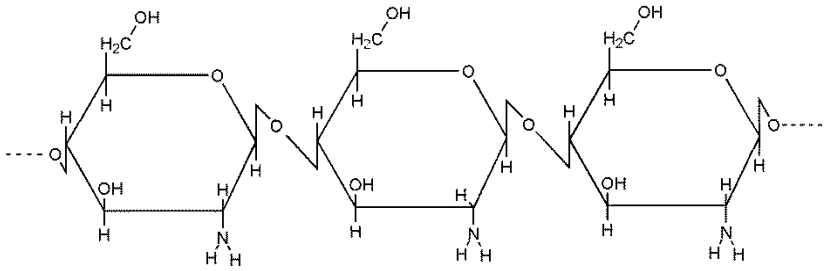

(a) chitosan

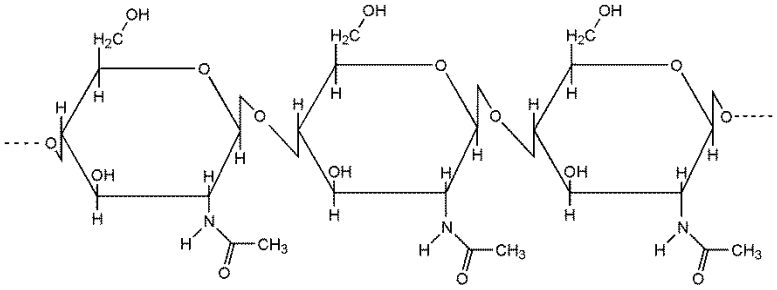

(b) chitin

Figure 3.1 Structures of chitosan and chitin (Gerente et al., 2007)

To fully explore chitosan's potential as a promising selective flotation depressant in the minerals industry for the differential flotation separation of Cu-Pb sulfides, one of the most widely used commercial copper and lead metal production

technologies, the interaction mechanism between chitosan and the minerals needs to be understood. It has been well-documented that chitosan binds with certain metal ions and forms metal-chitosan complex. The mechanism of complex formation is attributed to chelation (Boddu et al., 2003; Burke et al., 2002; Gerente et al., 2007; Lasko and Hurst, 1999; Muzzarelli, 1977; Ngah et al., 2010; Nomanbhay and Palanisamy, 2005; Onsosyen and Skaugrud, 1990). The amino groups (Chui et al., 1996; Stöhr et al., 2001; Vold et al., 2003), together with the hydroxyl groups (Deans and Dixon, 1992; Kamiński and Modrzejewska, 1997; Lerivrey et al., 1986; Monteiro and Airoldi, 1999; Sun and Wang, 2006; Wang et al., 2004), were considered as the major binding sites for the uptake of metal ions in aqueous solutions by chitosan.

Much work is ongoing aimed at delineating the mechanism of complex formation, but the conclusions on the formation of chitosan-metal complex is still contradictory. Different models were proposed concerning the structure of the complexes, including the bridge model (Blair and Ho, 1981; Schlick, 1986) and the pendant model (Domard, 1987; Piron and Domard, 1998; Roberts et al., 1992). The major differences for the formation models were the bonding structure of nitrogen atoms and metal ions in space.

Among the extensive investigation of chitosan as an absorbent, the growing literature show that the formation of chitosan-metal ion complexes can be affected by many parameters, such as the degree of deacetylation of chitosan (Guibal et al., 1999; Ishii et al., 1995; Kurita et al., 2003; Peter, 1995; Vold et al., 2003), solution pH (Guibal et al., 1994; Jha et al., 1988; Saucedo et al., 1993) and physical type of chitosan (Gerente et al., 2007; Hsien and Rorrer, 1997; Kawamura, 1991; Rorrer et al., 1993). These factors greatly influenced the adsorption capacity of chitosan and made the chelation mechanism of chitosan complicated. The degree of deacetylation is one of the key factors in the complex formation. The amino groups, as a result of deacetylation, bind with metal ions. Thus, chitosan with higher degrees of deacetylation has a stronger capacity to

chelate with metal ions. The degree of deacetylation has the potential influence on the effect of chitosan as a selective depressant in mineral flotation separation.

The aim of this study was to gain an understanding of the interaction mechanisms of chitosan with minerals in the differential flotation of Cu-Pb sulfides. Attenuated total reflection Fourier transform infrared spectroscopy (ATR-FTIR), time-of-flight secondary ion mass spectroscopy (ToF-SIMS), and X-ray photoelectron spectroscopy (XPS) were used to identify the bonds formed between chitosan and mineral surfaces, as well as the stable molecular fragments after ion bombardment of the mineral surfaces following chitosan adsorption.

3.2 Materials and Methods

3.2.1 Materials

Two chitosan samples were used in this study. Both had similar reported molecular weights (MW), ranging from 100,000 to 300,000. One chitosan (designated as CT) was obtained from Sigma-Aldrich Canada, which had a reported degree of deacetylation of 75%-85%. The other chitosan (designated as HCT), with a higher reported degree of deacetylation (>90%), was purchased from Acros Organics, USA. CT was used throughout this work, while HCT was only used in the flotation tests to compare its effectiveness with CT. Solutions of both chitosan samples were prepared by dissolving the chitosan in diluted hydrochloric acid (0.2 mol/L). Hydrochloric acid and sodium hydroxide were purchased from Fisher Scientific Canada and were used to adjust pH. Potassium ethyl xanthate (KEX, $CH_3CH_2OCS_2K$) courtesy of Prospec Chemicals Ltd, Canada, was used as a collector in the flotation tests. It was purified with ethyl ether anhydrous and acetone (Fisher Scientific, Canada) following the protocol of Foster (Foster, 1928) before using. Distilled water was used throughout the experimental work.

The copper and lead sulfide minerals (chalcopyrite, $CuFeS_2$, and galena, PbS) were purchased from Ward's Scientific Establishment, Ontario, Canada. X-ray diffraction spectra of the chalcopyrite and galena samples showed that they were of high purity with minor amounts of quartz in chalcopyrite and no impurities in galena. The chalcopyrite sample assayed 29.26% Cu, indicating a purity of 84% chalcopyrite, and galena assayed 84.00% Pb, representing a purity of 97% galena. The lumps of the chalcopyrite and galena were separately crushed (Retsch Jaw Crusher, USA) and pulverized (Fritsch Mortar Grinder Pulverisette 2, Germany) to a particle size of smaller than 75 μm, then dry screened to different size fractions. The sample powder larger than 38 μm but smaller than 75 μm (-75+38 μm) was used in the flotation tests, while the powder smaller than 20 μm (-20 μm) was used in ATR-FTIR, ToF-SIMS and XPS analyses. All mineral samples were sealed in plastic bottles and stored in a freezer at -10°C to minimize oxidation.

Quantachrome Autosorb 1MP (Quantachrome Instruments, USA) was used to determine the specific surface areas of both chalcopyrite and galena using the BET method. The specific surface area of the -75+38 μm chalcopyrite was 0.38 m^2/g, and that of the -20 μm chalcopyrite was 1.19 m^2/g. The specific surface area of the -75+38 μm galena was 0.15 m^2/g, and that of the -20 μm galena was 0.50 m^2/g.

3.2.2 ATR-FTIR measurements

Attenuated total reflectance Flourier transform infrared (ATR-FTIR) spectra were recorded by a Nicolet 8700 (Thermo, USA) FTIR spectrophotometer, using the Smart Speculator Collector for ATR. The number of scans for each spectrum was 64, with a resolution of 4 cm^{-1}. Zinc Selenide (ZnSe) with standard 45 degree angle of incidence was used as crystal material (internal reflection element) on a Spectra-tech A.R.K trough plate kit.

A 0.5 mL of a mineral-water mixture with mineral concentration of 0.1 g/L was added into the sample container to form a flat surface on top of the ZnSe substrate. A background spectroscopy collection was performed by setting both mineral surface and ZnSe substrate as the background before adding 0.5 mL chitosan (CT) solution (5 g/L) into the container to obtain the mineral-chitosan suspension at pH 4. The FTIR spectra of the samples were collected after 15 minutes following the addition of the chitosan solution.

3.2.3 ToF-SIMS measurements

ToF-SIMS measurements were conducted with a ToF-SIMS IV spectrometer (ION-TOF GmbH) using 25 keV Bi^+ primary ions. The area of each sample for spectra acquisition was 64 μm × 64 μm. The positive ion spectra, as a function of mass, were calibrated using the H^+, CH_3^+ and Na^+ peaks. Images were generated by mapping the mass-selected ion intensity in a burst alignment mode with 128 × 128 pixels per image.

The spectra of four samples were recorded, including two pure chitosan samples and two mineral samples, respectively. For the pure chitosan samples, one was chitosan (CT) powder as received while the other was prepared by dissolving chitosan (CT) in an acidic solution at pH 4 and dried in an oven at 50-60°C. The mineral samples were prepared by mixing chalcopyrite and galena at a weight ratio of 1:1 in 100 mL distilled water at pH 4, and adding 0.3 mg of chitosan. The suspension was conditioned in a shaking incubator for 30 min equilibrated at 25ºC, and the minerals were filtered, washed with 200 mL distilled water through the filtration funnel and dried in a desiccator under vacuum before analysis. To minimize oxidation, the ToF-SIMS analysis was conducted within 12 hours after mineral sample preparation.

3.2.4 XPS measurements

XPS analysis was carried out with an AXIS 165 X-ray photoelectron spectrometer (Kratos Analytical, USA) equipped with a monochromatic Al Kα X-ray source (hν = 1486.6 eV). The vacuum pressure inside the analytical chamber was below 3×10^{-8} Pa. For data acquisition, the survey scans and high-resolution scans were collected using analyzer pass energies of 160 eV and 20 eV, respectively. As the particle size of samples was -20 μm, the area of 400 μm × 700 μm on the sample surface was considered as representative analyzed area in the XPS analysis, while the overall information depth for the XPS analysis was approximately 10 nm. Therefore, the recorded spectra can provide information about the surfaces of the samples. Charge neutralization did not apply in the spectra collection. All the high-resolution spectra were processed by the CasaXPS Version 2.3.15 instrument software. To resolve binding energy peaks, individual Gaussian-Lorentzian peaks were employed after the Shirley-type background subtraction to optimize the high-resolution spectra. The processed spectra were imported and calibrated according to previously publish data by a graphic software package (Origin, OriginLab Corp) for displaying the optimized fitting peaks of the high-resolution spectra.

For sample preparation for the XPS analysis, 2 mg of chitosan (CT) was added in the mineral slurry of 1 g mineral (chalcopyrite or galena) mixed with 100 mL distilled water at pH 4. The mineral samples were filtered and washed with 200 mL distilled water after conditioning in an incubator at 25°C for 30 min. Afterwards, the sample was deposited to dehydrate in a desiccator in vacuum station before XPS analysis. All the XPS measurements were conducted within 12 hours after sample preparation to minimize oxidation.

3.2.5 Flotation and contact angle measurement

Froth flotation tests were performed in a modified small-scale flotation tube, the construction of which was described in detail by Cao and Liu (2006). This tube minimizes mechanical entrainment through the narrow throat that connects the

flotation tube to the collection bulb, which only allows one gas bubble to pass through at a time with attached particles. Particles that were not attached to the bubble were abraded off. For a typical test, 1.5 g of the -75+38 μm mineral powders (single mineral or mineral mixtures with weight ratio 1:1) were conditioned for 3 min in a 250-mL beaker with 150 mL distilled water at a specific pH adjusted by either hydrochloric acid or sodium hydroxide. The addition of an appropriate amount of chitosan and KEX were followed sequentially into the slurry and conditioned for 3 min each. The conditioned slurry was then transferred to the flotation tube and floated for 3 min using N_2 gas. The concentrate and tailings were dried and collected to calculate mineral recovery. Both the froth and tailings were dissolved with aqua regia, followed by the analysis of solutions using a Varian SpectrAA-220FS (Varian, USA) atomic absorption spectrometer (AAS). The recoveries of chalcopyrite and galena in the artificial mixture flotation were calculated through the concentrations of Cu and Pb in the flotation products determined by the AAS.

A Krüss drop shape analysis system (DSA 10-MK2, Germany) using a sessile drop method was applied to determine the contact angle of water on the surface of a 10 mm diameter pressed pellet of powdered mineral samples. The pellet was prepared from 0.2-0.4 g of fine mineral (-20 μm) under a pressure of 2500 psi (170 atm) (ICL International Crystal Laboratories, USA) for 5 minutes. A drop of distilled water was placed on the surface of the pressed pellet and a microscopic image of the drop and the pellet was taken immediately. The contact angle was determined by fitting an outline to the shape of the sessile drop on the microscopic image.

3.3 Results and Discussion

3.3.1 ATR-FTIR spectra of sulfide minerals after treatment with chitosan

The ATR-FTIR spectra of chitosan (CT), CT on galena surface and CT on chalcopyrite surface are presented in Figure 3.2 in the spectral range of 1700-1000 cm^{-1}. The spectrum of CT, with a degree of deacetylation of 85.6% (the value was verified by XPS, see following section), displayed the characteristic vibrations of the acetyl groups and the deacetylated amine groups. The acetyl groups of chitosan showed peaks at 1655 cm^{-1}, 1551 cm^{-1} and 1312 cm^{-1}, which were consistent with previous reports (Amaral et al., 2005; Muzzarelli, 1973a; Pearson et al., 1960). These peaks corresponded to amide I (C=O stretching), amide II (N–H in plane deformation) and amide III (C–N stretching) vibrations, respectively. The band at 1580 cm^{-1} was assigned to the N–H deformation vibration from amine, which was of relatively high absorbance intensity in the spectrum (Lawrie et al., 2007). Since chitosan protonation reaches equilibrium at pH 6.5 (Crini and Badot, 2008; Guibal, 2005; Sorlier et al., 2001), at pH 4, it was mostly the protonated amine ($–NH_3^+$) that was present in the CT solution. The band appearing at 1625 cm^{-1} was due to the asymmetric deformation vibration of the protonated amine. The symmetric $–NH_3^+$ deformation vibration at 1520 cm^{-1} was not observed in the spectrum, probably caused by overlapping with the strong peaks of N-H deformation vibrations of amide and amine.

The spectra of CT adsorbed on the two minerals are also shown in Figure 3.2. The increase in absorbance at 1559 cm^{-1}, corresponding to the peak of 1551 cm^{-1} of amide II of chitosan, was the result of the reaction between amide group of chitosan and the surfaces of both minerals. The peak due to protonated amine, at 1625 cm^{-1}, shifted to 1615 cm^{-1} upon adsorption on chalcopyrite but only showed up as an almost un-noticeable shoulder after adsorption on galena. It is therefore possible that only the amide II (N–H) group was involved in the interaction between chitosan and galena, while both the amide II (N–H) and the protonated amine groups were involved in the interaction between chitosan and chalcopyrite.

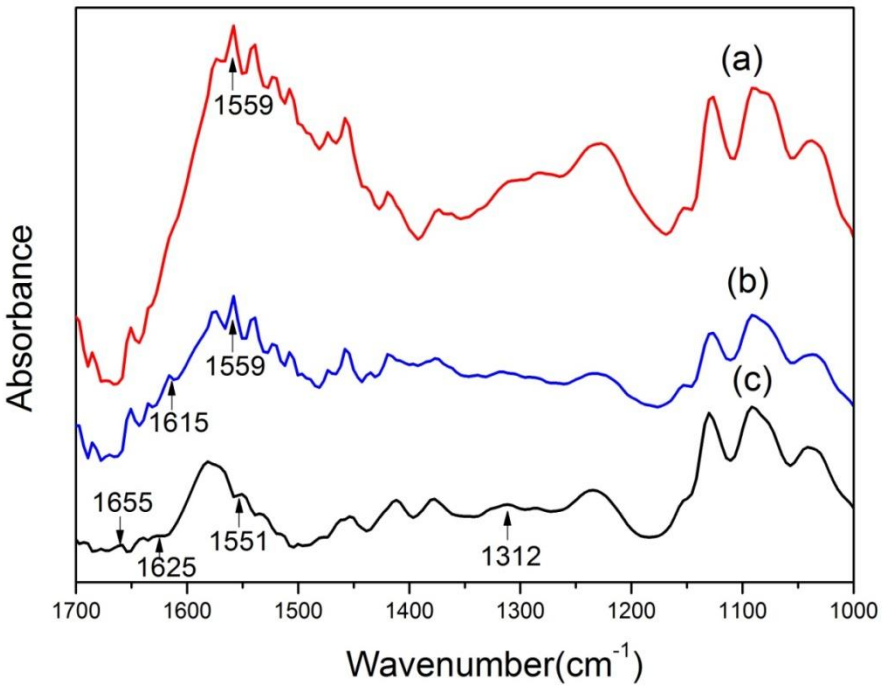

Figure 3.2 ATR-FTIR spectra of (a) chitosan on galena surface, (b) chitosan on chalcopyrite surface and (c) chitosan.

Table 3.1 FTIR bands of chitosan with assignments

Wavenumber (cm^{-1})	Assignment	References
1312	amide III (C–N stretching)	Amaral et al., 2005; Muzzarelli, 1973a; Pearson et al., 1960
1551	amide II (N–H in plane deformation)	Amaral et al., 2005; Muzzarelli, 1973a; Pearson et al., 1960
1580	N–H deformation vibration from amine	Lawrie et al., 2007
1625	protonated amine (NH_3^+)	Crini and Badot, 2008; Guibal, 2005; Sorlier et al., 2001
1655	amide I (C=O stretching)	Amaral et al., 2005; Muzzarelli, 1973a; Pearson et al., 1960

3.3.2 ToF-SIMS analyses of sulfide minerals after treatment with chitosan

Figure 3.3a and Figure 3.3b show the positive ion images of Cu^+ and Pb^+ from chalcopyrite-galena mixtures treated with chitosan. As chalcopyrite and galena were the only sources of Cu^+ and Pb^+, respectively, the positive ion distribution images were used to represent the chalcopyrite and galena minerals. The fragment of $C_6H_{11}O_4N^+$, as the monomer unit of chitosan, was identified and used to represent the distribution of chitosan (Figure 3.3c). The mineral distribution images (Figure 3.3a and Figure 3.3b) of the 64 μm × 64 μm surface region confirmed that the particle size of the chalcopyrite and galena samples were indeed about 20 μm. By comparing the images shown in Figure 3.3, it was obvious that Figure 3.3c (chitosan) had similar pattern as Figure 3.3a (chalcopyrite) but completely different from Figure 3.3b (galena). The areas rich in chalcopyrite (bright spots in Figure 3.3a) were also rich in chitosan (bright spots in Figure 3.3c). On the other hand, areas rich in galena (bright spots in Figure 3.3b) were devoid of chitosan (dark spots in Figure 3.3c). This indicates that chitosan selectively adsorbed on chalcopyrite but not on galena in the mineral mixtures.

The positive ion mass spectra of pure chitosan and chalcopyrite-galena mixtures treated with chitosan were acquired to identify the interaction species between chitosan and the minerals. Figure 3.4a and Figure 3.4b show the positive ion mass spectra of NH_2^+, NH_3^+ and NH_4^+ from both the original chitosan powder (CT) and the chitosan that had been dissolved in water and then dried. The spectra in Figure 3.4a was recorded from the chitosan as received without any treatment. It can be seen from Figure 3.4a that of the three ionic species (NH_2^+, NH_3^+ and NH_4^+), NH_3^+ had the highest intensity. However, it is known that $-NH_2$ is the original group in the chitosan and it should be dominant. The inconsistency was probably caused by cationization of $-NH_2$ groups during the ToF-SIMS measurements (Vickerman et al., 2001). Cationization led to the formation of NH_3^+ from NH_2. Figure 3.4b shows that when the chitosan was dissolved in water then dried for

ToF-SIMS analysis, the intensity of NH_4^+ was higher than the other two ionic species. As the *p*Ka for the protonation of chitosan is 6.5 (Crini and Badot, 2008; Guibal, 2005; Sorlier et al., 2001), NH_3^+ should be the dominant species for the chitosan at pH 4. Again, the observed dominance of NH_4^+ was likely due to the cationization effect of NH_3^+ during the ToF-SIMS measurements.

Part of the positive ion mass spectra of the CT-chalcopyrite-galena system at pH 4 is shown in Figure 3.4c. As can be seen, the intensity of NH_4^+ was much higher than NH_2^+ and NH_3^+, in agreement with the results shown in Figure 3.4b. By mapping NH_4^+, it was found that the NH_4^+ positive ion image (Figure 3.5a) had the same pattern as Figure 3.3a which was the distribution of chalcopyrite on the mineral mixture surface. For the metal-NH_x^+ species (x = 1-4), significant intensity difference was identified between $CuNH_4^+$ and $PbNH_4^+$, i.e., the intensity of $CuNH_4^+$ was much higher than that of $PbNH_4^+$, while the intensity of the rest fragments were low and similar. The images of $CuNH_4^+$ and $PbNH_4^+$ were shown in Figure 3.5b and Figure 3.5c, respectively. By comparing with the image of chalcopyrite distribution (Figure 3.3a), the same distribution of $CuNH_4^+$ and chalcopyrite were identified, indicating that $CuNH_4^+$ was the dominant species which originated from the interaction of chitosan with the mixture of chalcopyrite and galena during the ToF-SIMS measurements. In fact, $CuNH_4^+$ was probably the result of cationization of $CuNH_3^+$. The dominance of the $CuNH_4^+$ species during ToF-SIMS measurements indicates the high stability of the Cu-NH_3 bonds and the strong interaction between NH_3^+ and surface Cu on chalcopyrite, which was the reason for the selective adsorption of chitosan on chalcopyrite in chalcopyrite-galena mixtures.

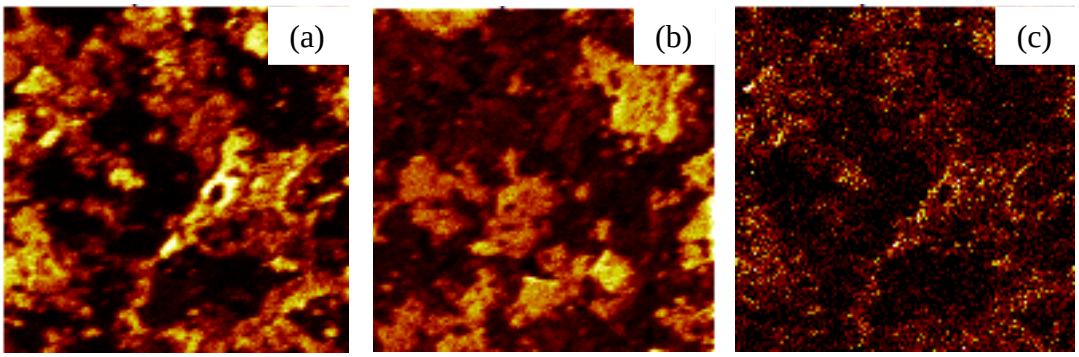

Figure 3.3 Positive-ion images of a 64 μm × 64 μm region from the surface of a mixture of chalcopyrite and galena (weight ratio 1:1) after chitosan adsorption. (a) image of Cu^+; (b) image of Pb^+; (c) image of $C_6H_{11}O_4N^+$.

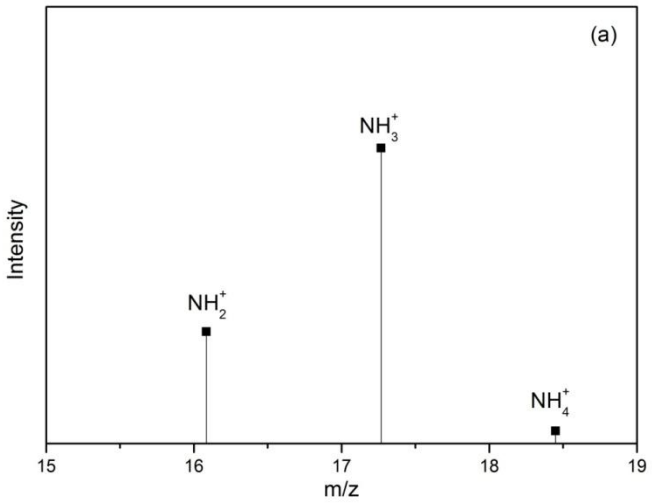
(a)
Intensity
NH_3^+
NH_2^+
NH_4^+
15
16
17
18
19
m/z

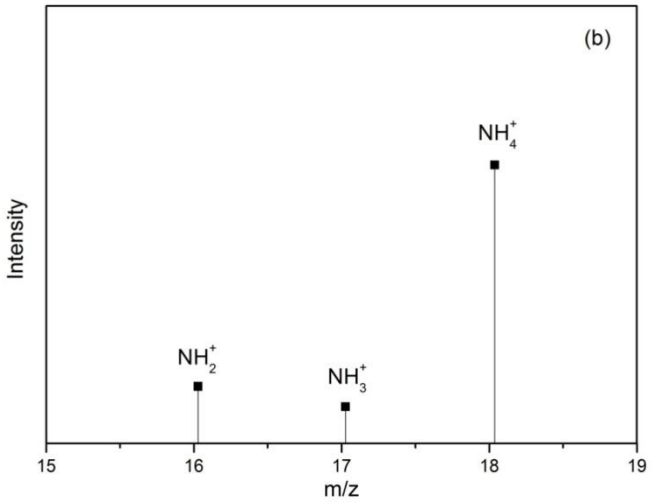
(b)
Intensity
NH_4^+
NH_2^+
NH_3^+
15
16
17
18
19
m/z

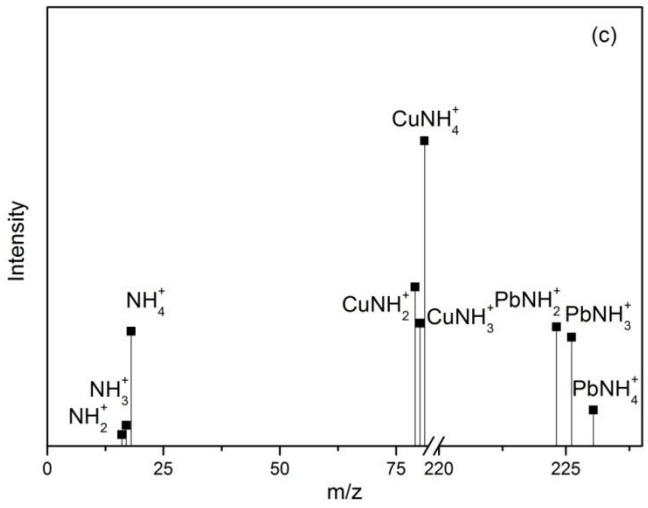

Figure 3.4 Part of the positive ion ToF-SIMS spectra of a 64 μm × 64 μm region from the surface of (a) chitosan (CT), (b) chitosan (CT) at pH 4 and (c) a mixture of chalcopyrite alena (1:1) after chitosan adsorption.

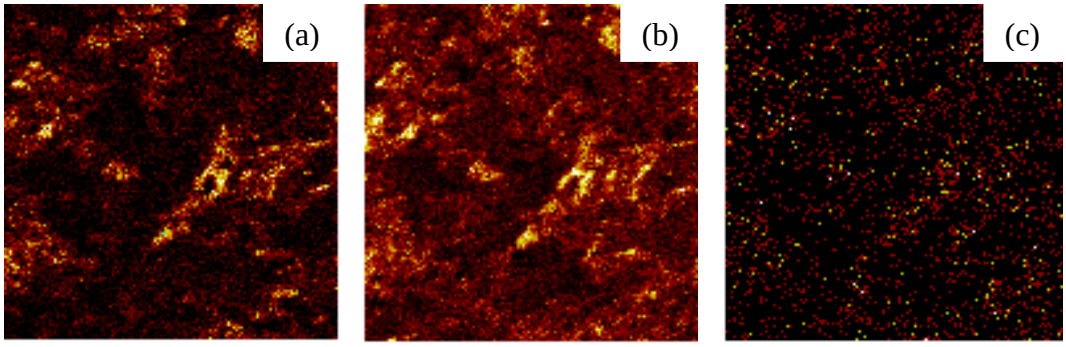

Figure 3.5 Positive-ion images of a 64 μm × 64 μm region from the surface of a mixture of chalcopyrite and galena (weight ratio 1:1) after chitosan adsorption. (a) image of NH_4^+; (b) image of $CuNH_4^+$; (c) image of $PbNH_4^+$.

3.3.3 XPS analyses of sulfide minerals after treatment with chitosan

The XPS spectra were obtained from chalcopyrite and galena single minerals, respectively, that were treated with chitosan (CT) at pH 4. As charging occurred in the measurement, the Cu $2p^{3/2}$ component (BE = 932.0 eV) and Pb $4f^{7/2}$ component (BE = 137.5 eV) were used as internal standards to calibrate the entire XPS spectra of chalcopyrite and galena samples. In order to avoid the interference of carbon from chitosan, the commonly used internal standard, C 1s (BE = 285.0 eV) of contaminated hydrocarbons, was not used for binding energy calibration.

The as-received chitosan (CT) powder was measured as a reference. In the XPS survey scan of the chitosan, the presence of carbon, oxygen and nitrogen peaks were confirmed from the XPS spectrum, in accordance with the chemical formula of chitosan. No significant contamination was detected on the tested chitosan surface. The high-resolution spectra of N 1s and O 1s electrons were acquired for the chitosan (CT). The slight shift due to charging was observed and referenced to the N 1s peak at 399.5 eV (Amaral et al., 2005; Lawrie et al., 2007). The deconvoluted N 1s and O 1s high-resolution spectra of CT are shown in Figure 3.6. As can be seen, the N 1s spectrum consists of three binding energy peaks, at 399.5, 400.5 and 401.9 eV. The peaks were in good agreement with literature data (Amaral et al., 2005; Ignatova et al., 2009; Lawrie et al., 2007). The first peak (399.5 eV) was assigned to $-\underline{N}H_2$ (amine) (Amaral et al., 2005; Lawrie et al., 2007) as the basic structural unit of chitosan. The second peak (400.5 eV) was originated from O=C–<u>N</u>H– (amide) (Lawrie et al., 2007). The last peak (401.9 eV) was due to $-\underline{N}H_3^+$ (protonated amine) (Amaral et al., 2005). Calculation using integrated peak areas showed that the concentrations of amine ($-\underline{N}H_2$) and protonated amine ($-\underline{N}H_3^+$) were 76.2% and 9.5%, respectively. Both the amine and protonated amine were deacetylation units, thus the degree of deacetylation of the chitosan (CT) sample from its parent compound, chitin, should be 85.7% (i.e., the sum of 76.2% and 9.5%), which is on the high end specified by the vendor (75%-85%).

The O 1s spectrum of chitosan (CT) was deconvoluted into three peaks (Figure 3.6b). Considering the chemical structure of chitosan, the peaks at 531.8 eV and 533.0 eV were assigned to oxygen in O=C–NH– and –C–O–C– (Amaral et al., 2005; Ignatova et al., 2009; Lawrie et al., 2007). The peak at 533.6 eV originates from C-OH in the basic structural unit of chitosan (Amaral et al., 2005).

The high-resolution spectra of N 1s were recorded on chalcopyrite and galena before and after chitosan adsorption, and the results are shown in Figures 3.7a, 7c, 8a and 8b. As can be seen from Figure 3.7a and 8a, no N 1s peaks were observed on the high-resolution spectra of chalcopyrite and galena before chitosan treatment. After reacting with chitosan, nitrogen was detected on both minerals by XPS survey scan. The N 1s spectrum of chitosan-treated chalcopyrite (Figure 3.7c) was deconvoluted into three components. The major peak at 401.5 eV was from the nitrogen atoms in protonated amine ($–NH_3^+$), while the other two peaks, at 399.6 eV and 400.9 eV, were attributed to $–NH_2$ and O=C–NH–, respectively. The N 1s high-resolution spectrum of chitosan-treated galena is shown in Figure 3.8b. It was deconvoluted into two peaks. The first peak at 399.4 eV was due to $–NH_2$, while the second peak at 400.5 eV originated from O=C–NH–. Compared to the N 1s spectrum of chitosan-treated chalcopyrite, no peak corresponding to the protonated amine was identified on the N 1s spectrum of treated galena. It is worth noting that the binding energy shifts of amine (–0.1 eV) and amide (0.0 eV) on galena are much smaller than the obvious binding energy shifts of amide (+0.4 eV) and the appearance of ammonium (401.5 eV) on chalcopyrite. The relatively large binding energy shifts of amide and the existence of ammonium on chitosan-treated chalcopyrite suggest a chemical adsorption mechanism of chitosan on chalcopyrite.

Therefore, the adsorption of chitosan on galena cannot be attributed to chemical adsorption since there are no obvious binding energy shifts of N 1s electrons. A physical adsorption mechanism, possibly through the hydrophobic force between chitosan and galena surface, is proposed to explain the adsorption of chitosan on

galena. The wettability of galena and chalcopyrite surfaces by water before and after chitosan adsorption was characterized by contact angle measurements. The contact angles of galena and chalcopyrite before chitosan adsorption were measured to be $82.6^{o}\pm2.5^{o}$ and $27^{o}\pm1.6^{o}$, respectively, which shows that galena was much more hydrophobic than chalcopyrite. The origin of the hydrophobicity of galena is still open to debate - there were opinions that it was due to the moderate degrees of oxidization of S^{2-} into S^{o} on the surface (Gardner and Woods, 1979) while other investigators insist on other reasons (Luttrell and Yoon, 1984; Yin et al., 1995). The rest potentials of sulfide minerals at pH 4 was measured and the flotation tests proved that the collector-less floatability (which is a reflection of surface hydrophobicity) of sulfide minerals was inversely proportional to their rest potentials (Hayes et al., 1987). In Hayes et al.'s measurements, the rest potentials of galena and chalcopyrite were 0.40 V and 0.56 V, respectively, indicating that galena was more hydrophobic than chalcopyrite, which is in agreement with the contact angle measurement in this study. XPS measurements indicated that the percentage of amide group in the chitosan was only 14.3% (Figure 3.6a). However, it is important to note that 69% of the nitrogen species adsorbed on galena surfaces were amide and only 31% were amine, indicating that most of the adsorbed chitosan on galena surfaces is the acetyl unit of chitosan (i.e., chitin). According to the structure of the acetyl group, $-CH_3$ is hydrophobic, which would enable its adsorption the galena surface by hydrophobic interaction. This further supports the hypothesis that the main factor driving chitosan adsorption on galena is probably hydrophobic force.

In addition to N 1s spectra, high-resolution spectra of O 1s were also acquired from chitosan (CT) as well as from chalcopyrite and galena surface treated with chitosan (CT). The O 1s spectra of galena did not show any difference before and after chitosan treatment. On the contrary, binding energy shift was observed from the O 1s spectra of chalcopyrite after chitosan adsorption. As can be seen from Figure 3.7d, three peaks were found to fit the spectrum. The peaks at 530.0 eV and 531.9 eV are assigned to oxygen in the hydroxides and oxides components on

the chalcopyrite surface (Farquhar et al., 2003; Mielczarski et al., 1996), which have almost the same value as the corresponding peaks of the chalcopyrite spectrum (Figure 3.7b). However, the upward shift of the third peak (BE = 533.7 eV) was detected from Figures 3.7b and 7d. The third peak was assigned to C–OH (Amaral et al., 2005), while the corresponding peak (BE = 533.3 eV) on chalcopyrite surface was from the adsorbed water (Farquhar et al., 2003; Mielczarski et al., 1996). The C–OH component is the basic molecular structure unit of chitosan. The adsorbed chitosan could be detected by the shift of this peak, from 533.3 eV to 533.7 eV. Therefore, the hydroxyl groups attached to the carbon atoms from chitosan enhanced the adsorption of chitosan on chalcopyrite. The results further support the stronger reaction between chitosan and chalcopyrite than between chitosan and galena.

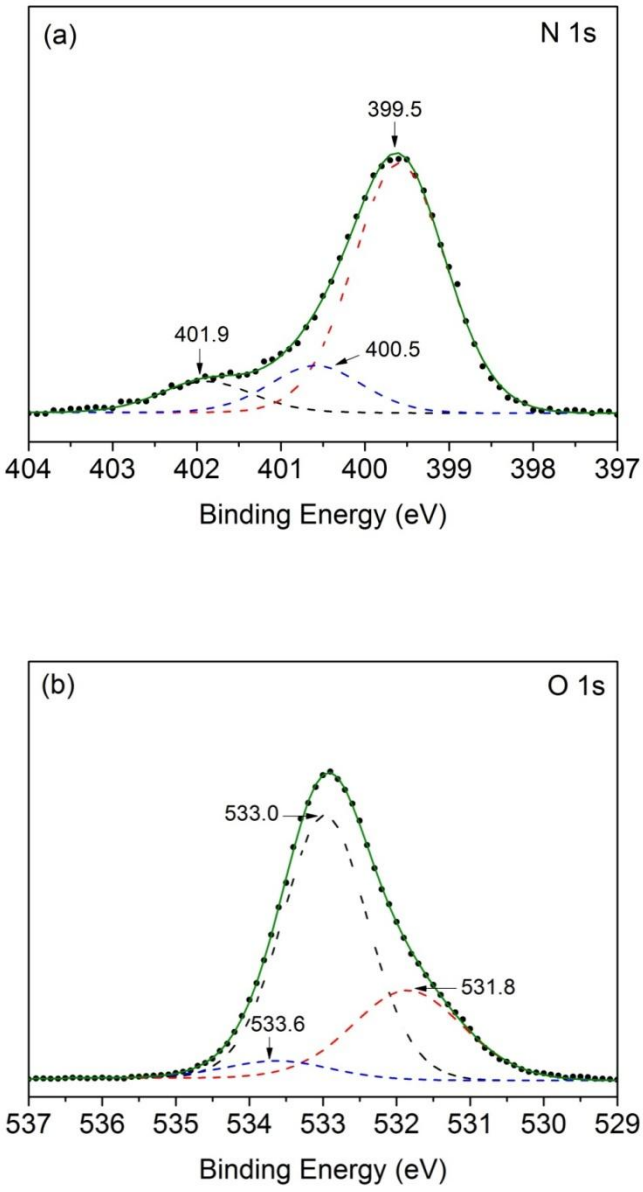

Figure 3.6 XPS peak fitting for narrow scan spectra of chitosan, (a) N 1s spectrum (b) O 1s spectrum.

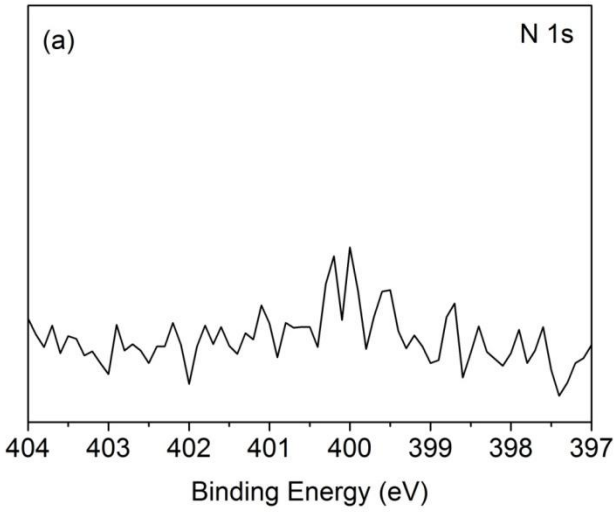
(a)
N 1s
404 403 402 401 400 399 398 397
Binding Energy (eV)

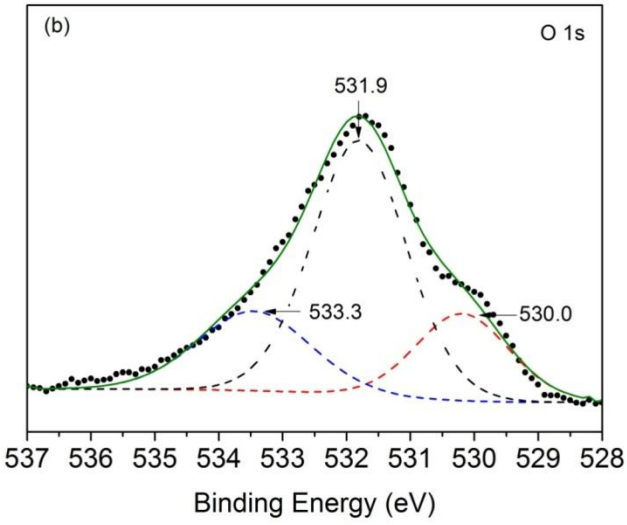
(b)
O 1s
531.9
533.3
530.0
537 536 535 534 533 532 531 530 529 528
Binding Energy (eV)

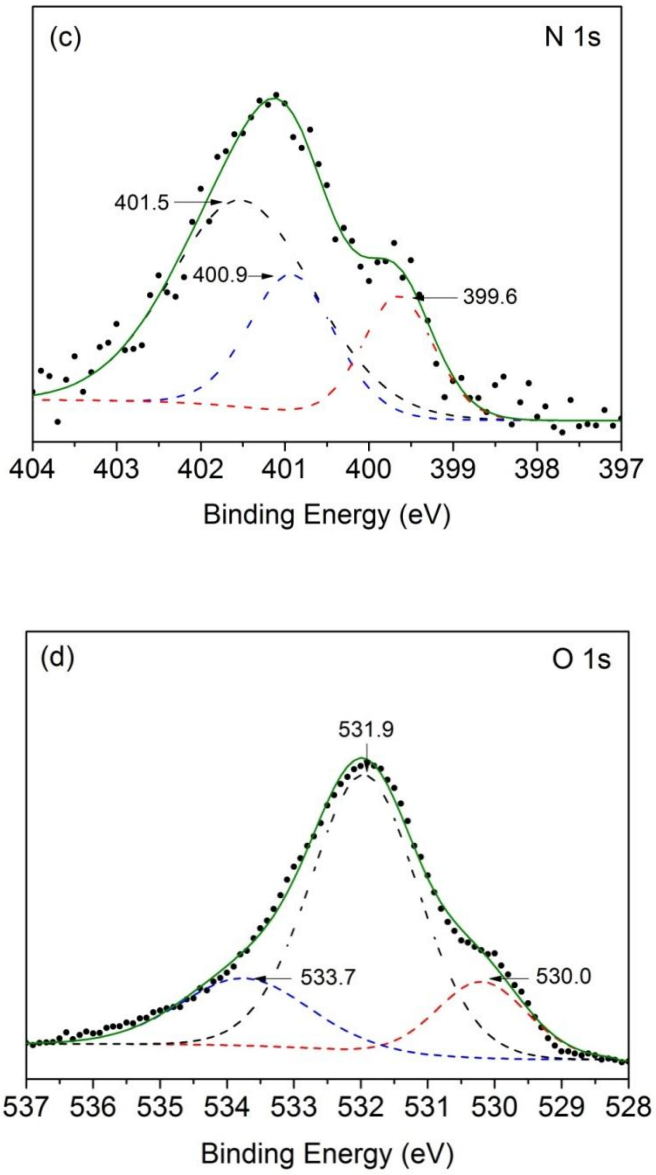

Figure 3.7 XPS narrow scan spectra with the curve fitting of chalcopyrite, (a) N 1s spectrum (b) O 1s spectrum, and chalcopyrite adsorbed with chitosan (CT), (c) N 1s spectrum (d) O 1s spectrum.

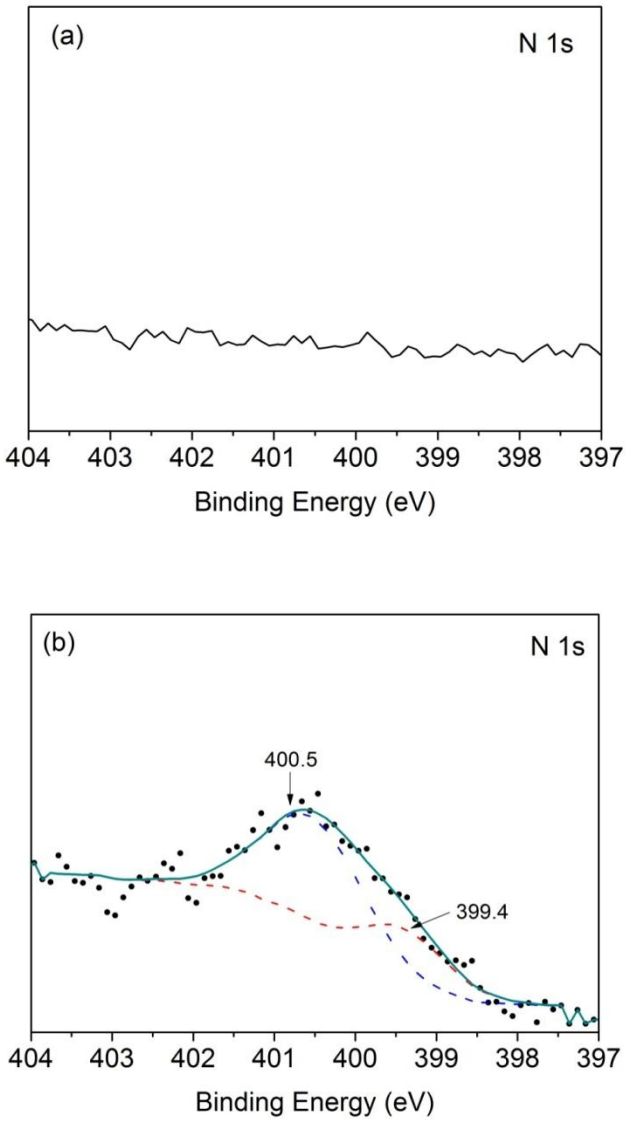

Figure 3.8 XPS N 1s peak fitting of galena before (a) and after (b) chitosan (CT) adsorption.

3.3.4 Chitosan with different degrees of deacetylation as flotation depressants

The foregoing description shows that chitosan adsorbs on galena probably by the acetyl unit (amide), while it adsorbs on chalcopyrite by the deacetylation unit (amine). Thus, the degree of deacetylation of chitosan from its parent compound, chitin, should have a great influence on the mineral recovery when chitosan with different degrees of deacetylation were used as depressants. A different chitosan sample, designated as HCT, with a specified degree of deacetylation of 91.7% (confirmed by XPS measurements), was used in the flotation tests to examine its effect and to compare with the results of chitosan with a degree of deacetylation of 85.7% (which was designated as CT).

Figure 3.9 shows the flotation recovery of chalcopyrite and galena with CT and HCT as a depressant in single mineral flotation. Both chalcopyrite and galena were depressed by chitosan to some degree within the tested pH range. When comparing the recoveries of galena with CT and HCT in Figure 3.9, significant difference can be seen in the acidic solution, while similar recoveries were observed in the rest of the pH range. With CT (lower degree of deacetylation, i.e., higher percentage of acetyl groups), the recovery of galena dropped from 80% to a plateau of 40% between pH 3 to 6. However, with HCT (higher degree of deacetylation, i.e., lower percentage of acetyl groups), between pH 3 and 5, the recovery of galena only slightly decreased from 80% to 70%, and sharply decreased from 70% to 40% in the pH range of 5 to 6. The flotation results were consistent with the postulation that the acetyl groups were responsible for chitosan adsorption on galena.

On the other hand, regarding the flotation of chalcopyrite, Figure 3.9 shows the same tendency of both CT and HCT used in the single mineral flotation of chalcopyrite, except that the recovery of chalcopyrite with HCT was marginally lower than that with CT. As the majority of the functional groups in both CT and

HCT were the deacetylated amine groups, their adsorption on chalcopyrite was not expected to be much different, so were the flotation results.

The chitosan with different degrees of deacetylation (CT and HCT) were tested as depressants in the differential sulfide minerals flotation separation of the mixtures of chalcopyrite and galena. The metal grade and the recovery of minerals in the floated concentrate are shown in Figure 3.10a and Figure 3.10b, respectively. Figure 3.10a also shows the metal grade of the mineral mixtures before flotation. In these tests, galena was separated from chalcopyrite in acidic solution when using either CT or HCT. But when HCT was used, the recovery of galena was higher than that of CT at pH less than 5 (Figure 3.10b), consistent with the single mineral flotation results of galena (Figure 3.9). The recovery of chalcopyrite was almost the same for either CT or HCT, confirming the results of single mineral flotation (Figure 3.9).

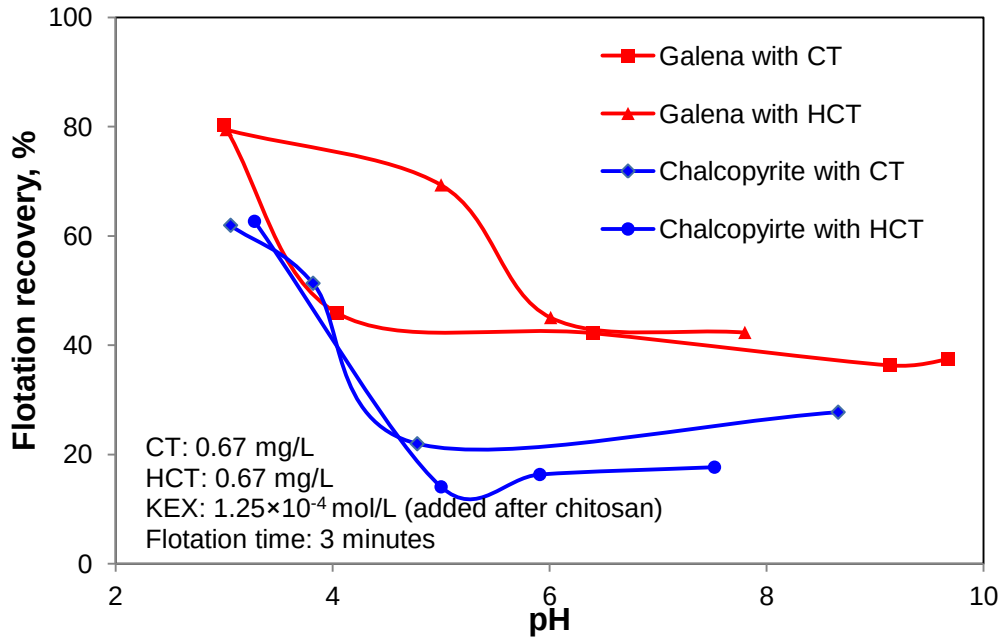

Figure 3.9 Flotation of single minerals of chalcopyrite and galena as a function of pH with chitosan (CT or HCT) as a depressant. (KEX: 1.25×10^{-4} mol/L; CT or HCT: 0.67 mg/L; Condition time: 3 min; Flotation time: 3 min)

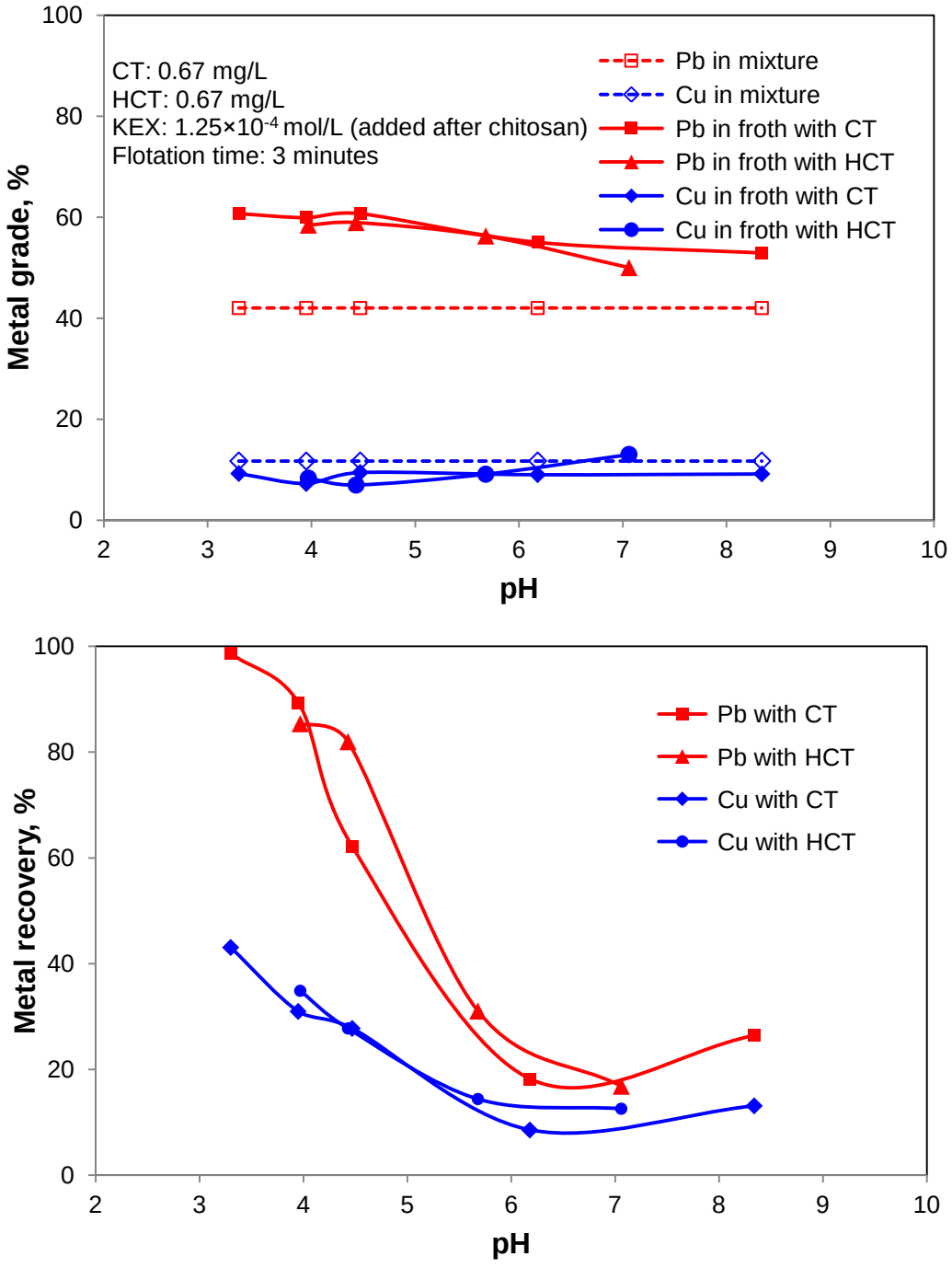

Figure 3.10 Flotation of mixtures of chalcopyrite and galena as a function of pH. (a). Metal grade in froth products; (b). Metal recovery in froth products. (KEX: 1.25×10^{-4} mol/L; CT or HCT: 0.67 mg/L; Condition time: 3 min; Flotation time: 3 min)

3.4 Conclusions

In this study, the mechanisms of interaction of chitosan with two sulfide minerals, chalcopyrite ($CuFeS_2$) and galena (PbS), were investigated by ATR-FTIR, ToF-SIMS and XPS. These complementary surface analysis techniques revealed that the deacetylated unit (amine) and the hydroxyl groups on chitosan were involved in the strong chitosan-chalcopyrite chemical interaction. However, chitosan-galena interaction was possibly due to weaker hydrophobic association through the acetyl (amide) units of chitosan, which are present in chitosan as a result of incomplete deacetylation. The above hypothesis was tested and proven by two chitosan samples, with different degrees of deacetylation (85.7% versus 91.7%), in the flotation of single minerals of chalcopyrite and galena, as well as their mixtures. The results showed that the chitosan with the higher degree of deacetylation indeed depressed galena to a lesser degree than the chitosan with a lower degree of deacetylation. Clearly, pure chitosan with complete deacetylation would be a very selective flotation depressant in the differential separation of copper sulfide from lead sulfide, which could provide a viable alternative to sodium cyanide and sodium dichromate that are routinely used in commercial Cu-Pb flotation separation circuits.

3.5 References

Aider, M., 2010. Chitosan application for active bio-based films production and potential in the food industry: Review. LWT-Food Science and Technology 43, 837-842.

Amaral, I., Granja, P., Barbosa, M., 2005. Chemical modification of chitosan by phosphorylation: an XPS, FT-IR and SEM study. Journal of Biomaterials Science, Polymer Edition 16, 1575-1593.

Blair, H.S., Ho, T.C., 1981. Studies in the adsorption and diffusion of ions in chitosan. Journal of Chemical Technology and Biotechnology 31, 6-10.

Boddu, V.M., Abburi, K., Talbott, J.L., Smith, E.D., 2003. Removal of hexavalent chromium from wastewater using a new composite chitosan biosorbent. Environmental science & technology 37, 4449-4456.

Burke, A., Yilmaz, E., Hasirci, N., Yilmaz, O., 2002. Iron (III) ion removal from solution through adsorption on chitosan. Journal of applied polymer science 84, 1185-1192.

Cao, M., Liu, Q., 2006. Reexamining the functions of zinc sulfate as a selective depressant in differential sulfide flotation--The role of coagulation. Journal of colloid and interface science 301, 523-531.

Choy, K.K.H., Porter, J.F., Mckay, G., 2001. A film-pore-surface diffusion model for the adsorption of acid dyes on activated carbon. Adsorption 7, 231-247.

Chui, V., Mok, K., Ng, C., Luong, B., Ma, K., 1996. Removal and recovery of copper (II), chromium (III), and nickel (II) from solutions using crude shrimp chitin packed in small columns. Environment international 22, 463-468.

Chung, Y.S., Lee, K.K., Kim, J.W., 1998. Durable press and antimicrobial finishing of cotton fabrics with a citric acid and chitosan treatment. Textile research journal 68, 772.

Crini, G., Badot, P.M., 2008. Application of chitosan, a natural aminopolysaccharide, for dye removal from aqueous solutions by adsorption processes using batch studies: A review of recent literature. Progress in Polymer Science 33, 399-447.

Deans, J.R., Dixon, B.G., 1992. Uptake of Pb2+ and Cu2+ by novel biopolymers. Water Research 26, 469-472.

Domard, A., 1987. pH and cd measurements on a fully deacetylated chitosan: application to Cu(II)--polymer interactions. International journal of biological macromolecules 9, 98-104.

Egger, G., Cameron-Smith, D., Stanton, R., 1999. The effectiveness of popular, non-prescription weight loss supplements. Med J Aust 171, 604-608.

Farquhar, M.L., Wincott, P.L., Wogelius, R.A., Vaughan, D.J., 2003. Electrochemical oxidation of the chalcopyrite surface: an XPS and AFM study in solution at pH 4. Applied surface science 218, 34-43.

Foster, L.S., 1928. Preparation of xanthates and other organic thiocarbonates. Utah Eng. Exp. Sta.

Gardner, J., Woods, R., 1979. An electrochemical investigation of the natural flotability of chalcopyrite. International Journal of Mineral Processing 6, 1-16.

Gerente, C., Lee, V., Cloirec, P.L., McKay, G., 2007. Application of chitosan for the removal of metals from wastewaters by adsorption-mechanisms and models review. Critical reviews in environmental science and technology 37, 41-127.

González Siso, M., Lang, E., Carreno-Gomez, B., Becerra, M., Otero Espinar, F., Blanco Mendez, J., 1997. Enzyme encapsulation on chitosan microbeads. Process Biochemistry 32, 211-216.

Guibal, E., 2005. Heterogeneous catalysis on chitosan-based materials: a review. Progress in Polymer Science 30, 71-109.

Guibal, E., Dambies, L., Milot, C., Roussy, J., 1999. Influence of polymer structural parameters and experimental conditions on metal anion sorption by chitosan. Polymer international 48, 671-680.

Guibal, E., Saucedo, I., Roussy, J., Le Cloirec, P., 1994. Uptake of uranyl ions by new sorbing polymers: discussion of adsorption isotherms and pH effect. Reactive polymers 23, 147-156.

Hayes, R., Price, D., Ralston, J., Smith, R., 1987. Collectorless flotation of sulfide minerals. Mineral Procesing and Extractive Metallurgy Review 2, 203-234.

Hsien, T.Y., Rorrer, G.L., 1997. Heterogeneous cross-linking of chitosan gel beads: kinetics, modeling, and influence on cadmium ion adsorption capacity. Industrial & engineering chemistry research 36, 3631-3638.

Huang, P., Cao, M., Liu, Q., 2012. Using chitosan as a selective depressant in the differential flotation of Cu–Pb sulfides. International Journal of Mineral Processing 106–109, 8-15.

Ignatova, M., Manolova, N., Markova, N., Rashkov, I., 2009. Electrospun Non-Woven Nanofibrous Hybrid Mats Based on Chitosan and PLA for Wound-Dressing Applications. Macromolecular bioscience 9, 102-111.

Ilium, L., 1998. Chitosan and its use as a pharmaceutical excipient. Pharmaceutical Research 15, 1326-1331.

Ishii, H., Minegishi, M., Lavitpichayawong, B., Mitani, T., 1995. Synthesis of chitosan-amino acid conjugates and their use in heavy metal uptake. International journal of biological macromolecules 17, 21-23.

Jha, I., Iyengar, L., Rao, A.V.S.P., 1988. Removal of cadmium using chitosan. Journal of Environmental Engineering 114, 962.

Jocić, D., Julia, M., Erra, P., 1997. Application of a chitosan/nonionic surfactant mixture to wool assessed by dyeing with a reactive dye. Journal of the Society of Dyers and Colourists 113, 25-31.

Kamiński, W., Modrzejewska, Z., 1997. Application of chitosan membranes in separation of heavy metal ions. Separation Science and Technology 32, 2659-2668.

Kawamura, S., 1991. Effectiveness of natural polyelectrolytes in water treatment. Journal American Water Works Association 83, 88-91.

Kim, S.K., Rajapakse, N., 2005. Enzymatic production and biological activities of chitosan oligosaccharides (COS): A review. Carbohydrate Polymers 62, 357-368.

Koide, S., 1998. Chitin-chitosan: properties, benefits and risks. Nutrition research 18, 1091-1101.

Kurita, K., Akao, H., Yang, J., Shimojoh, M., 2003. Nonnatural branched polysaccharides: synthesis and properties of chitin and chitosan having disaccharide maltose branches. Biomacromolecules 4, 1264-1268.

Lasko, C.L., Hurst, M.P., 1999. An investigation into the use of chitosan for the removal of soluble silver from industrial wastewater. Environmental science & technology 33, 3622-3626.

Lawrie, G., Keen, I., Drew, B., Chandler-Temple, A., Rintoul, L., Fredericks, P., Grøndahl, L., 2007. Interactions between alginate and chitosan biopolymers characterized using FTIR and XPS. Biomacromolecules 8, 2533-2541.

Lerivrey, J., Dubois, B., Decock, P., Micera, G., Urbanska, J., Kozlowski, H., 1986. Formation of D-glucosamine complexes with Cu (II), Ni (II) and Co (II) ions. Inorganica chimica acta 125, 187-190.

Loke, W.K., Lau, S.K., Yong, L.L., Khor, E., Sum, C.K., 2000. Wound dressing with sustained anti-microbial capability. Journal of biomedical materials research, Part A 53, 8-17.

Luttrell, G., Yoon, R., 1984. Surface studies of the collectorless flotation of chalcopyrite. Colloids and surfaces 12, 239-254.

Martino, A., Pifferi, P., Spagna, G., 1996. Immobilization of [beta]-glucosidase from a commercial preparation. Part 2. Optimization of the immobilization process on chitosan. Process Biochemistry 31, 287-293.

Mielczarski, J., Cases, J., Alnot, M., Ehrhardt, J., 1996. XPS characterization of chalcopyrite, tetrahedrite, and tennantite surface products after different conditioning. 1. Aqueous solution at pH 10. Langmuir 12, 2519-2530.

Monteiro, O.A.C., Airoldi, C., 1999. Some thermodynamic data on copper-chitin and copper-chitosan biopolymer interactions. Journal of colloid and interface science 212, 212-219.

Mourya, V., Inamdar, N.N., 2008. Chitosan-modifications and applications: Opportunities galore. Reactive and functional polymers 68, 1013-1051.

Muzzarelli, R., 1989. Amphoteric derivatives of chitosan and their biological significance. Chitin and chitosan. New York: Elsevier Applied Science, 87–99.

Muzzarelli, R.A.A., 1973. Natural chelating polymers; alginic acid, chitin and chitosan. Pergamon Press.

Muzzarelli, R.A.A., 1977. Chitin. Pergamon Press New York.

Ngah, W., Teong, L., Hanafiah, M., 2010. Adsorption of dyes and heavy metal ions by chitosan composites: A review, Carbohydrate Polymers. Elsevier, pp. 1446-1456.

Nomanbhay, S.M., Palanisamy, K., 2005. Removal of heavy metal from industrial wastewater using chitosan coated oil palm shell charcoal. Electronic Journal of Biotechnology 8, 43-53.

Onsosyen, E., Skaugrud, O., 1990. Metal recovery using chitosan. Journal of Chemical Technology & Biotechnology 49, 395-404.

Pearson, F., Marchessault, R., Liang, C., 1960. Infrared spectra of crystalline polysaccharides. V. Chitin. Journal of Polymer Science 43, 101-116.

Peter, M.G., 1995. Applications and environmental aspects of chitin and chitosan. Journal of Macromolecular Science, Part A: Pure and Applied Chemistry 32, 629-640.

Piron, E., Domard, A., 1998. Interactions between chitosan and [alpha] emitters: 238Pu and 241Am. International journal of biological macromolecules 23, 121-125.

Ravi Kumar, M.N.V., 2000. A review of chitin and chitosan applications. Reactive and functional polymers 46, 1-27.

Roberts, G., Taylor, K., Brine, C., Sanford, P., Zikakis, J., 1992. Surface activity and foam-enhancing properties of N-(2-hydroxyalkyl) chitosans. Advances in Chitin and Chitosan, Elsevier, Amsterdam. 179-186.

Rorrer, G.L., Hsien, T.Y., Way, J.D., 1993. Synthesis of porous-magnetic chitosan beads for removal of cadmium ions from wastewater. Industrial & engineering chemistry research 32, 2170-2178.

Saucedo, I., Guibal, E., Roussy, J., Roulph, C., Le Cloirec, P., 1993. Uranium sorption by glutamate glucan: A modified chitosan Part I: Equilibrium studies. WATER SA-PRETORIA- 19, 113-113.

Schlick, S., 1986. Binding sites of copper2+ in chitin and chitosan. An electron spin resonance study. Macromolecules 19, 192-195.

Se-Kwon, K., 2010. Chitin, Chitosan, Oligosaccharides and Their Derivatives : Biological Activities and Applications. 69-70.

Shahidi, F., Arachchi, J.K.V., Jeon, Y.J., 1999. Food applications of chitin and chitosans. Trends in Food Science & Technology 10, 37-51.

Shin, Y., Yoo, D.I., 1998. Use of chitosan to improve dyeability of DP-finished cotton (II). Journal of applied polymer science 67, 1515-1521.

Sorlier, P., Denuzière, A., Viton, C., Domard, A., 2001. Relation between the degree of acetylation and the electrostatic properties of chitin and chitosan. Biomacromolecules 2, 765-772.

Srinivasa, P., Baskaran, R., Ramesh, M., Harish Prashanth, K., Tharanathan, R., 2002. Storage studies of mango packed using biodegradable chitosan film. European Food Research and Technology 215, 504-508.

Stöhr, C., Horst, J., Höll, W.H., 2001. Application of the surface complex formation model to ion exchange equilibria: Part V. Adsorption of heavy metal salts onto weakly basic anion exchangers. Reactive and functional polymers 49, 117-132.

Struszczyk, M., 2002. Chitin and chitosan—Part II. Applications of chitosan. Polimery 47, 396-403.

Sun, S., Wang, A., 2006. Adsorption properties and mechanism of cross-linked carboxymethyl-chitosan resin with Zn (II) as template ion. Reactive and functional polymers 66, 819-826.

Teixeira, M.A., Paterson, W.J., Dunn, E.J., Li, Q., Hunter, B.K., Goosen, M.F.A., 1990. Assessment of chitosan gels for the controlled release of agrochemicals. Industrial & engineering chemistry research 29, 1205-1209.

Vickerman, J.C., Briggs, D., Limited, S., 2001. ToF-SIMS: surface analysis by mass spectrometry. IM Publications Chichester, UK.

Vold, I., Varum, K.M., Guibal, E., Smidsrod, O., 2003. Binding of ions to chitosan--selectivity studies. Carbohydrate Polymers 54, 471-477.

Wang, L., Khor, E., Wee, A., Lim, L.Y., 2002. Chitosan-alginate PEC membrane as a wound dressing: Assessment of incisional wound healing. Journal of biomedical materials research, Part A 63, 610-618.

Wang, X., Du, Y., Liu, H., 2004. Preparation, characterization and antimicrobial activity of chitosan-Zn complex. Carbohydrate Polymers 56, 21-26.

Yin, Q., Kelsall, G., Vaughan, D., England, K., 1995. Atmospheric and electrochemical oxidation of the surface of chalcopyrite (CuFeS2). Geochimica et cosmochimica acta 59, 1091-1100.

CHAPTER 4

SELECTIVE DEPRESSION OF SPHALERITE BY CHITOSAN IN DIFFERENTIAL Pb-Zn FLOTATION*

4.1 Introduction

As the major sources of lead and zinc, galena (PbS) and sphalerite (ZnS) are usually found in association in nature. It is known that galena is readily floatable with a thiol collector such as xanthate, while sphalerite does not respond well to flotation with short-chain xanthate at moderate concentrations due to the relative high solubility of zinc xanthate (Fuerstenau et al., 1974; Laskowski et al., 1997). It would thus appear that galena could be separated from Pb-Zn sulfide ores with short-chain xanthate as a collector. However, in the complex commercial flotation pulp where many metal ions such as lead and copper are present, the sphalerite is usually activated and becomes floatable, even with short chain xanthate collectors (Chandra and Gerson, 2009; Finkelstein, 1997; Prestidge et al., 1997).

Therefore, for the differential flotation separation of Pb-Zn sulfides, in most cases the combination of NaCN and $ZnSO_4$ is employed to de-activate and depress sphalerite while galena is floated by xanthate. However, increasingly stringent environmental regulations demand that more environmentally benign reagents be used in these processes. In this study, chitosan, as a naturally occurring polymer, was tested as a potential depressant in the differential Pb-Zn sulfide flotation separation.

---

* This paper was published in International Journal of Mineral Processing in 2013: P. Huang, M. Cao and Qi Liu, 2013. Selective Depression of Sphalerite by Chitosan in Differential Pb-Zn Flotation. International Journal of Mineral Processing, Vol. 122, 29-35. http://dx.doi.org/10.1016/j.minpro.2013.04.010.

Chitosan is a partial deacetylation product from chitin, which is contained in crustacean shells of seafood such as prawn, shrimp, crab and lobster (Tokura and Tamura, 2007). As a copolymer, the main components of chitosan are β-(1-4)-linked D-glucosamine and β-(1-4)-linked N-acetyl-D-glucosamine (Figure 4.1). Chitosan has outstanding properties of biodegradability, biocompatibility, non-toxicity and strong metal ion chelation ability due to the presence of functional amine and hydroxyl groups on the monomer (Ngah et al., 2010; Se-Kwon, 2010). These advantageous characteristics have been studied and tested for applications in a number of areas. In wastewater treatment, chitosan is used as an adsorbent for heavy metals to meet environmental regulations before discharge (Boddu et al., 2003; Burke et al., 2002; Ravi Kumar, 2000); In paper and textile industry, chitosan has been used as a surface treatment agent during processing to enhance the dyeing and water repelling abilities (Choy et al., 2001; Chung et al., 1998; Houshyar and Amirshahi, 2002; Jocić et al., 1997; Shin and Yoo, 1998; Struszczyk, 1987). As chitosan is extracted from the exoskeleton of living organisms, it is widely studied and used in biomedical engineering (Koide, 1998; Loke et al., 2000; Struszczyk, 2002; Wang et al., 2002), healthcare (González Siso et al., 1997; Ilium, 1998; Martino et al., 1996; Muzzarelli, 1989), and agriculture and food industry (Crini and Badot, 2008; Egger et al., 1999; Gerente et al., 2007; Srinivasa et al., 2002; Teixeira et al., 1990).

In the mineral processing industry, chitosan was recently found to be a potential selective depressant in the differential flotation of Cu-Pb sulfides (Huang et al., 2012a, b). Huang et al. (2012a, b) showed that chalcopyrite ($CuFeS_2$) was depressed by chitosan while galena (PbS) was floated by xanthate at acidic pH from mixtures of chalcopyrite and galena.

In this paper, we report results of a study to use chitosan in the differential flotation of Pb-Zn sulfides. Small-scale flotation tests were conducted to examine the selective depressive action of chitosan, and ToF-SIMS and XPS analyses were

performed to study the mechanisms of the selective depression of sphalerite by chitosan.

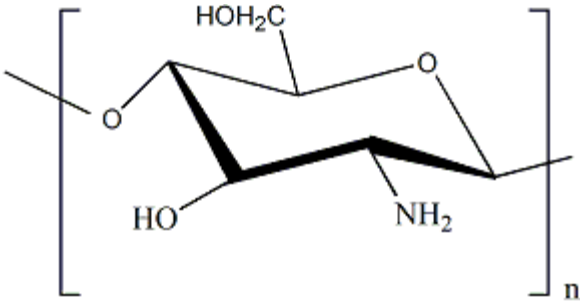

(a) chitosan

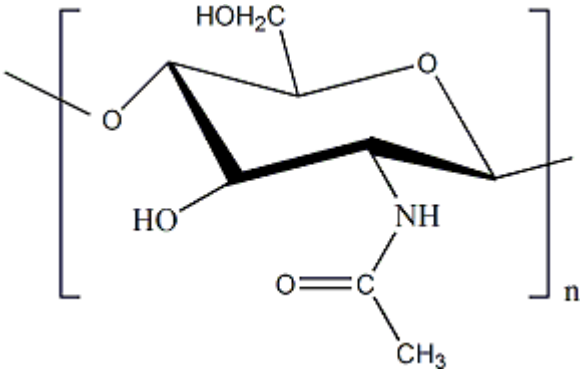

(b) chitin

Figure 4.1 Structures of chitosan and chitin (Rinaudo, 2006).

4.2 Materials and Methods

4.2.1 Materials

Chitosan (abbreviated as CT) was obtained from Sigma-Aldrich Canada. The chitosan had a degree of deacetylation of 75-85% and a molecular weight (MW) ranging from 100,000 to 300,000 (reported by vendor). It was dissolved by dilute hydrochloric acid (0.2 mol/L) before using. Hydrochloric acid and sodium

hydroxide were used to adjust pH and they were purchased from Fisher Scientific Canada. $Cu(NO_3)_2$ (Fisher Scientific, Canada) was used for sphalerite activation. Potassium ethyl xanthate (KEX), courtesy of Prospec Chemicals Ltd, Canada, was used as a collector throughout the flotation tests. The KEX was purified with ethyl ether anhydrous and acetone (Fisher Scientific, Canada) following the protocol of Foster (1928). EDTA (Fisher Scientific, Canada) was added in the flotation slurry to remove the contaminating metal ions when necessary. Distilled water was used throughout.

The sphalerite and galena were purchased from Ward's Scientific Establishment. X-ray diffraction patterns of the sphalerite and galena samples showed that both minerals were of high purity with no detectable impurity peaks. The sphalerite sample assayed 63.00% zinc, indicating a purity of 98% sphalerite, and the galena sample assayed 84.00% Pb, representing a purity of 97% galena. The lumps of the sphalerite and galena were separately crushed (Retsch BB200 Jaw Crusher, USA) and pulverized (Fritsch Agate Mortar Grinder Pulverisette 2, Germany) to -75 μm, and screened to collect the -75+38 μm particles for the flotation tests and ToF-SIMS measurements, and the -20 μm particles for XPS studies. All the mineral samples were sealed in plastic bottles and stored in a freezer at -10 ℃.

4.2.2 Experimental methods

4.2.2.1 Flotation

A small-scale glass flotation tube, which was designed to minimize mechanical entrainment, was used to conduct the flotation tests. The details of the construction of the flotation tube was described by Cao and Liu (2006).

In a typical flotation test, 1.5 g of the -75+38 μm mineral mixture (galena and sphalerite mixed at a weight ratio of 1:1) were conditioned for 3 min in a 250-mL beaker with 150 mL distilled water at a specific pH. This was followed by the addition of an appropriate amount of EDTA (when used), chitosan (when used) and KEX sequentially with 3 min conditioning after each addition. The

conditioned suspension was then transferred to the flotation tube and floated for 3 min using N_2 (The alternative was to use compressed air. However, nitrogen gas was used to avoid the influence from flotation gas as air is an oxidative gas. Compressed air was used in selected tests and no difference in the flotation behaviors was observed, possibly due to the short flotation time). The concentrate and tailings were collected, dried and analyzed to calculate mineral recovery. Both the concentrate and tailings were dissolved in aqua regia, followed by the determination of Pb and Zn concentrations using a Varian SpectrAA-220FS (Varian, USA) atomic absorption spectrometer (AAS).

For the flotation of mixtures of galena with copper-coated sphalerite, the 0.75 g -75+38 μm sphalerite were treated with 100 mL 3×10^{-3} mol/L $Cu(NO_3)_2$ for 3 min at pH 5.5. The sphalerite was filtered and washed with 100 mL distilled water, and mixed with 0.75 g galena to carry out the flotation tests.

4.2.2.2 ToF-SIMS measurements

ToF-SIMS spectra were acquired with a ToF-SIMS IV spectrometer (ION-TOF GmbH) using 25 keV Bi^+ primary ions. An area of 171 μm × 171 μm was analyzed for spectra acquisition. As the particle size of the sample was -75+38 μm, the test area can cover enough particles for reliable analysis. The positive spectra were calibrated using the H^+, CH_3^+ and Na^+ peaks before fragment identification. Images were then generated by mapping the mass-selected ion intensity in a burst alignment mode with pixels of 128 × 128 per image.

Two sphalerite samples were analyzed for SIMS spectra acquisition. One sample was chitosan treated sphalerite. The sample was prepared by mixing 1.5 g -20 μm sphalerite in 150 mL distilled water at pH 4, and adding 0.1 mg of chitosan (1 mL 0.1 g/L chitosan stock solution). The other sample was chitosan treated copper-coated sphalerite. This sample was prepared by first reacting 1.5 g sphalerite with 100 mL 3×10^{-3} mol/L $Cu(NO_3)_2$ for 3 min at pH 5.5. After the reaction, the sphalerite was filtered and washed with 100 mL distilled water, then mixed with

0.1 mg chitosan (1 mL 0.1 g/L chitosan stock solution) in 150 mL distilled water at pH 4. The sphalerite-chitosan suspensions in both cases were agitated in an incubator for 30 min, and the minerals were filtered, washed with 200 mL distilled water through the filtration funnel and dried in a desiccator under vacuum. To minimize oxidation, the ToF-SIMS analysis was conducted within 12 hours after mineral sample preparation.

4.2.2.3 XPS measurements

An AXIS 165 X-ray photoelectron spectrometer (Kratos Analytical, USA) was used to carry out the XPS analyses for the mineral samples. The instrument was equipped with a monochromatic Al Kα X-ray source ($h\nu$ = 1486.6 eV). The vacuum pressure inside the analytical chamber was lower than 3×10^{-8} Pa. For data acquisition, the survey scans and high-resolution scans were collected using analyzer pass energy of 160 eV and 20 eV, respectively. An area of 400 μm × 700 μm on the sample surface was analyzed, while the overall information depth for the XPS analysis was approximate 10 nm. Therefore, the recorded spectra can provide surface information of the samples. All the high-resolution spectra were processed by the CasaXPS Version 2.3.15 instrument software. To resolve the obtained binding energy peaks, individual Gaussian-Lorentzian peaks were employed after the Shirley-type background subtraction to optimize the high-resolution spectra. The processed spectra were imported and calibrated according to previously publish data by a graphic software (Origin, OriginLab Corp) package for displaying the optimized fitting peaks of the high-resolution spectra.

To prepare the samples for XPS analysis, 1 g -20 μm mineral (sphalerite or galena) was mixed with 100 mL distilled water at pH 4 with the addition of 2 mg of chitosan (when used). The mineral samples were filtered and washed with 200 mL distilled water after agitating in an incubator at 25 ℃ for 30 min. Afterwards, the sample was deposited on a filter paper to dry in a vacuum desiccator before XPS analysis. All the XPS measurements were conducted within 12 hours after sample preparation.

4.3 Results and Discussion

4.3.1 Flotation of sphalerite-galena mixtures

Figure 4.2 shows the flotation of galena-sphalerite mixtures (1:1 weight ratio) using potassium ethyl xanthate (KEX) with and without chitosan (CT) or EDTA. The results were plotted as a function of EDTA concentration, and the concentration of chitosan was 0.67 mg/L when used. As can be seen, when no EDTA was used (i.e., the data points on the left vertical axis), both the galena and sphalerite were floatable with recoveries of over 90% in the absence of chitosan. However, after adding 0.67 mg/L chitosan, the recovery of sphalerite dropped to slightly over 20% and that of galena dropped to slightly over 40%. There was no selective separation whether chitosan was used or not.

The observed results were thought to be due to the contamination of sphalerite by lead ions (Pb^{2+}). Similar sphalerite contamination was reported by other researchers in galena-sphalerite flotation separation (Basilio et al., 1996; Rashchi and Finch, 2006) albeit without chitosan. The contamination of sphalerite surface by the lead ions at the test pH (pH 4) made the sphalerite behave like galena. It was interesting to note that the recovery of galena from the galena-sphalerite mixtures in the presence of 0.67 mg/L chitosan was the same as that in single mineral flotation under the same conditions as reported earlier (Huang et al., 2012b).

EDTA was used to clean the sphalerite surface of lead ions. As can be seen from Figure 4.2, EDTA itself served as a selective depressant for the separation of galena from sphalerite using KEX as a collector. In the absence of chitosan, when EDTA concentration was increased from zero to 5×10^{-4} mol/L, the sphalerite recovery dropped from over 90% to about 10%, while the galena recovery was only slightly affected and remained at about 90%. The improved separation

efficiency was probably due to the removal of lead ions from the sphalerite surfaces, so that the sulfide mineral surfaces were returned to their pristine states.

In the single mineral flotation tests with KEX, the recovery of sphalerite was only about 10%. The addition of chitosan further lowered its recovery to 5% (results not shown). In the differential flotation of Zn-Pb sulfide mixtures, EDTA slightly assisted with the depression of sphalerite caused by chitosan. As can be seen from Figure 4.2, sphalerite recovery dropped from slightly above 20% in the absence of EDTA, to about 10% after adding 5×10^{-4} mol/L EDTA. Also, the addition of EDTA significantly improved galena recovery, from slightly above 40% in the absence of EDTA to over 80% after adding 5×10^{-4} mol/L EDTA.

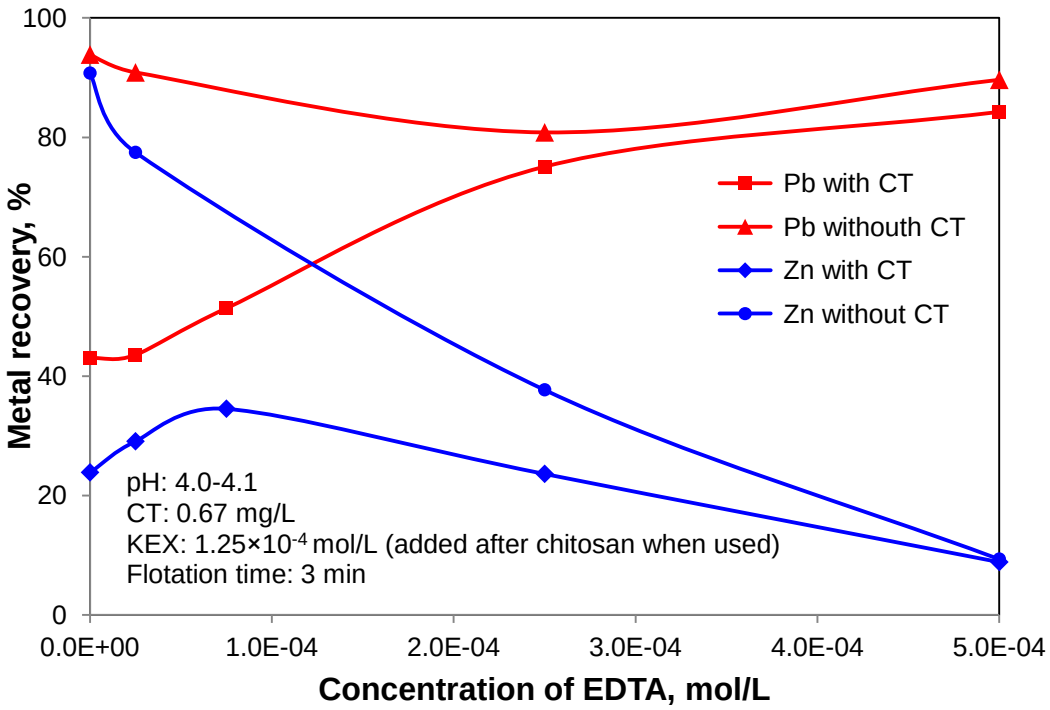

Figure 4.2 Flotation recovery of sphalerite and galena from their mixtures as a function of EDTA concentration. KEX: 1.25×10^{-4} mol/L; Chitosan: 0.67 mg/L when used; Condition time: 3 min; Flotation time: 3 min.

What may have happened in the flotation system was probably the removal of lead ions from sphalerite surface by the EDTA, and the removal of the oxidation products from galena surfaces, both of which probably helped lowering the amount of chitosan adsorbed on galena surfaces. The EDTA-cleaned sphalerite surface had a higher affinity to chitosan, adsorbed more chitosan and was thus more severely depressed at low EDTA concentration as can be seen from Figure 4.2 in the co-presence of EDTA and chitosan. As galena had a lower affinity to chitosan than sphalerite, the preferential adsorption of the chitosan on sphalerite would reduce the amount of chitosan available to galena, thus restoring its flotation recovery, as observed from Figure 4.2. In the meantime, the EDTA should also have removed the metal oxidation products from galena surface. This

may also lower the amount of chitosan that could adsorb on galena surface, leading to improved flotation recovery.

To verify, the sphalerite sample was treated with cupric nitrate so that the sphalerite was coated with copper. The copper-coated sphalerite was removed from the copper nitrate solution, dried and mixed with galena to carry out the flotation tests at pH 4. As can be seen from Figure 4.3, the Pb and Zn recoveries as a function of pH were very similar to the Pb and Cu recoveries in the galena-chalcopyrite mixtures reported earlier (Huang et al., 2012b). Galena was floated from the mixtures while sphalerite was depressed between pH 3.5-4.5. The results seem to indicate that when the flotation tests were conducted on galena-sphalerite mixtures at pH 4, the lead ions could adsorb on sphalerite surface making it indistinguishable from galena surface to chitosan. However, when the sphalerite surface was coated with copper ions, the lead ions did not show the detrimental effects.

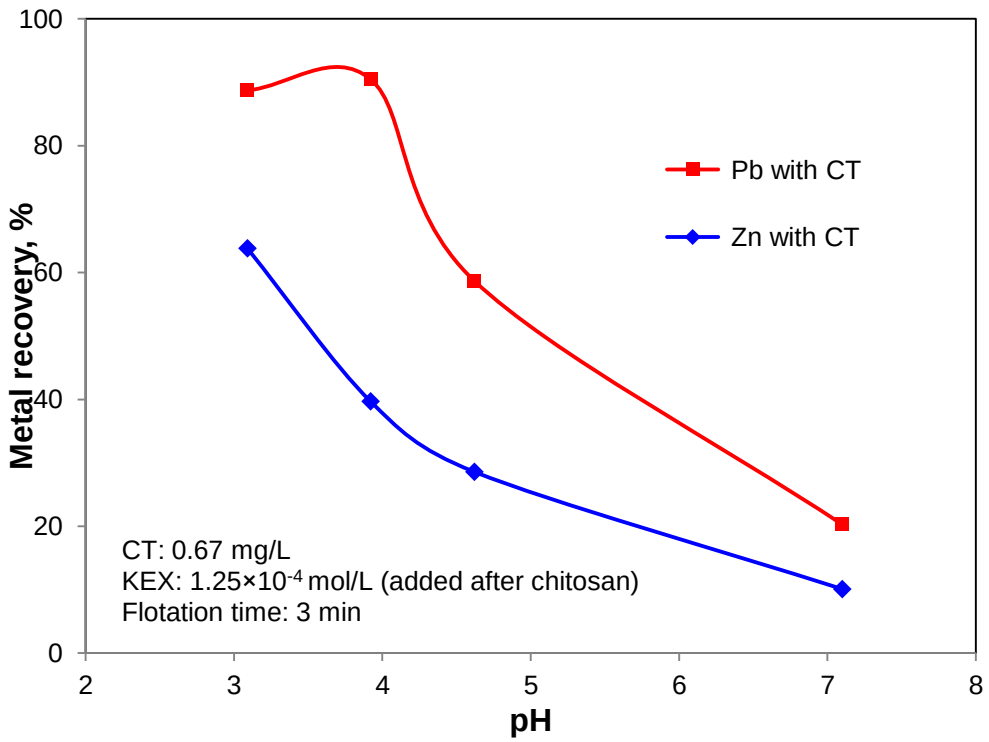

Figure 4.3 Flotation recovery of galena and copper-coated sphalerite from their mixtures as a function of pH. KEX: 1.25×10-4 mol/L; Chitosan: 0.67 mg/L; Condition time: 3 min; Flotation time: 3 min.

4.3.2 ToF-SIMS analyses of sphalerite after treatment with chitosan

To identify the stable reaction products between sphalerite and chitosan, positive ion mass spectra were recorded from sphalerite treated by chitosan and from copper-coated sphalerite treated by chitosan. Figure 4.4a shows part of the ion mass spectra of sphalerite treated by chitosan at pH 4. For the NH_x^+ species (x = 2, 3 and 4), NH_4^+ has the highest intensity compared with the other two species (NH_2^+ and NH_3^+). It is worth noting that due to cationization effect during ToF-SIMS measurements, the intensities of NH_4^+, NH_3^+ and NH_2^+ in fact reflect the concentrations of NH_3, NH_2 and NH in the sample, respectively. Therefore, the samples contained relatively higher concentrations of NH_3 than NH_2 and NH. This is consistent with literature as it has been reported that the *p*Ka of chitosan is

around 6.5 (Crini and Badot, 2008; Guibal, 2005; Sorlier et al., 2001), so that at pH 4 the amine groups ($–NH_2$) in chitosan should have been protonated. Meanwhile, Figure 4.4a shows that the intensity of $ZnNH_3^+$ was much higher than that of $ZnNH_2^+$ and $ZnNH_4^+$. Due to the cationization effect, $ZnNH_3^+$ represents $ZnNH_2$, indicating that strong interaction occurred between $–NH_2$ and zinc on sphalerite surface. This hypothesis was further supported by the XPS results (i.e., amine group NH_2 was the dominant species on high-resolution N 1s spectrum of sphalerite after chitosan treatment, as will be discussed later in section 4.3.3).

Part of the positive ion mass spectra of the copper-coated sphalerite treated by chitosan at pH 4 were shown in Figure 4.4b. Similar to Figure 4.4a, NH_4^+ was the predominant species of NH_x^+. However, for the metal-NH_x^+ species, $CuNH_4^+$ had the highest intensity in comparison with other Cu-NH_x^+. The results were very similar to the ToF-SIMS spectra obtained from chalcopyrite treated by chitosan reported earlier (Huang et al., 2012b).

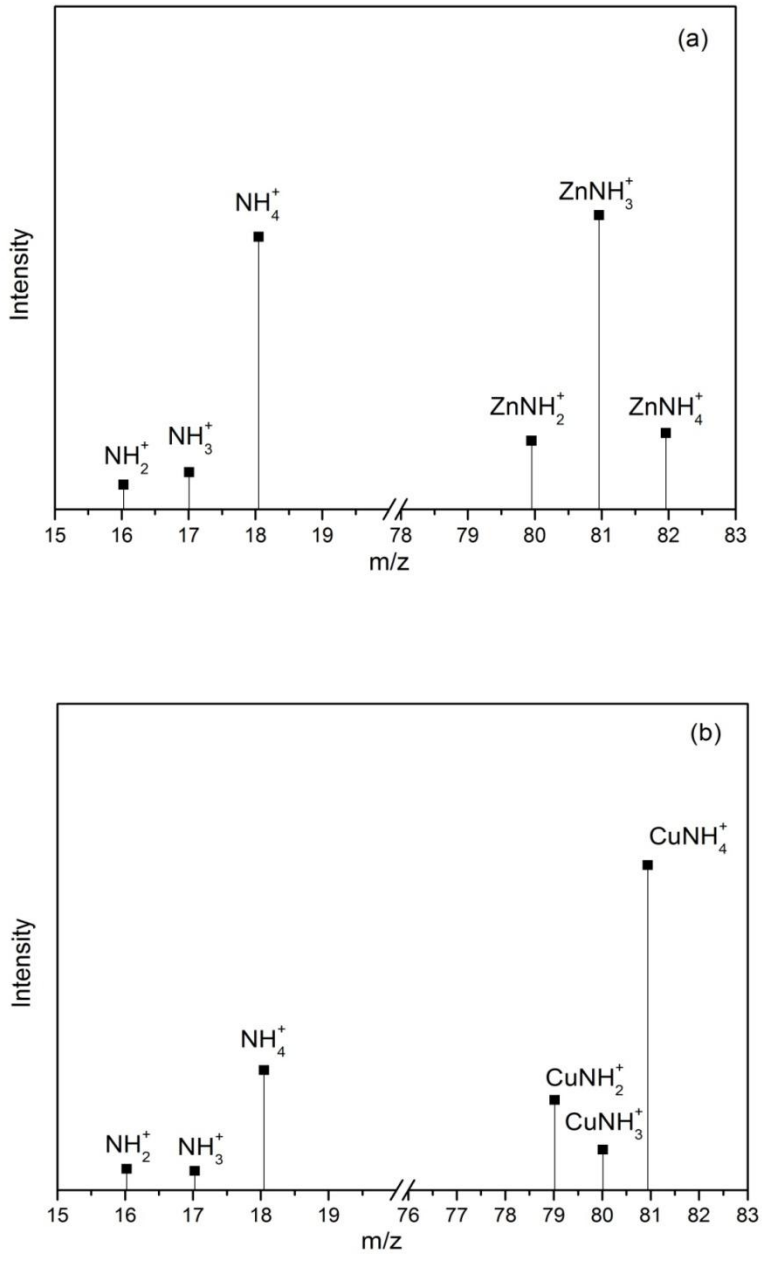

Figure 4.4 Part of the positive ion ToF-SIMS spectra of 171 μm × 171 μm region from the surface of (a) sphalerite-chitosan; (b) copper-coated sphalerite-chitosan.

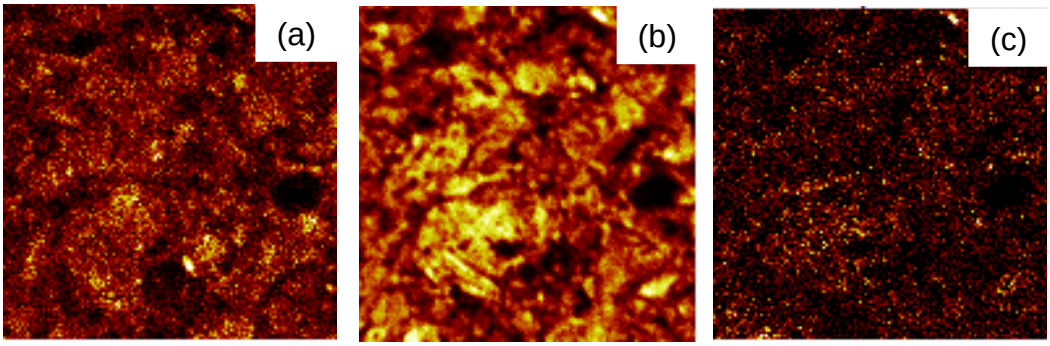

Figure 4.5 Positive-ion images of 171 μm × 171 μm region from the surface of copper-coated sphalerite after chitosan adsorption. (a) image of sphalerite (Zn^+); (b) image of Cu^+; (c) image of chitosan ($C_6H_{11}O_4N^+$).

Figure 4.5a shows the positive ion image of Zn^+ from copper-coated sphalerite treated by chitosan. As sphalerite was the only source of Zn^+, the distribution of Zn^+ can be considered as showing the presence of sphalerite. To study the effect of Cu^{2+} coating, the positive ion image of Cu^+ was also obtained and shown in Figure 4.5b. By comparison to Figure 4.5a, it can be seen that the image of Cu^+ in Figure 4.5b had similar pattern as sphalerite in Figure 4.5a, indicating that Cu^{2+} was indeed adsorbed on sphalerite surfaces. Furthermore, much higher intensity (brighter) was observed for Cu^+ than for Zn^+, showing that the sphalerite surface was dominated by copper ions but not by zinc ions. The mass fragment of $C_6H_{11}O_4N^+$ was selected and used to map the distribution of chitosan, which was shown in Figure 4.5c. It was obvious that chitosan was adsorbed on the copper-coated sphalerite surface.

4.3.3 XPS analyses of sphalerite and copper-coated sphalerite after treatment with chitosan

XPS analyses were used to examine the sphalerite and copper-coated sphalerite surfaces before and after chitosan treatment. The surface species, which

contribute to the flotation behaviours, were identified through the deconvoluted peaks of the photoelectron binding energy spectra. Comparing the XPS spectra before and after treatment with chitosan, significant binding energy shifts can be used to infer chemical interactions between sphalerite and chitosan. Due to the interference of carbon from chitosan, the binding energy of C 1s was not used as internal standard for peak calibration. The Zn $2p^{3/2}$ component was used to calibrate the binding energy peaks in the XPS analyses (Buckley et al., 1989; Fornasiero and Ralston, 2006; Kartio et al., 1998).

The high-resolution spectra were acquired on sphalerite with or without treatment with chitosan and are shown in Figure 4.6. Figure 4.6a and 6b show the N 1s and O 1s binding energy spectra of sphalerite at pH 4 without chitosan treatment, respectively. As can be seen from Figure 4.6a, the intensity of nitrogen is very low and can be considered as coming from background noise, thus it indicates that there was no nitrogen on the sphalerite sample. For the O 1s spectrum (Figure 4.6b), the broad O 1s peak could be fitted by two components, at 533.2 eV and 531.6 eV, respectively, for oxygen in hydroxides and oxides on sphalerite surface. The N 1s and O 1s spectra of the sphalerite after treatment by chitosan at pH 4 are shown in Figure 4.6c and 6d, respectively. As can be seen from Figure 4.6c, the relative high intensity of nitrogen indicates the adsorption of chitosan on sphalerite. The spectrum was fitted by three peaks. The peaks at 399.6 eV and 400.5 eV were originated from the amine ($–\underline{N}H_2$) and amide (O=C–$\underline{N}$H–) groups, respectively. The third peak at 401.6 eV was assigned to the protonated amine ($–\underline{N}H_3^+$). The three peaks for the pure chitosan were at 399.5, 400.5, and 401.9 eV, respectively (Huang et al., 2012b) The spectral deconvolution indicated that 63.4% and 23.6% of the nitrogen species adsorbed on sphalerite surfaces were amine and protonated amine, respectively. The remaining species (13.0%) was amide group. It seems that the amine, as the basic structure on the chitosan monomer, was the major species involved in the chitosan-sphalerite interaction. The shift of -0.3 eV of the protonated amine after reacting with sphalerite, which was significant as

the resolution of the instrument is 0.1 eV, probably indicated a chemisorption of the chitosan on sphalerite.

Figure 4.6d shows the O 1s spectral deconvolution of sphalerite after reacting with chitosan. Compared with Figure 4.6b, a new peak at 534.4 eV was observed while the other two peaks were almost identical. The new peak was assigned to C–OH (Amaral et al., 2005), which is the basic molecular structure unit of chitosan. Huang et al. (2012b) reported that the position of the O 1s peak in C-OH in chitosan was at 533.6 eV. The +0.8 eV binding energy shift shows that the hydroxyl groups from chitosan were involved in the adsorption of chitosan on sphalerite surface.

Similarly, Figure 4.7 shows the high-resolution spectra of N 1s and O 1s of copper-coated sphalerite before and after chitosan adsorption. As can be seen from Figure 4.7a, no nitrogen was detected on copper-coated sphalerite surface. After chitosan treatment, nitrogen was observed and three peaks were used to fit the spectrum. The major peak at 399.5 eV was assigned to amine ($–\underline{N}H_2$). The peaks at 400.3 eV and 401.7 eV were assigned to amide (O=C–<u>N</u>H–) and protonated amine ($–\underline{N}H_3^+$), respectively. The spectrum shows that 72.8% (the sum of amine and protonated amine) of the nitrogen species adsorbed on copper-coated sphalerite surfaces were deacetylated units while only 27.2% of the nitrogen species was acetyl units (amide). The results were consistent with that of nitrogen species adsorbed on chalcopyrite surfaces reported by Huang et al. (2012a), who showed that 77% of the nitrogen was from the deacetylated units and 23% was acetyl units.

Figure 4.7d shows the O 1s spectrum of copper-coated sphalerite after chitosan treatment. As can be seen, three peaks were found to fit the spectrum. Compared with the spectrum without chitosan treatment (Figure 4.7b), a new peak at 532.4 eV was identified in Figure 4.7d, and it was assigned to C–<u>O</u>H (Amaral et al., 2005). Compared with the O 1s binding energy of pure chitosan, 533.6 eV (Huang et al., 2012b), a binding energy shift of -1.2 eV was observed, indicating that the

hydroxyl groups in chitosan participated in the interaction between the copper-coated sphalerite and chitosan.

Huang et al. (2012b, Chapter 3 of this thesis) studied the XPS spectra of galena before and after chitosan adsorption. Chitosan was identified on galena surfaces after chitosan adsorption. However, by resolving the N 1s spectrum, they found that the acetyl units, which are from the parent compound chitin, were the major species responsible for adsorption. No protonated amine was observed on galena surface. In addition, there was no binding energy shift or the appearance of new peak on the galena surfaces after reacting with chitosan. The results indicate that the adsorption of chitosan on galena was through a different mechanism and was weaker than on either chalcopyrite or sphalerite.

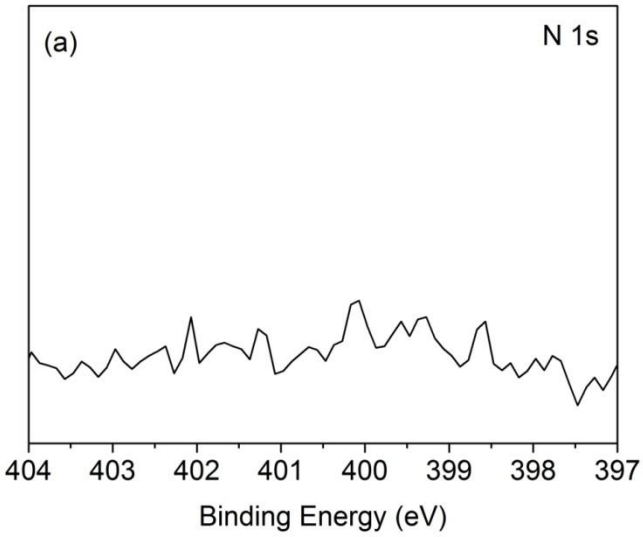

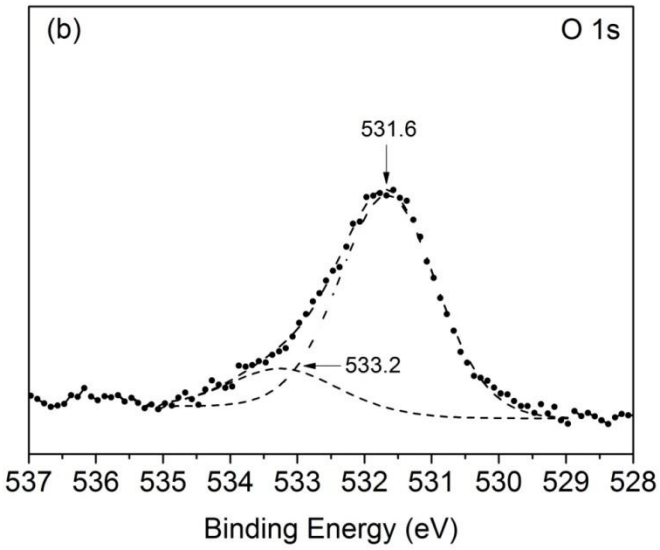
(b)
O 1s
531.6
533.2
537 536 535 534 533 532 531 530 529 528
Binding Energy (eV)

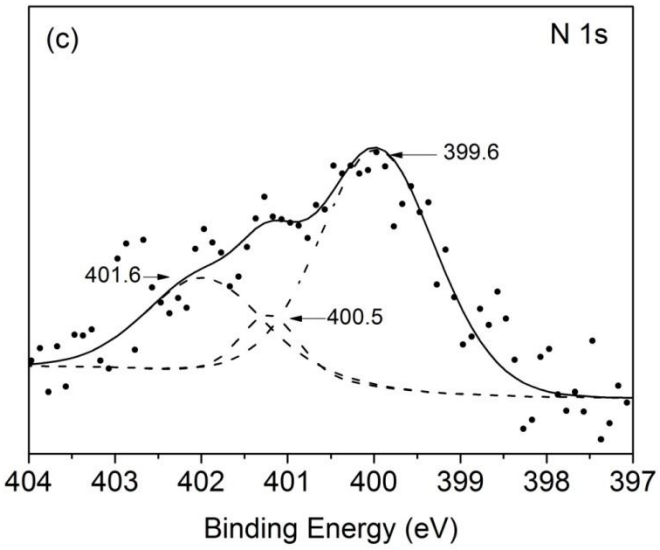
(c)
N 1s
399.6
401.6
400.5
404 403 402 401 400 399 398 397
Binding Energy (eV)

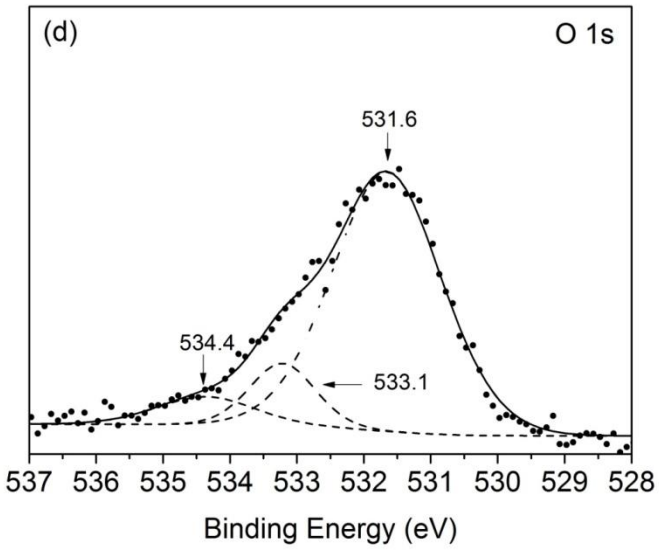

Figure 4.6 XPS narrow scan spectra with deconvoluted peaks for sphalerite: (a) N 1s spectrum, (b) O 1s spectrum; and chitosan-treated sphalerite: (c) N 1s spectrum, (d) O 1s spectrum.

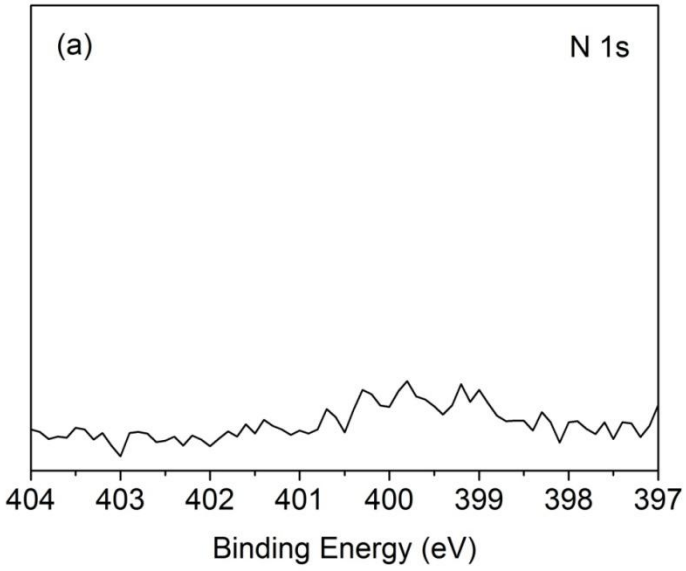
(a)
N 1s
404
403
402
401
400
399
398
397
Binding Energy (eV)

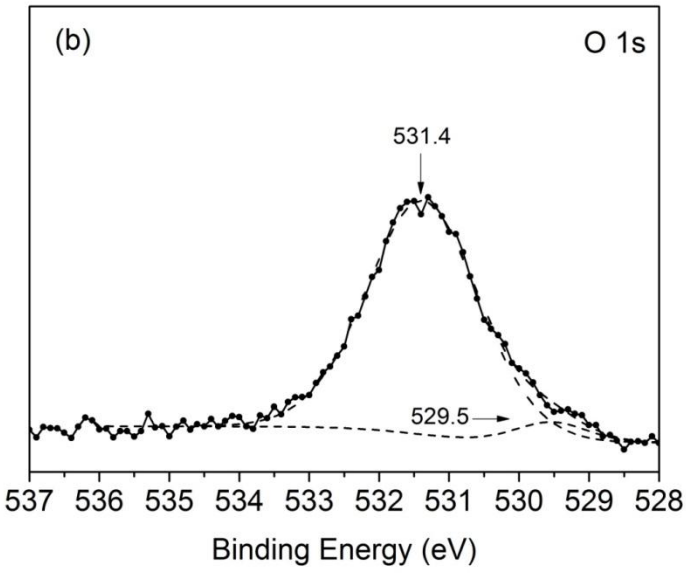
(b)
O 1s
531.4
529.5
537
536
535
534
533
532
531
530
529
528
Binding Energy (eV)

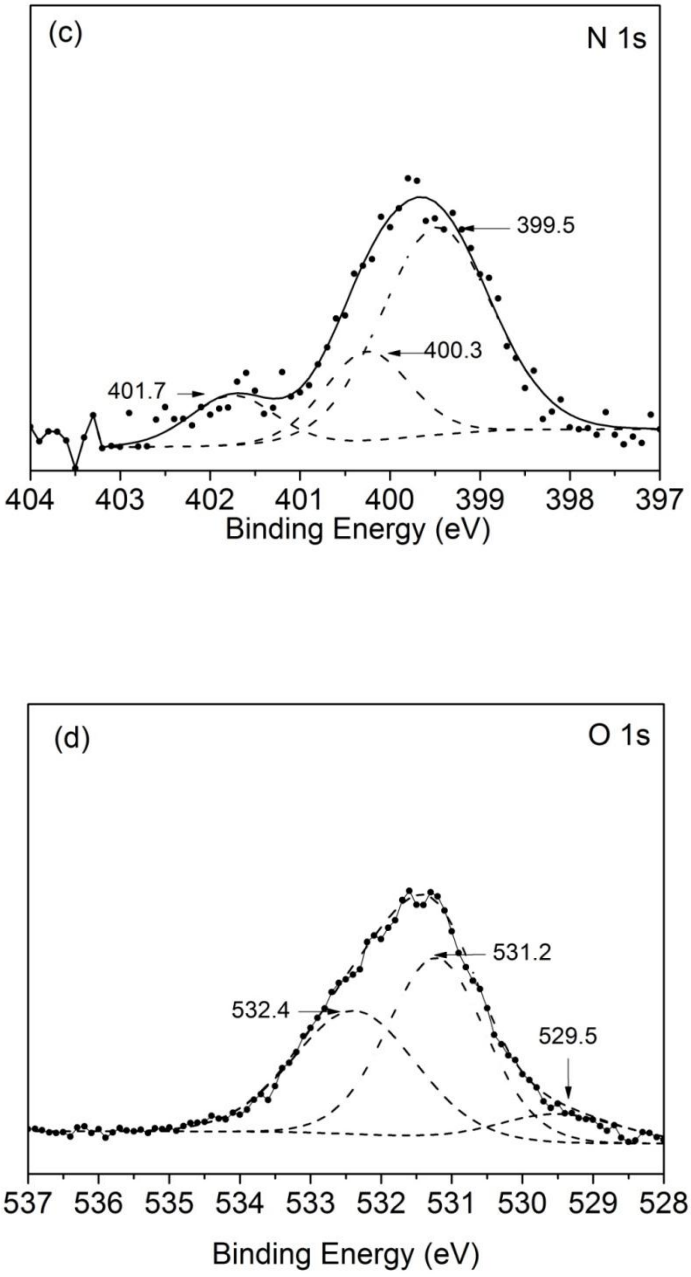

Figure 4.7 XPS narrow scan spectra with deconvoluted peaks for copper-coated sphalerite (a) N 1s spectrum (b) O 1s spectrum, and chitosan treated copper-coated sphalerite (c) N 1s spectrum (d) O 1s spectrum.

4.4. Conclusions

The application of chitosan as a potential selective depressant in the differential flotation of sphalerite-galena was studied. In the flotation of galena and sphalerite mixtures, it was observed that the addition of chitosan caused both minerals to be severely depressed. This was caused by the contamination of the sphalerite surface by lead ions, which likely came from the dissolution of oxidized galena in weakly acidic suspension. The addition of EDTA was found to enable the depression of sphalerite by chitosan while allowing galena to be floated at pH 4. On the other hand, when the sphalerite was previously coated by Cu^{2+} ions before mixing with galena, the addition of chitosan caused the sphalerite to be depressed while galena could be floated at pH 3.5-4.5, without the addition of EDTA.

ToF-SIMS and XPS analyses were performed to investigate the interactions of chitosan with sphalerite and copper-coated sphalerite. It was found that both the amine ($-NH_2$) and the hydroxyl (-OH) groups from chitosan were involved in its adsorption on sphalerite and copper-coated sphalerite, possibly through chemical interaction due to the observed binding energy shifts of both N 1s and O 1s electrons. Interestingly, ToF-SIMS analysis showed that on the chitosan-treated sphalerite surface, the $ZnNH_2$ was the dominant species, while on chitosan-treated copper-coated sphalerite surfaces, the $Cu\text{-}NH_3$ was the dominant species. Chitosan only showed weak interactions with galena as reported previously (Huang et al., 2012b), which explains the observed separation between galena and sphalerite with the use of chitosan.

4.5 References

Amaral, I., Granja, P. and Barbosa, M., 2005. Chemical modification of chitosan by phosphorylation: an XPS, FT-IR and SEM study. Journal of Biomaterials Science, Polymer Edition, 16(12): 1575-1593.

Basilio, C., Kartio, I. and Yoon, R.H., 1996. Lead activation of sphalerite during galena flotation. Minerals Engineering, 9(8): 869-879.

Boddu, V.M., Abburi, K., Talbott, J.L. and Smith, E.D., 2003. Removal of hexavalent chromium from wastewater using a new composite chitosan biosorbent. Environmental science & technology, 37(19): 4449-4456.

Buckley, A., Woods, R. and Wouterlood, H., 1989. An XPS investigation of the surface of natural sphalerites under flotation-related conditions. International Journal of Mineral Processing, 26(1-2): 29-49.

Burke, A., Yilmaz, E., Hasirci, N. and Yilmaz, O., 2002. Iron (III) ion removal from solution through adsorption on chitosan. Journal of applied polymer science, 84(6): 1185-1192.

Cao, M. and Liu, Q., 2006. Reexamining the functions of zinc sulfate as a selective depressant in differential sulfide flotation--The role of coagulation. Journal of colloid and interface science, 301(2): 523-531.

Chandra, A.P. and Gerson, A.R., 2009. A review of the fundamental studies of the copper activation mechanisms for selective flotation of the sulfide minerals, sphalerite and pyrite. Advances in colloid and interface science, 145(1-2): 97-110.

Choy, K.K.H., Porter, J.F. and Mckay, G., 2001. A film-pore-surface diffusion model for the adsorption of acid dyes on activated carbon. Adsorption, 7(3): 231-247.

Chung, Y.S., Lee, K.K. and Kim, J.W., 1998. Durable press and antimicrobial finishing of cotton fabrics with a citric acid and chitosan treatment. Textile research journal, 68(10): 772.

Crini, G. and Badot, P.M., 2008. Application of chitosan, a natural aminopolysaccharide, for dye removal from aqueous solutions by adsorption processes using batch studies: A review of recent literature. Progress in Polymer Science, 33(4): 399-447.

Egger, G., Cameron-Smith, D. and Stanton, R., 1999. The effectiveness of popular, non-prescription weight loss supplements. Med J Aust, 171(11-12): 604-8.

Finkelstein, N.P., 1997. The activation of sulfide minerals for flotation: a review. International Journal of Mineral Processing, 52(2-3): 81-120.

Fornasiero, D. and Ralston, J., 2006. Effect of surface oxide/hydroxide products on the collectorless flotation of copper-activated sphalerite. International Journal of Mineral Processing, 78(4): 231-237.

Foster, L.S., 1928. Preparation of xanthates and other organic thiocarbonates. Utah Eng. Exp. Sta.

Fuerstenau, M., Clifford, K. and Kuhn, M., 1974. The role of zinc-xanthate precipitation in sphalerite flotation. International Journal of Mineral Processing, 1(4): 307-318.

Gerente, C., Lee, V., Cloirec, P.L. and McKay, G., 2007. Application of chitosan for the removal of metals from wastewaters by adsorption-mechanisms and models review. Critical reviews in environmental science and technology, 37(1): 41-127.

González Siso, M. et al., 1997. Enzyme encapsulation on chitosan microbeads. Process Biochemistry, 32(3): 211-216.

Guibal, E., 2005. Heterogeneous catalysis on chitosan-based materials: a review. Progress in Polymer Science, 30(1): 71-109.

Houshyar, S. and Amirshahi, S.H., 2002. Treatment of cotton with chitosan and its effect on dyeability with reactive dyes. Iranian Polymer Journal, 11: 295-302.

Huang, P., Cao, M. and Liu, Q., 2012a. Using chitosan as a selective depressant in the differential flotation of Cu–Pb sulfides. International Journal of Mineral Processing, 106–109(0): 8-15.

Huang, P., Cao, M. and Liu Q., 2012b. Adsorption of chitosan on chalcopyrite and galena in aqueous suspensions. Colloids and Surfaces A: Physicochemical and Engineering Aspects, 409: 167-175.

Ilium, L., 1998. Chitosan and its use as a pharmaceutical excipient. Pharmaceutical Research, 15(9): 1326-1331.

Jocić, D., Julia, M. and Erra, P., 1997. Application of a chitosan/nonionic surfactant mixture to wool assessed by dyeing with a reactive dye. Journal of the Society of Dyers and Colourists, 113(1): 25-31.

Kartio, I., Basilio, C. and Yoon, R.H., 1998. An XPS study of sphalerite activation by copper. Langmuir, 14(18): 5274-5278.

Koide, S., 1998. Chitin-chitosan: properties, benefits and risks. Nutrition research, 18(6): 1091-1101.

Laskowski, J.S., Liu, Q. and Zhan, Y., 1997. Sphalerite activation: Flotation and electrokinetic studies. Minerals Engineering, 10(8): 787-802.

Loke, W.K., Lau, S.K., Yong, L.L., Khor, E. and Sum, C.K., 2000. Wound dressing with sustained anti-microbial capability. Journal of biomedical materials research, Part A, 53(1): 8-17.

Martino, A., Pifferi, P. and Spagna, G., 1996. Immobilization of [beta]-glucosidase from a commercial preparation. Part 2. Optimization of the immobilization process on chitosan. Process Biochemistry, 31(3): 287-293.

Muzzarelli, R., 1989. Amphoteric derivatives of chitosan and their biological significance. Chitin and chitosan. New York: Elsevier Applied Science: 87–99.

Ngah, W., Teong, L. and Hanafiah, M., 2010. Adsorption of dyes and heavy metal ions by chitosan composites: A review, Carbohydrate Polymers. Elsevier, pp. 1446-1456.

Prestidge, C.A., Skinner, W.M., Ralston, J. and Smart, R.S.C., 1997. Copper (II) activation and cyanide deactivation of zinc sulfide under mildly alkaline conditions. Applied Surface Science, 108(3): 333-344.

Rashchi, F. and Finch, J.A., 2006. Deactivation of Pb-contaminated sphalerite by polyphosphate. Colloids and Surfaces A: Physicochemical and Engineering Aspects, 276(1-3): 87-94.

Ravi Kumar, M.N.V., 2000. A review of chitin and chitosan applications. Reactive and functional polymers, 46(1): 1-27.

Rinaudo, M., 2006. Chitin and chitosan: Properties and applications. Progress in Polymer Science, 31(7): 603-632.

Se-Kwon, K., 2010. Chitin, Chitosan, Oligosaccharides and Their Derivatives : Biological Activities and Applications. 69-70.

Shin, Y. and Yoo, D.I., 1998. Use of chitosan to improve dyeability of DP-finished cotton (II). Journal of applied polymer science, 67(9): 1515-1521.

Sorlier, P., Denuzière, A., Viton, C. and Domard, A., 2001. Relation between the degree of acetylation and the electrostatic properties of chitin and chitosan. Biomacromolecules, 2(3): 765-772.

Srinivasa, P., Baskaran, R., Ramesh, M., Harish Prashanth, K. and Tharanathan, R., 2002. Storage studies of mango packed using biodegradable chitosan film. European Food Research and Technology, 215(6): 504-508.

Struszczyk, H., 1987. Microcrystalline chitosan. I. Preparation and properties of microcrystalline chitosan. Journal of applied polymer science, 33(1): 177-189.

Struszczyk, M., 2002. Chitin and chitosan—Part II. Applications of chitosan. Polimery, 47(6): 396-403.

Teixeira, M.A. et al., 1990. Assessment of chitosan gels for the controlled release of agrochemicals. Industrial & engineering chemistry research, 29(7): 1205-1209.

Tokura, S. and Tamura, H., 2007. Chitin and chitosan. Comprehensive Glycoscience from Chemistry to Systems biology, 2: 449-474.

Wang, L., Khor, E., Wee, A. and Lim, L.Y., 2002. Chitosan-alginate PEC membrane as a wound dressing: Assessment of incisional wound healing. Journal of biomedical materials research, Part A, 63(5): 610-618.

CHAPER 5

SELECTIVE DEPRESSION OF PYRITE WITH CHITOSAN IN Pb-Fe SULFIDE FLOTATION*

5.1 Introduction

Pyrite (FeS_2), the most widely occurring sulfide mineral, is usually found associated with other base-metal minerals and coal. Pyrite is readily floatable up to pH 11 with thiol collectors (such as xanthate) (King, 1982; Wang and Eric Forssberg, 1991). Therefore, pyrite is easily floated to the concentrate and compromises the concentrate grade of value sulfide minerals. Due to the high sulfur content in pyrite (53.45% from its chemical formula), its inclusion in the concentrate raises the sulfur content of the froth product and reduces its economic value. It also increases the energy consumption in the subsequent metal extraction and refining operations, and causes potential environmental pollution through sulfur dioxide emissions.

The rejection of pyrite requires a suitable depressant during flotation. To reject pyrite during the flotation of lead sulfide (galena), sodium cyanide together with lime is commonly used as selective depressants for pyrite while xanthate is used as a collector to float galena (Atalay, 1996; King, 1982). As it is desirable to replace sodium cyanide with environmentally benign chemicals, organic polymers have been tested and some have shown to be selective depressants that could potentially replace the toxic inorganic depressants (Atalay, 1996; Boulton et al., 2001). A recent report by Huang et al. has indicated that chitosan could be used as a depressant in Cu-Pb and Zn-Pb separation (Huang et al., 2012a; Huang et al., 2012b, i.e., Chapters 2 and 3 of this thesis). Huang et al showed that chitosan

* This paper was published in Minerals Engineering in 2013: P. Huang, M. Cao and Qi Liu, 2013. Selective depression of pyrite with chitosan in Pb-Fe sulfide flotation. Minerals Engineering, Vol. 46-47, 45-51. http://dx.doi.org/10.1016/j.mineng.2013.03.027.

specifically absorbed on chalcopyrite and sphalerite surface but not on galena surface. Motivated by these observations, in this work, chitosan was tested as an alternative depressant for pyrite in the differential flotation of Pb-Fe sulfides.

Chitosan and its derivatives have been used as adsorbents to remove heavy metal ions and dyes from industrial wastewater. The outstanding properties of chitosan were principally due to the amine and the hydroxyl groups in the polymer structure, which react with metal ions through chelation (Boddu et al., 2003; Burke et al., 2002; Choy et al., 2001; Chung et al., 1998; Jocić et al., 1997; Onsosyen and Skaugrud, 1990; Ravi Kumar, 2000; Shin and Yoo, 1998). In the study of chitosan application in single sulfide mineral flotation, it was observed that chalcopyrite, galena and sphalerite were all depressed to some extent (Huang et al., 2012a; Huang et al., 2013, Chapters 2 and 4 of this thesis), which was consistent with the results of metal ion adsorption on chitosan from aqueous solution. However, in the flotation of mineral mixtures, competitive adsorption occurred and chitosan predominately adsorbed on chalcopyrite (Huang et al., 2012a) and sphalerite (Huang et al., 2013) but not on galena. The competitive adsorption is in general agreement with results of selective adsorption of metal ions on chitosan in binary metal species systems pointed out by Vold et al. (2003). The selective adsorption behaviors of adsorbents with functional groups such as amine, iminodiacetic and thiol have attracted significant amount of attention to study their prospective application (Guibal, 2004; Höll et al., 1991; Kiefer and Hoell, 2001; Lam et al., 2006a; Pavan et al., 2003; Stöhr et al., 2001; Vilensky et al., 2002). However, the selective adsorption mechanism has not been explained in detail, especially for chitosan. In this study, we have attempted to elucidate the adsorption mechanism and examine the prospective selective adsorption behavior of chitosan in sulfide flotation systems.

The complimentary surface analysis techniques, time-of-flight secondary ion mass spectrometry (ToF-SIMS) and X-ray photoelectron spectroscopy (XPS) were applied to investigate the mineral surfaces after treatment with chitosan.

Through the collection of the ToF-SIMS ion mass spectra, the chitosan distribution was mapped on the pyrite-galena mixtures, directly showing the adsorption of chitosan on pyrite or galena surfaces. Furthermore, the fragmentation pattern was derived from the spectral data which revealed the characteristic peaks corresponding to reaction species between minerals and chitosan. On the other hand, XPS measurements can identify the chemical states of individual elements. The combination of XPS and ToF-SIMS would shed light on the interaction mechanisms between chitosan and the studied sulfide minerals.

5.2 Experimental

5.2.1 Materials

Pyrite (FeS_2) and galena (PbS) samples were bulk-pack minerals purchased from Ward's Scientific Establishment, Ontario, Canada. The minerals were separately crushed and hand-picked to remove minor inclusions such as quartz and calcite. The hand-picked lumps of minerals were crushed and dry ground in a mechanized agate mortar/pestle grinder, and screened to -75+38 μm and -20 μm size fractions. The -75+38 μm particles were used in flotation tests (either single mineral or mineral mixtures). The -20 μm particles were used in surface analysis including ToF-SIMS and XPS. X-ray diffraction analysis showed that the samples were free from impurities. According to the chemical formula of pyrite (FeS_2) and galena (PbS), the chemical analysis results of iron and lead indicated that the pyrite sample contained 93.1% FeS_2 and the galena sample contained 97.0% PbS. To minimize surface oxidation, all the ground samples were sealed in plastic bottles and stored in a freezer at below -10 ℃.

Chitosan was purchased from Sigma-Aldrich Canada. The vendor's data showed that the molecular weight of the chitosan ranged from 100,000 to 300,000 Dalton and the degree of deacetylation was 75-85%. It was used without further

purification. Solution pH was modified by the addition of HCl and NaOH (Fisher Scientific Canada). Potassium ethyl xanthate (KEX), supplied by Prospec Chemicals Ltd., Canada, was added as a collector. It was purified by recrystallization with ethyl ether anhydrous and acetone (Fisher Scientific, Canada) following the protocol of Foster (1928). Manganese sulfate monohydrate ($MnSO_4 \cdot H_2O$), cupric chloride dihydrate ($CuCl_2 \cdot 2H_2O$) and calcium chloride anhydrous ($CaCl_2$) were purchased from Fisher Scientific Canada. All the chemicals were of analytical grade as received and were used in the experimental work without further purification. Distilled water was used to prepare all the solution in the study.

5.2.2 Flotation

Small-scale flotation tests were performed to examine the selective depressant function of chitosan in the flotation of pyrite-galena mixtures using a glass flotation tube made in-house. Details of the flotation tube were described elsewhere (Cao and Liu, 2006). In a typical flotation test, 1.5 g of the -75+38 μm mineral samples were stirred with 150 mL distilled water in a 250 mL beaker by a magnetic stir bar. Following pH adjustment, 1.0 mL of 0.1 g/L chitosan stock solution, and 1.0 mL of 3 g/L KEX stock solution, were added sequentially into the stirring pulp and conditioned for 3 min each. The conditioned mineral slurry was transferred to the flotation tube and floated for 3 min using high purity nitrogen gas at 5 mL/min. Both the froth product and the tailings were collected and dried for mineral recovery calculations. In the mineral mixture flotation tests, the froth product and the tailings were dissolved with aqua regia and the Fe and Pb contents were measured using a Varian SpectrAA-220FS (Varian, USA) atomic absorption spectrometer (AAS).

5.2.3 ToF-SIMS analysis

A ToF-SIMS IV spectrometer (ION-TOF GmbH) was utilized for the ToF-SIMS measurements by using 25 keV Bi^+ primary ions. The positive spectra were collected from each sample with an area of 177 μm × 177 μm. The targeted fragments were selected from the acquired spectra, and images were outlined by the mass-selected ion intensity in a burst alignment mode with pixels of 128 × 128 per image.

To prepare mineral samples for ToF-SIMS analysis, 1 g mineral mixture of pyrite and galena (weight ratio 1:1) were added to 100 mL distilled water at pH 4 or 6. The slurry was conditioned with 0.3 mg of chitosan (3 mL of 0.1 g/L chitosan) in a SI-600 shaking incubator (Jeio Tech, USA) for 30 min, and then filtered and dried. The ToF-SIMS spectra acquisition was conducted within 12 hours after sample preparation.

5.2.4 XPS measurements

As a complementary method to detect the type of mineral surface species after chitosan adsorption, XPS analysis was applied to acquire spectra from surface by an AXIS 165 X-ray photoelectron spectrometer (Kratos Analytical, USA) equipped with a monochromatic Al Kα X-ray source (hν = 1486.6 eV). The measurements were conducted inside the analytical chamber with vacuum pressure below 3×10^{-8} Pa. The analyzed sample was first subjected to a survey scan to identify chemical components, followed by high-resolution scans on a certain element from an area of 400 μm × 700 μm. The analyzer pass energy for the survey and high-resolution scans were 160 eV and 20 eV, respectively. Charge neutralization did not apply in the spectra collection. Casa XPS Version 2.3.15 instrument software was used to analyze all the obtained spectra. For the high-resolution spectra, individual Gaussian-Lorentzian peaks were employed to resolve binding energy peaks. The background was subtracted by the Shirley-type method. The processed spectra were imported and calibrated according to previously published data by a graphic software package (Origin, OriginLab Corp)

to display the optimal fitting peaks of the high-resolution spectra. Due to the slight charging identified in the measurement, the S 2p component (BE = 162.7 eV) was used as an internal standard to calibrate the spectra. In this equipment, a binding energy shift over 0.1 eV is considered significant.

The mineral samples for XPS measurements were prepared in a similar way as the samples for ToF-SIMS analysis, except that only single mineral was used. To prepare the sample, 1 g mineral (pyrite or galena) was mixed with 100 mL distilled water at pH 4 and 2 mg of chitosan (20 mL of 0.1 g/L chitosan) was added in the mineral slurry. The slurry was placed in an incubator and conditioned for 30 min at 25 ℃. Afterwards, the sample was filtered and deposited to dry in a desiccator in vacuum. To minimize oxidation, all the XPS measurements were conducted within 12 h after sample preparation.

5.2.5 Adsorption study

The adsorption of single and binary metal species on chitosan was measured after shaking the slurry in an incubator at 250 rpm, 25 ℃, for 30 min. Manganese sulfate monohydrate, cupric chloride dihydrate and calcium chloride anhydrous were used to prepare the metal salt solutions. Chitosan (0.1 g) was dispersed in 50 mL distilled water in a conical flask, and this was followed by the addition of a given amount of solution with preset metal ion concentration. The suspension was shaken for 30 min at 250 rpm and 25 ℃, and then filtered. The supernatant was used to determine the equilibrium concentrations of the metal ions using the Varian AAS. The adsorption density of the metal ions on chitosan was calculated by the difference between the initial concentration and the equilibrium concentration.

5.3 Results and Discussion

5.3.1 Flotation tests

Single mineral flotation tests of pyrite with and without chitosan as a depressant were carried out, and the results are shown in Figure 5. 1. The recoveries of single mineral flotation of galena are also plotted in Figure 5. 1 using data published earlier (Huang et al., 2012b, Chapter 3). As can be seen, in the presence of potassium ethyl xanthate (KEX), both pyrite and galena were readily floatable with recoveries over 90% in acidic and weakly alkaline solutions up to pH 8. When chitosan (0.67 mg/L) was added prior to KEX, pyrite recovery dropped from 95% to 37% at pH 3.2. At higher pH, the recovery of pyrite decreased further from 37% to 22% and stayed at 22-25% in the tested pH range (up to 9). After adding chitosan prior to KEX, the flotation of galena was also depressed and its recovery was approximately 40% between pH 4 and 9. Although pyrite was more severely depressed than galena, there was no indication of a separation window based on the single mineral flotation test results.

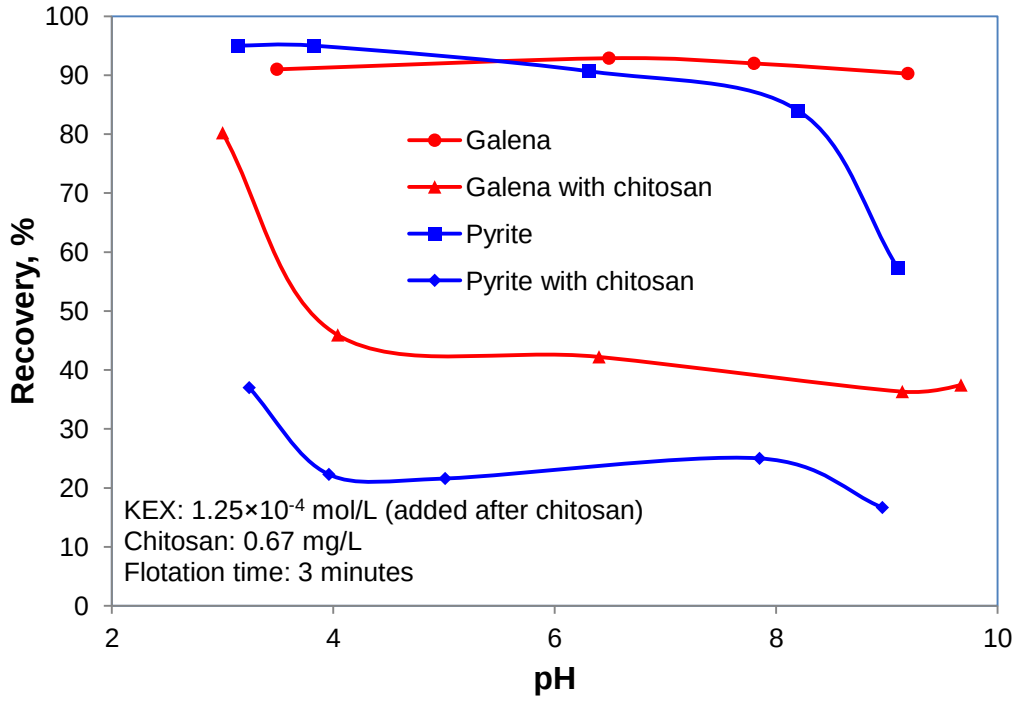

Figure 5.1 Flotation of single minerals of pyrite and galena as a function of pH in the presence and absence of chitosan as a depressant. (KEX: 1.25×10^{-4} mol/L; Chitosan: 0.67 mg/L; Condition time: 3 min; Flotation time: 3 min)

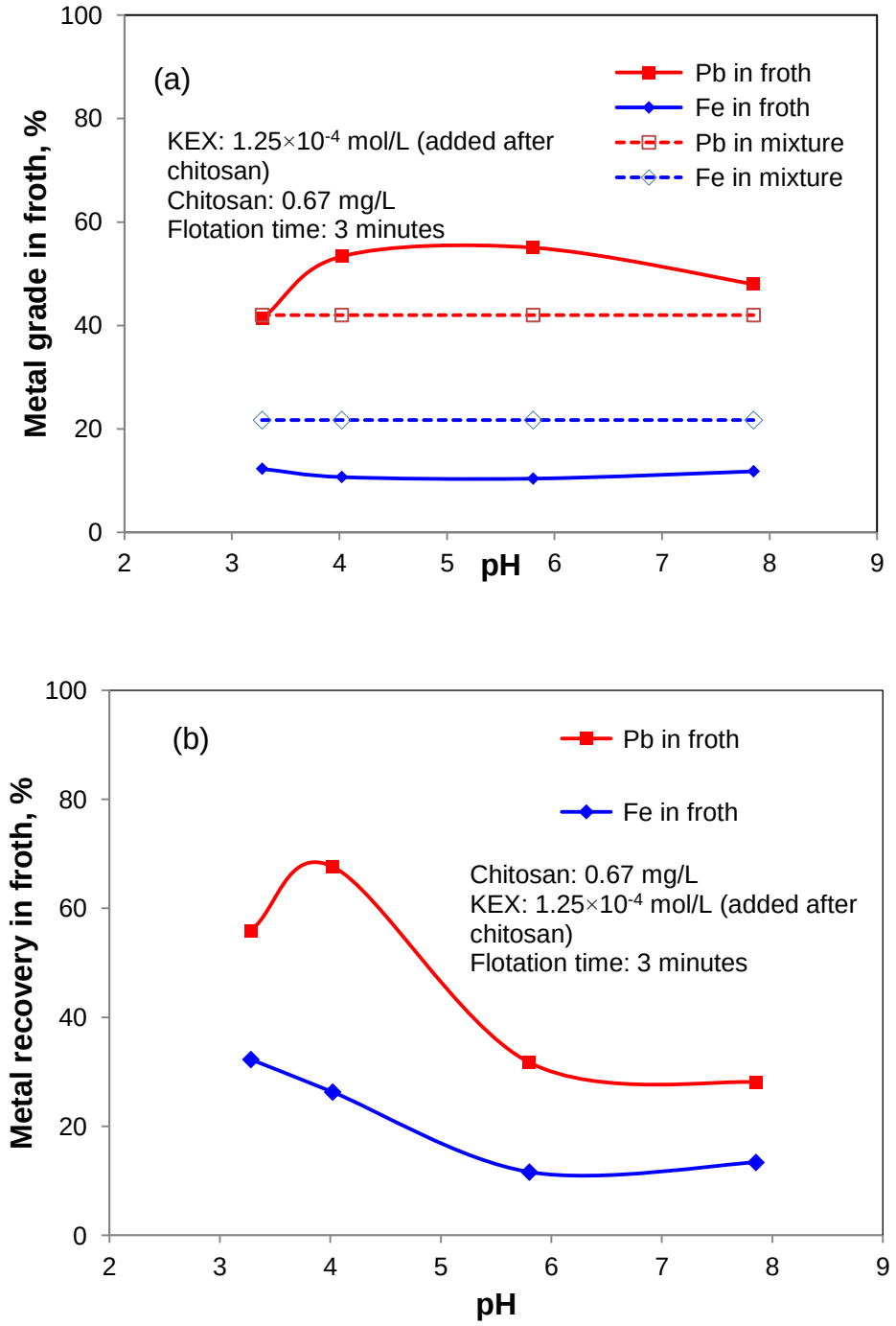

Figure 5.2 Flotation of mixtures of pyrite and galena (weight ratio 1:1) as a function of pH. (a). Metal grade in froth products; (b). Metal recovery in froth products. (KEX: 1.25×10^{-4} mol/L; Chitosan: 0.67 mg/L; Condition time: 3 min; Flotation time: 3 min)

Flotation tests were carried out on pyrite-galena mixtures (weight ratio 1:1) and the metal grade and recovery of pyrite and galena in the flotation concentrate were shown in Figure 5.2a and 2b, respectively. As can be seen, the Pb grade in the flotation concentrate was over 50% while it was 42% in the mixture before flotation. The Fe grade in the concentrate was 10%, representing a more than 50% reduction from the Fe grade in the flotation feed. The metal recovery (Figure 5.2b) shows that a separation window existed and the optimum was around pH 4. At this pH, galena recovery from the mixture was 68% while that of pyrite was 23%. Compared with single mineral flotation results (Figure 5.1), it can be seen that galena recovery was much higher (68% in the mixture versus 40% in the single mineral flotation). The difference shows that when both galena and pyrite were present in the suspension, chitosan probably preferentially adsorbed on pyrite.

5.3.2 Surface characterization

5.3.2.1 ToF-SIMS measurement of sulfide minerals treated with chitosan

The flotation results showed that pyrite was selectively depressed in the pyrite-galena mixture due to the addition of chitosan as a depressant. In order to verify the possible selective adsorption of chitosan on pyrite but not on galena, ToF-SIMS positive-ion mass spectra were obtained from the surface of pyrite-galena mixtures after chitosan treatment at pH 4 and 6. Figure 5.3 and Figure 5.4 show the positive-ion images of Fe^+, $C_6H_{11}O_4N^+$ and Pb^+, respectively, at pH 4 and pH 6. In the mineral mixture, pyrite was the only source for the fragment of Fe^+, so the spectra of Fe^+ can be considered as that of pyrite. Likewise, the image of Pb^+ was recognized as the distribution of galena in the mixture. The fragment of $C_6H_{11}O_4N^+$, as the monomer for chitosan, was considered to represent chitosan. As can be seen from Figure 5.3, at pH 4, even though the intensity of chitosan was low, the pattern of the image can be identified as similar to that of pyrite, and only overlapped with galena on rare spots.

Figure 5.2 shows that both pyrite and galena were more severely depressed at pH 6 than at pH 4. This was especially true for galena, and its recovery dropped from 68% (at pH 4) to 32% (at pH 6). However, the recovery difference between galena and pyrite was still as high as 21% (32% for galena and 11% for pyrite). The positive-ion mass spectra were collected from the mineral mixtures at pH 6, and the maps of specific fragments were generated by the ionic mass selected from the spectra. As can be seen, the relative intensity of chitosan to pyrite was higher at pH 6 (Figure 5.4) in comparison with pH 4 (Figure 5.3), indicating higher adsorption density of chitosan on pyrite at pH 6. By the same token, more similar areas with relative high intensity were observed when the images of chitosan and galena were compared (Figure 5.4b and 4c). The results indicated that chitosan adsorbed on both pyrite and galena but the intensity of chitosan on pyrite was higher than that on galena.

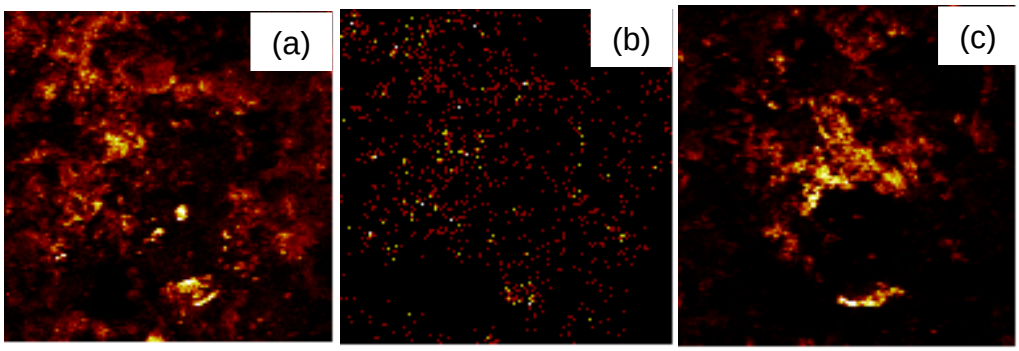

Figure 5.3 Positive-ion images of an 177 μm ×177 μm area from the surface of a mixture of pyrite and galena (weight ratio 1:1) after chitosan adsorption at pH 4. (a) image of Fe^+; (b) image of $C_6H_{11}O_4N^+$; (c) image of Pb^+.

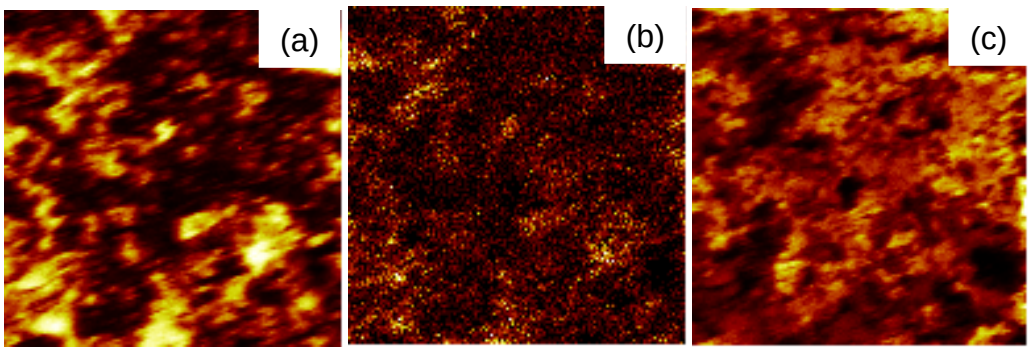

Figure 5.4 Positive-ion images of an 177 μm ×177 μm area from the surface of a mixture of pyrite and galena (weight ratio 1:1) after chitosan adsorption at pH 6. (a) image of Fe^+; (b) image of $C_6H_{11}O_4N^+$; (c) image of Pb^+.

5.3.2.2 XPS analyses of sulfide minerals treated with chitosan

XPS spectra were collected from the pyrite mineral surface before and after chitosan treatment at pH 4 and 6. The XPS analyses of galena after chitosan adsorption were reported earlier (Huang et al., 2012b). Figure 5.5a and 5c show the high-resolution spectra in the binding energy range for N 1s on pyrite before chitosan treatment at pH 4 and 6, and they show that, as expected, no N 1s peaks were observed on the pyrite surface. After treatment with chitosan, the XPS survey scans showed nitrogen peaks on pyrite at both pH 4 and 6, indicating that chitosan adsorbed on the mineral surface. In order to identify the chemical state of the adsorbed nitrogen, high-resolution scans were performed and the obtained spectra deconvoluted. The results are shown in Figure 5.5b and 5d. As can be see, two peaks were fitted to the spectra obtained at both pH 4 and 6. The major peak at 399.7 eV was assigned to amine ($-\underline{N}H_2$) and the peak at 401.8 eV probably originated from protonated amine ($-\underline{N}H_3^+$). The positions of the binding energy peaks of the two nitrogen components were the same at pH 4 and 6, but the peak intensities were different. At pH 4, the relative concentrations (calculated from relative peak intensities) of amine and protonated amine were 60% and 40%, respectively. When the pH was raised to 6, the concentration of amine increased

to 84% and the concentration of the protonated amine decreased to 16%. Compared to the N 1s spectrum of chitosan (Huang et al., 2012a), the binding energy of amine shifted from 399.5 eV to 399.8 eV, suggesting that a chemical adsorption may have occurred between chitosan and pyrite.

In addition to the N 1s binding energy spectra, high resolution binding energy spectra of O 1s were collected from pyrite treated with chitosan at pH 4 and 6. The obtained O 1s spectra for pyrite at pH 4 and pH 6 (Figure 5.6a and 6c) were deconvoluted into $\underline{O}H^-$ of the hydroxides (531.7 eV), O^{2-} ions of the oxides (530.3 eV) and H_2O on the surface (533.3 eV) (Bonnissel-Gissinger et al., 1998). After chitosan treatment at pH 4 and pH 6 (Figure 5.6b and 6d), the peaks at 531.7 eV and 530.2 eV did not shift, but the peak at 533.3 eV shifted to lower values, to 532.9 eV (pH 4) and 533.0 eV (pH 6), respectively. The shift was probably from the adsorbed chitosan, which was assigned to C-$\underline{O}$H in the basic structural unit of chitosan. It seems that the C-OH, combined with amine group, reacted with pyrite surface and formed a stable complex, which led to its flotation depression.

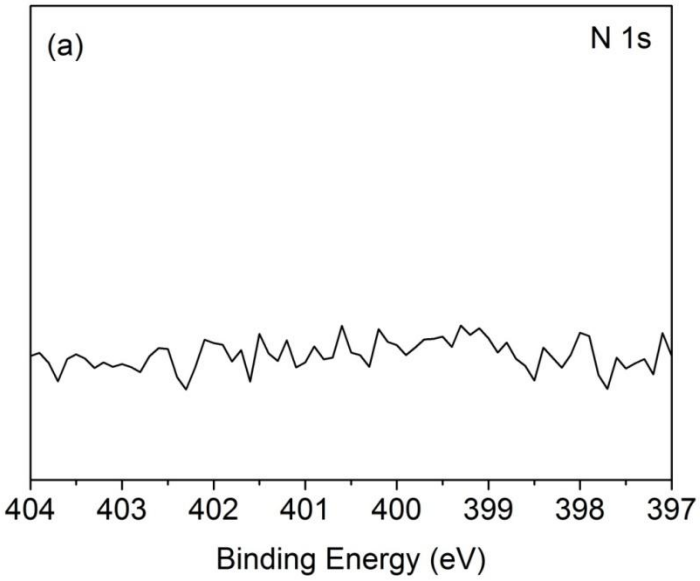
(a)
N 1s
404
403
402
401
400
399
398
397
Binding Energy (eV)

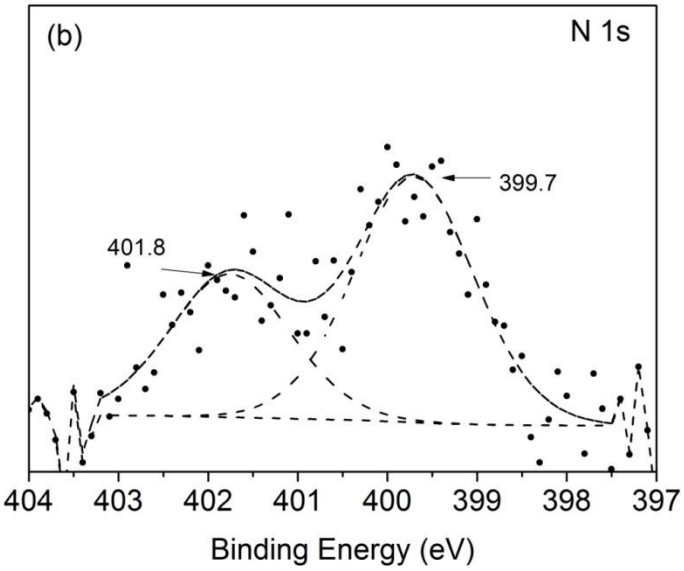
(b)
N 1s
399.7
401.8
404
403
402
401
400
399
398
397
Binding Energy (eV)

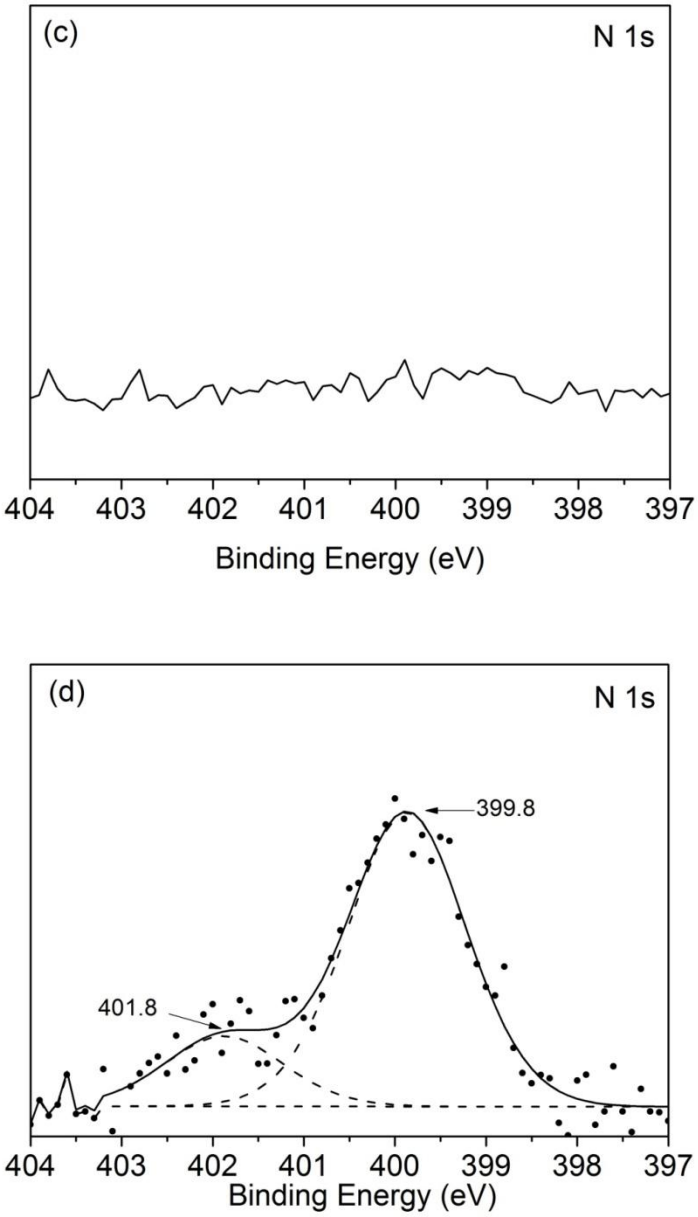

Figure 5.5 N 1s high resolution spectra with deconvoluted peaks: (a) pyrite at pH 4, (b) chitosan-treated pyrite at pH 4: (c) pyrite at pH 6, (d) chitosan-treated pyrite at pH 6.

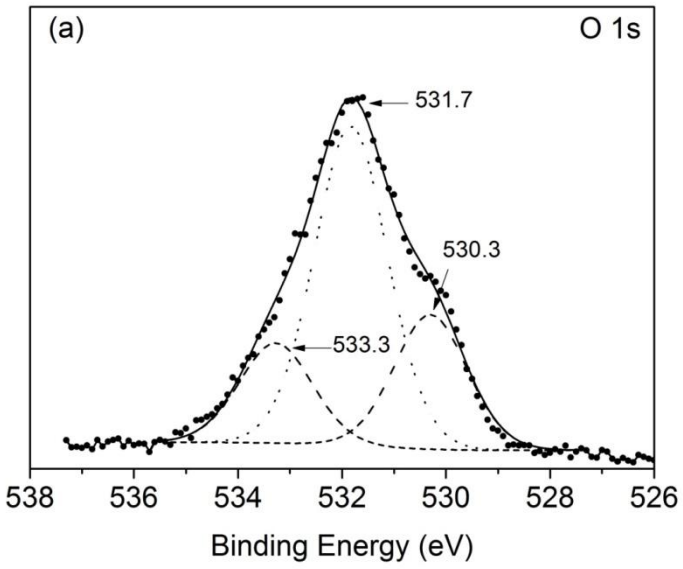
(a)
O 1s
531.7
530.3
533.3
538
536
534
532
530
528
526
Binding Energy (eV)

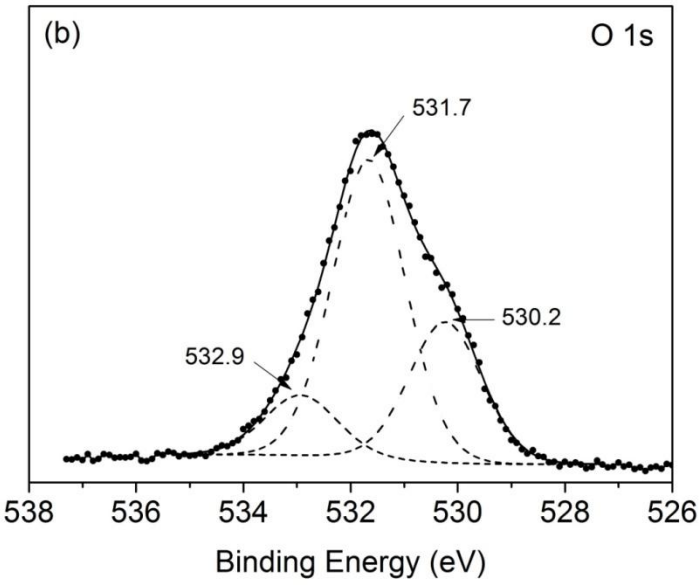
(b)
O 1s
531.7
530.2
532.9
538
536
534
532
530
528
526
Binding Energy (eV)

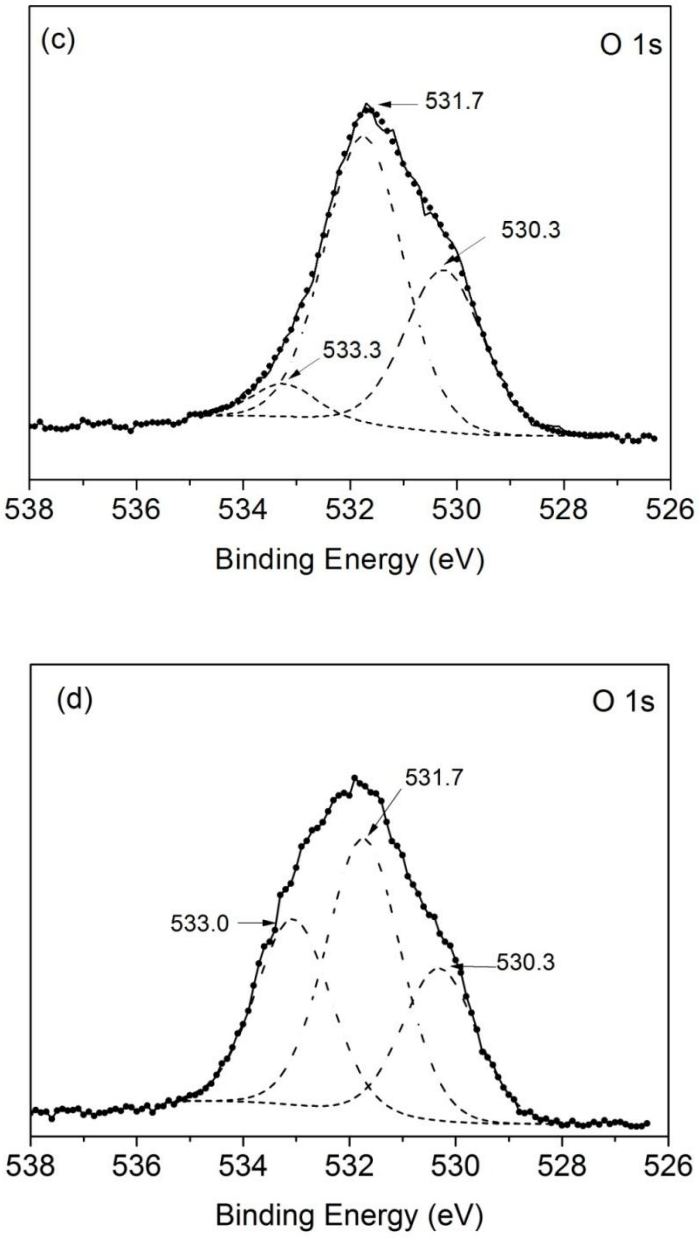

Figure 5.6 O 1s high resolution spectra with deconvoluted peaks: (a) pyrite at pH 4, (b) chitosan-treated pyrite at pH 4: (c) pyrite at pH 6, (d) chitosan-treated pyrite at pH 6.

5.3.3 Possible mechanisms for the selective adsorption

The single mineral flotation tests show that both pyrite and galena were depressed by chitosan in acidic solutions to some degree. However, in the mineral mixture flotation, galena was floated with a recovery of 68% at pH 4 and pyrite was depressed with a recovery of 23%. The flotation results indicated that competitive adsorption of chitosan occurred in the pyrite-galena mixtures. Similar flotation results were also observed in the flotation of chalcopyrite-galena mixtures and sphalerite-galena mixtures using chitosan (Huang et al., 2012a; Huang et al., 2012b). The mechanism studies revealed that amine ($–NH_2$) and hydroxyl (–OH) groups, which are parts of the basic structure of chitosan, were involved in the interaction between chitosan and the sulfide minerals (i.e., chalcopyrite, pyrite, and sphalerite), but the same interaction was not observed on galena (Huang et al., 2012a, b; Huang et al, 2013).

Chitosan, as one of the widely used adsorbents with nitrogen-based functional groups, has been examined for the selective adsorption behaviors in binary metal species systems (Vold et al., 2003). The adsorption performance shows that chitosan displayed selectivity in the adsorption of Cu^{2+} over Ni^{2+}, Zn^{2+} and Cd^{2+} in the binary mixtures at pH lower than 4.7. Furthermore, other adsorbents with nitrogen-based functional groups, such as DETA (diethylenetriamine)-functionalized polymeric adsorbent (P-DETA) and amine functionalized fine-grained activated carbon (NH_2-AC), were found to have the selective adsorption behaviors in aqueous solutions (Lam et al., 2006b; Liu et al., 2008; Yantasee et al., 2004). Based on FTIR and XPS results, Liu et al. (Liu et al., 2008) found that the nitrogen atoms in the amine groups of DETA in P-DETA formed coordination bonds with copper and lead ions in single metal species system. However, in the binary Cu-Pb metal species systems, they showed that considerable amount of copper ions were adsorbed on P-DETA with little lead ions being adsorbed (Liu et al., 2008). Yantasee et al. (2004) measured the competitive adsorption capacity of

Cu^{2+} on NH_2-AC in batch experiments. They found that the affinity of NH_2-AC toward metal ions follows the decreasing order of Cu^{2+}, Pb^{2+}, Ni^{2+}, and Cd^{2+}.

Even though literature shows an increasing interest in the research on the selective adsorption behaviors of chitosan towards different metal ionic species, the adsorption mechanisms were still not elucidated clearly at present. Pearson's hard-soft acids-bases (HSAB) principle is widely used to explain reaction mechanism of transition metals and coordination ligands (Lam et al., 2006b; Parr and Pearson, 1983; Pearson, 1963). According to the HSAB theory, hard acids and hard bases prefer to bind together to form ionic complexes and soft acids and soft bases prefer to bind together to form covalent complexes (Klopman, 1968; Pearson, 1963). Yantasee et al. (2004) applied the HSAB theory to explain the selective adsorption of metal ions on NH_2-AC. The copper ion, as a borderline cation, has the tendency to react with aniline nitrogen which was soft base. Lam et al. (2006b) designed an adsorbent containing NH_2 groups to selectively remove Cu^{2+} from the binary solution of Cu-Ag following the HSAB theory. However, the HSAB theory is used to provide a qualitative rather than quantitative explanation for the coordination reactions. It does not show the reaction intensity order of metal ions which are borderline cations with certain ligands. In terms of the competitive adsorption of copper and lead ions on chitosan, the adsorption tests indicated that chitosan prefer copper ions to lead ions in the binary solution (Huang et al., 2012b). Both lead and copper ions are borderline cations and the absolute hardness of these cations are similar, i.e., 8.3 eV for copper ion and 8.5 eV for lead ion (Parr and Pearson, 1983). Therefore the HSAB theory cannot fully explain the selective adsorption order in this case. At present, the adsorption study of chitosan confirmed its selectivity for copper ions over nickel, zinc, lead and cadmium ions (Huang et al., 2012b; Vold et al., 2003). Huang at al. (2013) showed that chitosan adsorbed more strongly on zinc ion (sphalerite) than lead ion (galena). Moreover, the present work indicated that chitosan preferentially adsorbed on pyrite (affinity to ferric/ferrous ions) but not on galena (lead ions).

It is worth noting that the tested selective adsorption of chitosan on the different minerals follows the table of electron affinity (A_S) for metal species in Pearson's absolute hardness study (Parr and Pearson, 1983). For instance, the A_S is 20.29 eV for copper ions while it is 15.03 eV for lead ions, which can explain the different affinities of the observed copper ions and lead ions to chitosan. In addition to such atomic parameter of the metal ions, the selective behaviors of chitosan in binary metal species solution also depends on the chitosan physical type, source and composition, etc.

To test the possible dependence of chitosan's interaction with metal ions on the electron affinities of the metal ions, adsorption tests were done in the binary system of Cu^{2+}/Mn^{2+} and Cu^{2+}/Ca^{2+}. The A_S values for Cu^{2+}, Mn^{2+} and Ca^{2+} are 20.29 eV, 15.14 eV and 11.87 eV, respectively. Figure 5.7 shows the adsorption isotherms of Cu^{2+}/Ca^{2+} and Cu^{2+}/Mn^{2+} in single and binary metal ions solutions. As can be seen, Ca^{2+} and Mn^{2+} did not adsorb on chitosan as strongly as Cu^{2+} ions in single metal ion adsorption tests. In the binary metal species system (Cu^{2+}/Ca^{2+} and Cu^{2+}/Mn^{2+}), the differences in the adsorption densities of Cu^{2+} and Ca^{2+}, and in the adsorption densities of Cu^{2+} and Mn^{2+}, were enlarged. The results indicated a competitive adsorption of the metal ions on the chitosan surface, i.e., the preferential adsorption of Cu^{2+} on chitosan reduced the adsorption densities of the Ca^{2+} and Mn^{2+} ions on the chitosan.

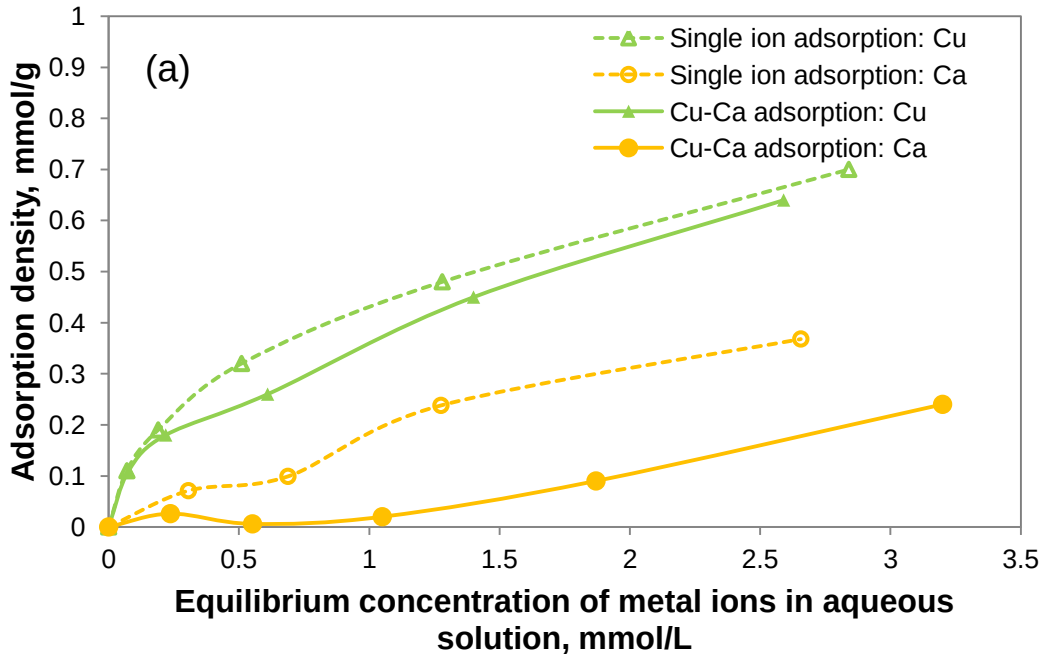

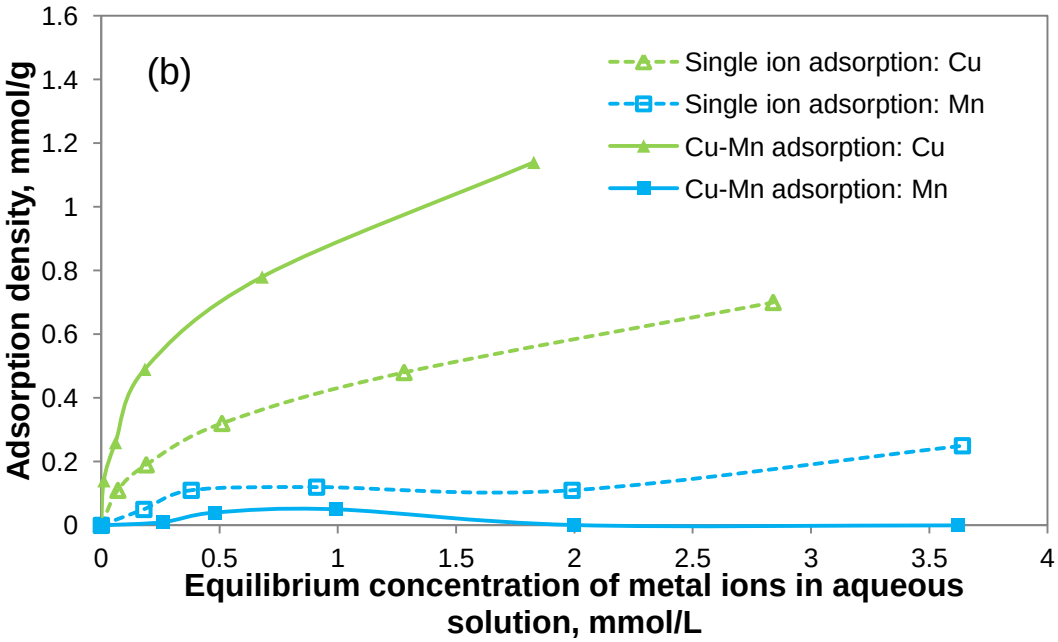

Figure 5.7 Adsorption density as a function of equilibrium concentration of metal ions in aqueous solution. (a). Cu^{2+} and Ca^{2+}; (b). Cu^{2+} and Mn^{2+}. (Temperature: 25 ℃ Adsorption time: 30 min)

5.4 Conclusions

In this study, the application of chitosan as a selective depressant in the differential flotation of galena and pyrite was tested. The single mineral flotation results showed that pyrite was depressed as well as galena by chitosan using potassium ethyl xanthate as a collector. However, in the flotation of pyrite-galena mixtures, due to the competitive adsorption of chitosan on pyrite surfaces, galena was floated from the mixture with a recovery of 68% at pH 4 while pyrite was depressed with a recovery of 23%. ToF-SIMS and XPS analyses showed that the amine groups and the hydroxyl groups in chitosan were involved in its reaction with pyrite, possibly through a chemisorption mechanism. But the adsorption of chitosan on galena was probably physisorption in nature, as shown previously in the chalcopyrite-galena and sphalerite-galena systems.

The preferential adsorption of chitosan on sulfide minerals such as chalcopyrite, sphalerite and pyrite, over galena, probably stems from the different affinities of the constituent metal ions in the minerals towards chitosan. It was hypothesized that the affinity of a metal ion towards chitosan is dependent on its electron affinity. The metal ion with a higher electron affinity has a stronger tendency to interact with the amine groups in chitosan, leading to its preferential adsorption on chitosan over other metal ions. The minerals containing such metal ion would adsorb chitosan more strongly than other minerals.

5.5 References

Atalay, U., 1996. Flotation behavior of galena and pyrite. Taylor & Francis, p. 229.

Boddu, V.M., Abburi, K., Talbott, J.L., Smith, E.D., Removal of hexavalent chromium from wastewater using a new composite chitosan biosorbent. Environ. Sci. Technol., 2003, 37(19), 4449-4456.

Bonnissel-Gissinger, P., Alnot, M., Ehrhardt, J.J., Behra, P., Surface oxidation of pyrite as a function of pH. Environ. Sci. Technol., 1998, 32(19), 2839-2845.

Boulton, A., Fornasiero, D., Ralston, J., Selective depression of pyrite with polyacrylamide polymers. Int. J. Miner. Process., 2001, 61(1), 13-22.

Burke, A., Yilmaz, E., Hasirci, N., Yilmaz, O., Iron (III) ion removal from solution through adsorption on chitosan. J. Appl. Polym. Sci., 2002, 84(6), 1185-1192.

Cao, M., Liu, Q., Reexamining the functions of zinc sulfate as a selective depressant in differential sulfide flotation--The role of coagulation. J. Colloid Interface Sci., 2006, 301(2), 523-531.

Choy, K.K.H., Porter, J.F., Mckay, G., A film-pore-surface diffusion model for the adsorption of acid dyes on activated carbon. Adsorption., 2001, 7(3), 231-247.

Chung, Y.S., Lee, K.K., Kim, J.W., Durable press and antimicrobial finishing of cotton fabrics with a citric acid and chitosan treatment. Text. Res. J., 1998, 68(10), 772.

Foster, L.S., Preparation of xanthates and other organic thiocarbonates. Utah Eng. Exp. Sta., 1928.

Guibal, E., Interactions of metal ions with chitosan-based sorbents: a review. Sep. Purif. Technol., 2004, 38(1), 43-74.

Höll, W.H., Horst, J., Wernet, M., Application of the surface complex formation model to exchange equilibria on ion exchange resins. Part II. Chelating resins. React. Polym., 1991, 14(3), 251-261.

Huang, P., Cao, M., Liu, Q., Adsorption of chitosan on chalcopyrite and galena from aqueous suspensions. Colloids Surf., A, 2012a. 409, 167-175.

Huang, P., Cao, M., Liu, Q., Using chitosan as a selective depressant in the differential flotation of Cu–Pb sulfides. Int. J. Miner. Process., 2012b, 106–109(0), 8-15.

Huang, P., Cao M., Liu, Q., Selective depression of sphalerite by chitosan in the differential Pb-Zn flotation. Int. J. Miner. Process., 2013, 122, 29-35. .

Jocić, D., Julia, M., Erra, P., Application of a chitosan/nonionic surfactant mixture to wool assessed by dyeing with a reactive dye. J. Soc. Dyers Colour., 1997, 113(1), 25-31.

Kiefer, R., Hoell, W.H., Sorption of heavy metals onto selective ion-exchange resins with aminophosphonate functional groups. Ind. Eng. Chem. Res., 2001, 40(21), 4570-4576.

King, R., Principles of flotation. South African Institute of Mining and Metallurgy, Kelvin House, 2 Holland St, Johannesburg, South Africa, 1982. 171.

Klopman, G., Chemical reactivity and the concept of charge-and frontier-controlled reactions. J. Am. Chem. Soc., 1968, 90(2), 223-234.

Lam, K.F., Yeung, K.L., McKay, G., An investigation of gold adsorption from a binary mixture with selective mesoporous silica adsorbents. J. Phys. Chem. B, 2006a, 110(5), 2187-2194.

Lam, K.F., Yeung, K.L., McKay, G., A rational approach in the design of selective mesoporous adsorbents. Langmuir, 2006b, 22(23), 9632-9641.

Liu, C., Bai, R., San Ly, Q., Selective removal of copper and lead ions by diethylenetriamine-functionalized adsorbent: Behaviors and mechanisms. Water Res., 2008, 42(6-7), 1511-1522.

Onsosyen, E., Skaugrud, O., Metal recovery using chitosan. J. Chem. Technol. Biotechnol., 1990, 49(4), 395-404.

Parr, R.G., Pearson, R.G., Absolute hardness: companion parameter to absolute electronegativity. J. Am. Chem. Soc., 1983, 105(26), 7512-7516.

Pavan, F.A., Lucho, A., Gonçalves, R.S., Costa, T.M.H., Benvenutti, E.V., Anilinepropylsilica xerogel used as a selective Cu (II) adsorbent in aqueous solution. J. Colloid Interface Sci., 2003, 263(2), 688-691.

Pearson, R.G., Hard and soft acids and bases. J. Am. Chem. Soc., 1963, 85(22), 3533-3539.

Ravi Kumar, M.N.V., A review of chitin and chitosan applications. React. Funct. Polym., 2000, 46(1), 1-27.

Shin, Y., Yoo, D.I., Use of chitosan to improve dyeability of DP - finished cotton (II). J. Appl. Polym. Sci., 1998, 67(9), 1515-1521.

Stöhr, C., Horst, J., Höll, W.H., Application of the surface complex formation model to ion exchange equilibria: Part V. Adsorption of heavy metal salts onto weakly basic anion exchangers. React. Funct. Polym., 2001, 49(2), 117-132.

Vilensky, M.Y., Berkowitz, B., Warshawsky, A., In situ remediation of groundwater contaminated by heavy-and transition-metal ions by selective ion-exchange methods. Environ. Sci. Technol., 2002, 36(8), 1851-1855.

Vold, I., Varum, K.M., Guibal, E., Smidsrod, O., Binding of ions to chitosan-selectivity studies. Carbohydr. Polym., 2003, 54(4), 471-477.

Wang, X.H., Eric Forssberg, K., Mechanisms of pyrite flotation with xanthates. Int. J. Miner. Process., 1991, 33(1-4), 275-290.

Yantasee, W., Lin, Y., Fryxell, G.E., Alford, K.L., Busche, B.J., Johnson, C.D., Selective removal of copper (II) from aqueous solutions using fine-grained activated carbon functionalized with amine. Ind. Eng. Chem. Res., 2004, 43(11), 2759-2764.

CHAPTER 6

CONCLUSIONS AND RECOMMENDATIONS

6.1 General Conclusions

Chitosan, a naturally occurring polymer, was exploited in the differential flotation of Cu-Pb (chalcopyrite and galena), Zn-Pb (sphalerite and galena), and Fe-Pb (pyrite and galena). The adsorption of chitosan on the sulfide minerals was studied to help elucidate the interaction mechanism and support the application of chitosan as a new depressant in sulfide minerals flotation. The study led to the following conclusions:

(1) In single mineral flotation of chalcopyrite and galena, both minerals were depressed by chitosan to different extents and the recovery of chalcopyrite was 40% while that of galena was 20% at pH 4. However, in the flotation of mixed mineral systems of chalcopyrite and galena, galena was floatable while chalcopyrite was depressed by chitosan in acidic solution between pH 3 and 5. The best results were observed at pH 4, where the recovery of galena was as high as 95% while chalcopyrite was depressed by 0.67 mg/L chitosan with low recovery (30%) in the presence of 5×10^{-4} mol/L potassium ethyl xanthate.

(2) The mechanisms of interaction of chitosan with the two sulfide minerals, chalcopyrite ($CuFeS_2$) and galena (PbS), were investigated by ATR-FTIR, ToF-SIMS and XPS. These complementary surface analysis techniques revealed that the deacetylated unit (amine) and the hydroxyl groups on chitosan were involved in the strong chitosan-chalcopyrite chemical interaction, while the un-deacetylated amide group may be responsible for adsorption on galena through a weaker interaction. The above hypothesis was tested and proven by two chitosan samples, with different degrees of

deacetylation (85.7% versus 91.7%), in the flotation of single minerals of chalcopyrite and galena, as well as in their mixtures. The results showed that the chitosan with the higher degree of deacetylation indeed depressed galena to a lesser degree than the chitosan with a lower degree of deacetylation.

(3) In the flotation of galena and sphalerite mixtures, it was observed that the addition of chitosan caused both minerals to be severely depressed. This was caused by the contamination of the sphalerite surface by lead ions, which likely came from dissolution of oxidized galena in weakly acidic suspension. The addition of EDTA was found to enable the depression of sphalerite by chitosan while allowing galena to be floated at pH 4. On the other hand, when the sphalerite was previously coated by Cu^{2+} ions before mixing with galena, the addition of chitosan caused the sphalerite to be depressed while galena could be floated at pH 3.5-4.5 without the addition of EDTA. ToF-SIMS and XPS analyses were performed to investigate the interactions of chitosan with sphalerite and copper-coated sphalerite. It was found that both the amine (-NH_2) and the hydroxyl (-OH) groups from chitosan were involved in its adsorption on sphalerite and copper-coated sphalerite, possibly through a chemical interaction due to the observed binding energy shifts of both N 1s and O 1s electrons. Interestingly, ToF-SIMS analysis showed that on the chitosan-treated sphalerite surface, the $ZnNH_2$ was the dominant species, while on chitosan-treated copper-coated sphalerite surfaces, the $CuNH_3$ was the dominant species. Chitosan only showed weak interactions with galena, which explains the observed separation between galena and sphalerite with the use of chitosan.

The results of the Pb-Zn differential flotation study also indicated that while Pb ions affected sphalerite flotation, such an effect was absent when the sphalerite was pre-activated by copper ions. On the other hand, when copper ions were added to galena-sphalerite mixtures which were then floated by chitosan and xanthate, both galena and sphalerite were depressed. The results

implied that while copper ions could adsorb on lead sulfide and zinc sulfide mineral surfaces, lead ions did not adsorb on mineral surfaces that are already covered by copper.

(4) The single mineral flotation results showed that pyrite was depressed as well as galena by chitosan using potassium ethyl xanthate as a collector. However, in the flotation of pyrite-galena mixtures, due to the competitive adsorption of chitosan on pyrite surfaces, galena was floated from the mixture with a recovery of 68% at pH 4 while pyrite was depressed with a recovery of 23%. ToF-SIMS and XPS analyses showed that the amine groups and the hydroxyl groups in chitosan were involved in its reaction with pyrite, possibly through a chemisorption mechanism. But the adsorption of chitosan on galena was probably physisorption in nature, as shown previously in the chalcopyrite-galena and sphalerite-galena systems.

(5) The preferential adsorption of chitosan on sulfide minerals such as chalcopyrite, sphalerite and pyrite, over galena, probably stems from the different affinities of the constituent metal ions in the minerals towards chitosan. It was hypothesized that the affinity of a metal ion towards chitosan is dependent on its electron affinity. The metal ion with a higher electron affinity has a stronger tendency to interact with the amine groups in chitosan, leading to its preferential adsorption on chitosan over other metal ions. The minerals containing such metal ion would adsorb on chitosan more strongly than other minerals.

6.2 Claims of Originality

(1) At present, toxic inorganic depressants are routinely used in the base metal sulfide ore flotation. With the increasingly stringent environmental regulations in the minerals industry, the toxic inorganic depressants need to be replaced by environmentally benign chemicals. Chitosan, an abundant natural polymer,

was shown to be a potential depressant in the differential flotation of Cu-Pb (chalcopyrite and galena), Zn-Pb (sphalerite and galena), and Fe-Pb (pyrite and galena). The study showed that chalcopyrite, sphalerite or pyrite was depressed while galena was floated by chitosan with xanthate as a collector in the differential flotation of Cu-Pb, Zn-Pb, and Fe-Pb mixtures.

(2) In this research it was observed that while single mineral flotation tests did not show possible separation windows between the tested sulfide minerals, selective separation was achievable in the flotation of mineral mixtures. This was due to the competitive preferential adsorption of chitosan on one mineral but not on the other. Therefore, the usual practice used in mineral flotation study, i.e., to identify separation windows based on single mineral flotation testwork, can be misleading. To find selective flotation depressants, mineral mixture flotation and adsorption mechanism study should be carried out in parallel, and the testwork should not be solely based on single mineral flotation study.

(3) The mechanism studies indicated that the functional groups from chitosan, namely the amine and the hydroxyl groups, were involved in the strong chemical interaction between chitosan and chalcopyrite, sphalerite and pyrite. Galena, on the other hand, may have reacted with the un-deacetylated amide group through weaker interactions, which explains the observed flotation selectivity. It was hypothesized that the different adsorption mechanisms of chitosan on the sulfide minerals was due to the electron affinity of the lattice metal ion. The mineral containing a metal ion with higher electron affinity has a stronger interaction with chitosan.

6.3 Suggestions for Future Work

In this work, the influences of the degree of deacetylation were studied in the flotation tests. It would be worthwhile to evaluate other factors affecting chitosan adsorption performance on mineral surfaces such as the source of chitosan.

As the flotation testwork results in this study are subject to some uncertainty, it would be worthwhile to repeat the key experiments and use standard deviation to estimate the reproducibility of the results.

The adsorption isotherms of single metal ions to chitosan have been extensively studied. However, in the case of binary metal ion adsorption on chitosan, much less studies have been carried out and the interpretation of the competitive adsorption behavior seems to be complicated. It would be worthwhile to study the competitive adsorption binary metal ion – chitosan adsorption systems.

The isothermal titration calorimetry technique can be applied to measure the heat of adsorption which is released from the interaction of chitosan and sulfide mineral. Mineral flotation systems other than the ones studied in this dissertation work may be studied. These include many non-sulfide minerals and ores such as oxides, salt-type minerals, naturally hydrophobic minerals, etc. Based on the results of this dissertation work, the electron affinity of the lattice metal ions may be used as a pre-screening criterion.

The optimal pH for chitosan application was pH 4 in the tested differential flotation systems of the sulfide minerals. The commercial flotation systems are typically operated in weakly acidic or alkaline solutions. It would be more practical to modify the chitosan by grafting other functional groups so that it would be soluble and can be used as effective selective depressant at other pH.

Appendix A: Adsorption Study of Divalent Metal Ions on Chitosan in Aqueous Solution[1]

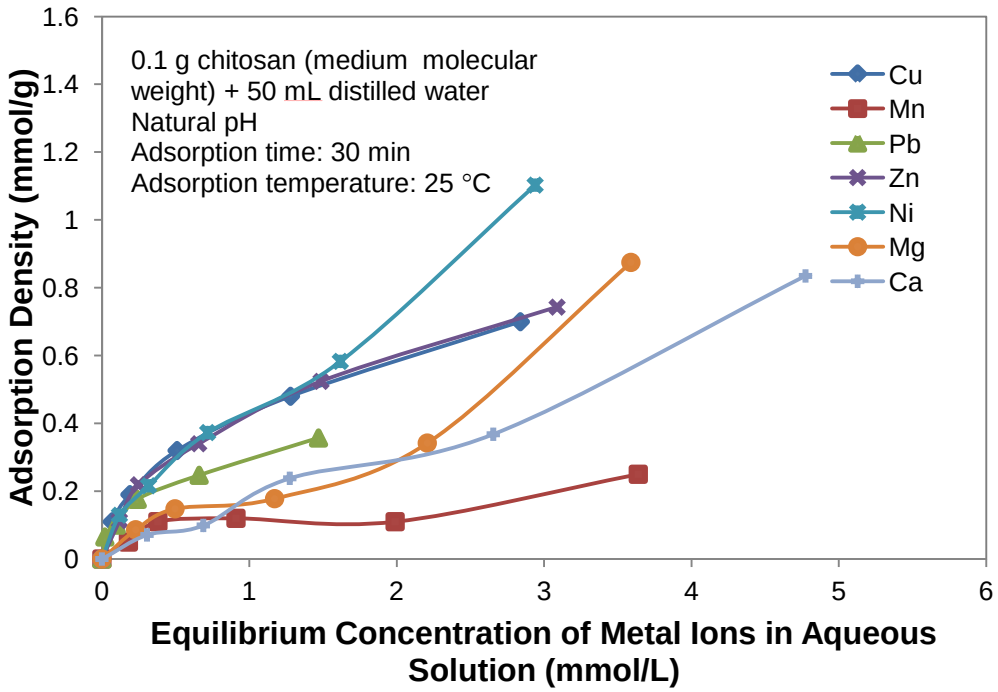

Figure 1. Adsorption isotherm in single metal species system

[1] Part of these experiments were conducted by Dr. Mingli Cao

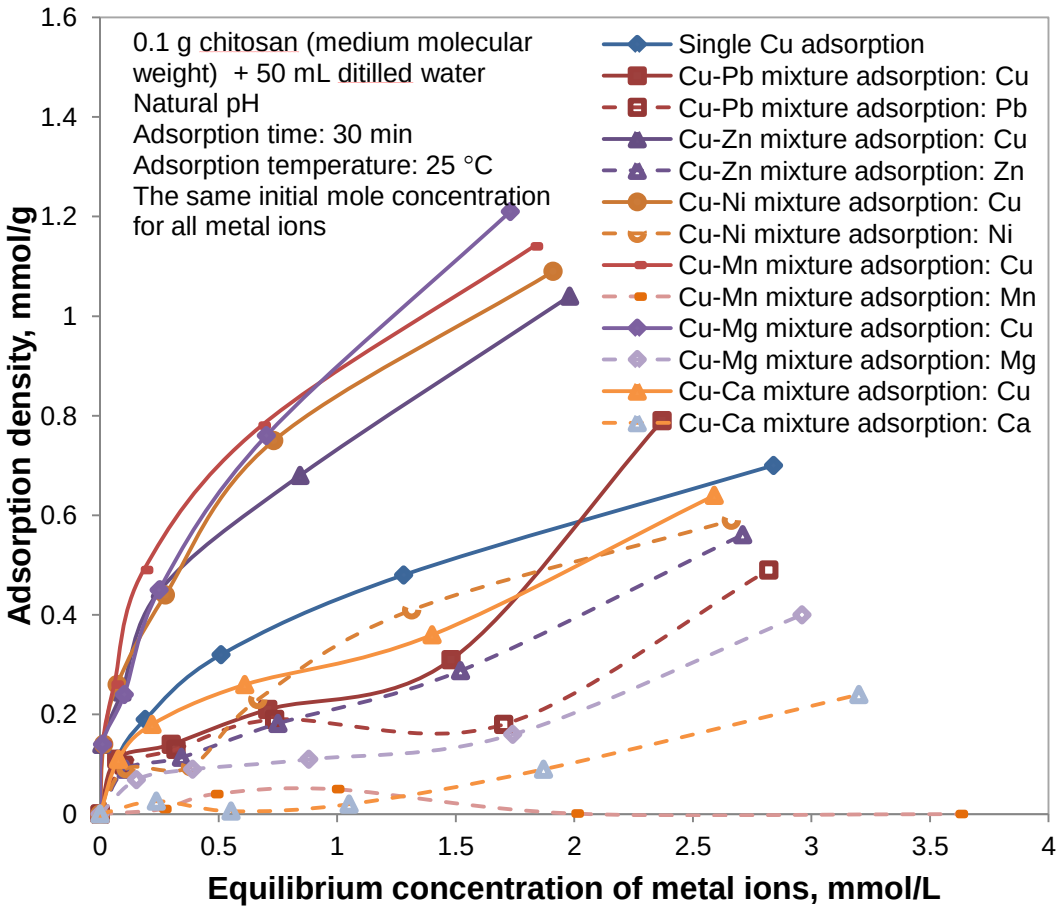

Figure 2. Adsorption isotherm in binary metal species system (1)

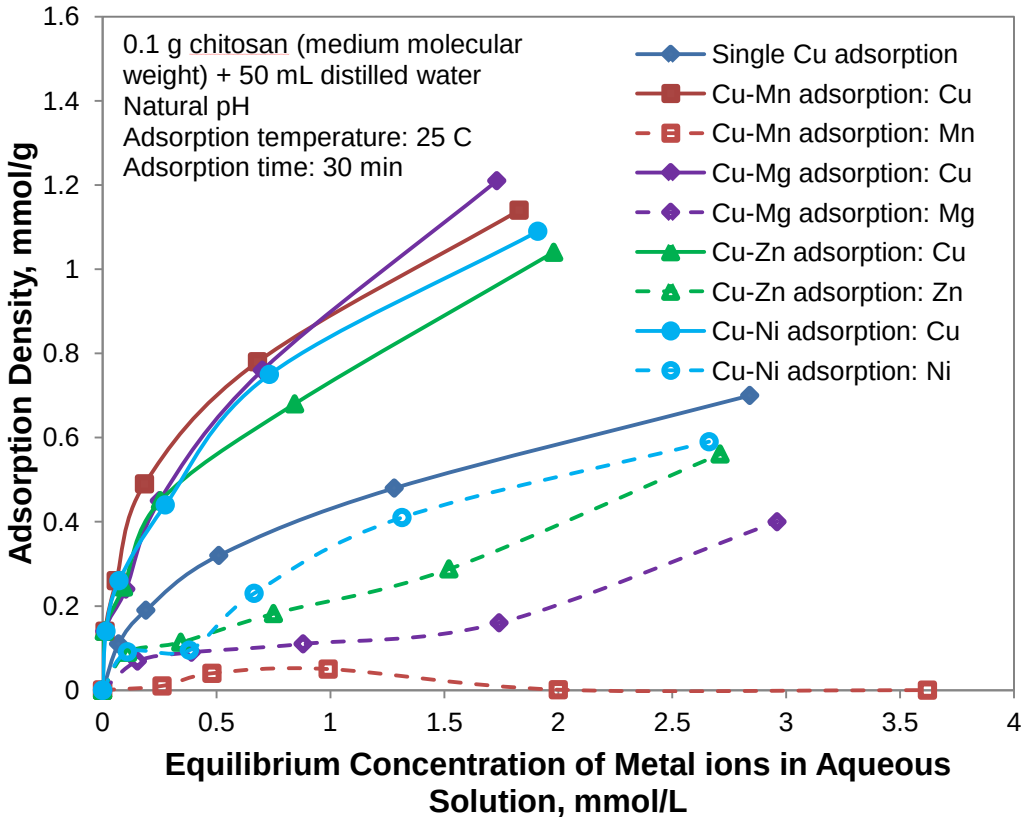

Figure 3. Adsorption isotherm in binary metal species system (2)

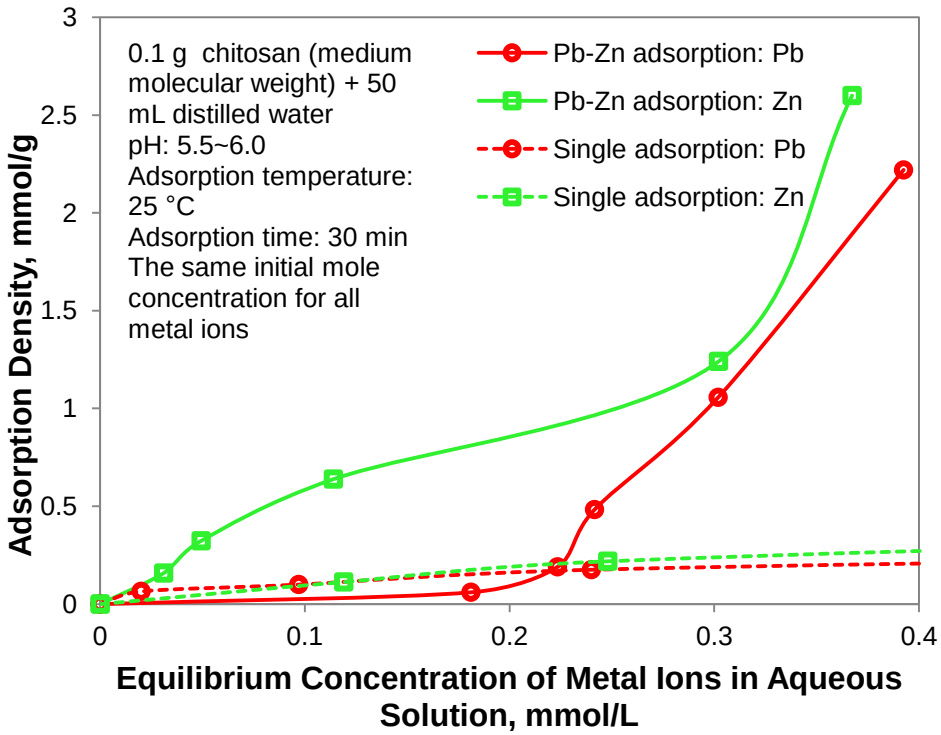

Figure 4. Adsorption isotherm in binary metal species system (3)

Appendix B: Experimental Methods

1. Flotation

In a typical test, 1.5 g of the -75+38 μm samples (single mineral or mineral mixtures with certain weight ratio) were mixed with 150 mL distilled water in a beaker for 3 min during which the solution pH was adjusted using either hydrochloric acid or sodium hydroxide. An appropriate amount of chitosan and KEX were added sequentially into the pulp and conditioned for 3 min each. The conditioned slurry was transferred to the flotation tube, and floated for 3 min using high purity nitrogen gas. After the flotation was finished, both the froth product and tailings were collected and dried to calculate mineral recovery. In the mineral mixture flotation tests, the metal contents in the froth and tailings were determined by dissolving the dried samples with aqua regia and analyzing the solutions using a Varian SpectrAA-220FS (Varian, USA) atomic absorption spectrometer (AAS).

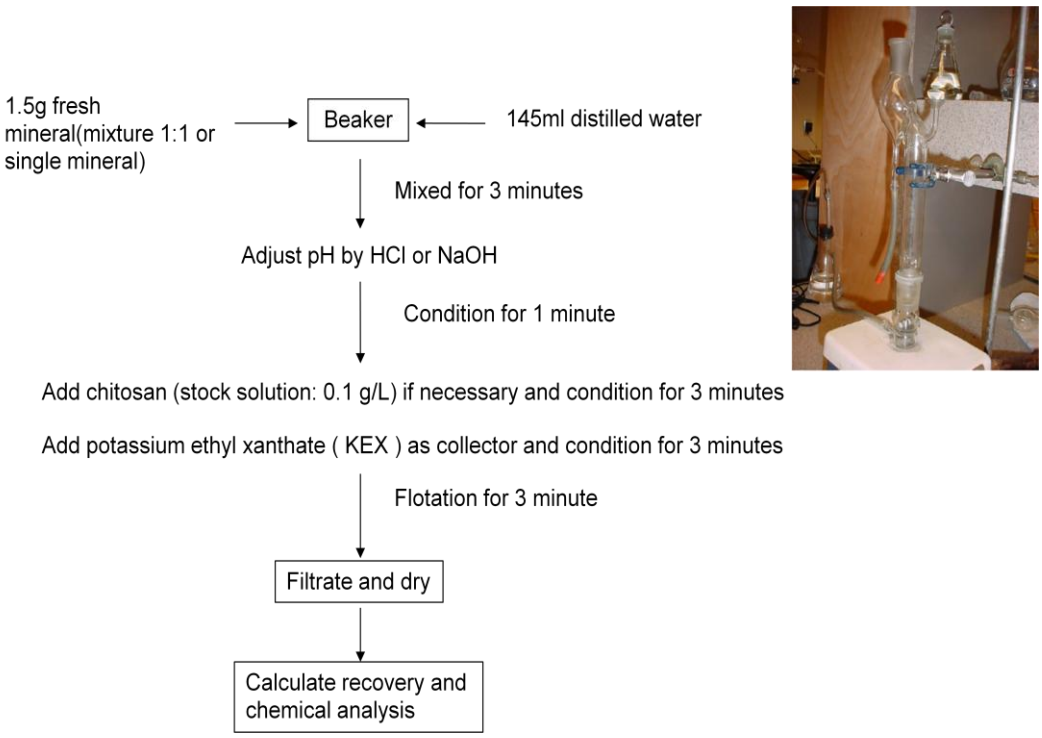

Figure 1. Small scale flotation tube and procedure

2. ToF-SIMS measurements

ToF-SIMS images and element maps of the chalcopyrite-galena mixture after treating with chitosan were obtained on a ToF-SIMS IV spectrometer (ION-TOF GmbH). For spectra acquisition, a high energy beam of Bi^+ ions (25 kV) was focused on the sample surface at an area such as 64 μm × 64 μm. The positive ion mass spectra were obtained and calibrated by the secondary ion peaks for H^+, CH_3^+ and Na^+. Images were then generated by mapping the mass-selected ion intensity in a burst alignment mode with pixels of 128 × 128 per image.

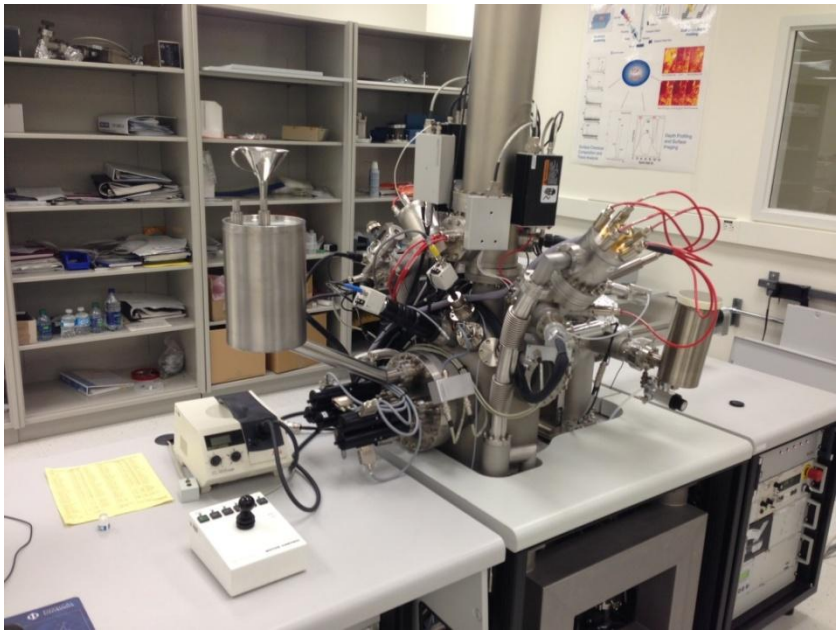

Figure 2. ToF-SIMS IV - 100 spectrometer (ION-TOF GmbH)

3. XPS measurements

XPS survey scan and high-resolution spectra were acquired on an AXIS 165 X-ray photoelectron spectrometer (Kratos Analytical). Monochromatic Al Kα source ($h\nu$ = 1486.6 eV) was used at a power of 210 W for all data acquisition. The vacuum pressure inside the analytical chamber was lower than 3×10^{-8} Pa. The analyzed area on the sample surface was 400 μm × 700 μm. The resolution of the instrument is 0.55 eV for Ag 3d and 0.70 eV for Au 4f peaks.

The survey scans were collected for binding energy range from 1100 eV to 0 eV with an analyzer pass energy of 160 eV and a step of 0.4 eV. To collect the high-resolution spectra, the pass-energy was set at 20 eV with a step of 0.1 eV. No charge neutralization was required through the spectra collection. XPS sampling depth for photoelectrons was 3-10 nm, which was more than enough to provide information of the mineral surfaces in this work. CasaXPS Version 2.3.15 instrument software was used to process the XPS data after spectra collection. The Shirley-type background subtraction was chosen to optimize the peak height through the high-resolution spectra analysis. And then, according to previously published data, the processed spectra were calibrated, resolved and refined into individual Gaussian-Lorentzian peaks and imported into a graphic software (Origin, OriginLab Corp) package for displaying the optimized fitting peaks from the high-resolution spectra.

Figure 3. Axis 165 X-ray Photoelectron Spectrometer (Kratos Analytical).

Appendix C: Supplemental Experimental Results

1. Parts of raw data

Table 1. Raw data of Figure 2.3

pH	weight of concentrate and filtration paper	weight of concentrate	recovery%▲
3.3	2.224	1.024	68.27
3.95	2.1401	0.9401	62.67
4.47	1.8453	0.6453	43.02
6.18	1.4085	0.2085	13.90
8.34	1.5146	0.3146	20.97

▲ The total sample weight was 1.5 g for each flotation test.

pH	Cu(mg/L)*	Cu% grade in concentrate °	Cu recovery in concentrate %■
3.30	0.923	9.23	43.07
3.95	0.723	7.23	30.97
4.47	0.944	9.44	27.76
6.18	0.9	9	8.55
8.34	0.915	9.15	13.12

pH	Pb(mg/L)*	Pb% grade in concentrate °	Pb recovery in concentrate %●
3.30	6.07	60.7	98.65
3.95	5.99	59.9	89.37
4.47	6.07	60.7	62.17
6.18	5.5	55	18.20
8.34	5.29	52.9	26.41

*0.050 g concentrate was dissolved in 10 mL aqua regia. The solution was heated to boil until particles were totally dissolved. 15 mL hydrochloric acid (50% V/V) was added to the solution. The solution was transferred to a 100-mL volumetric flask and distilled water was added to the 100 mL mark. This solution was diluted 50 times for AAS measurements.

°Cu/Pb% grade in concentrate = (Cu/Pb(mg/L)(read from AAS) × 50 times × 100 mL × 100)/0.05 g

■Cu recovery in froth% = Cu% grade in concentrate × weight of concentrate / (0.75 × 0.2926 (Cu% grade in chalcopyrite)

● Pb recovery in froth% = Pb% grade in concentrate × weight of concentrate / (0.75 × 0.8401 (Pb% grade in galena)

Table 2. Raw data of Figure 3.7c

calibration BE	CPS_Cu2p-#4/61	Cu 2p_1_Cu 2p-#4/61	Cu 2p_2_Cu2p-#4/61	Cu 2p_3_Cu2p-#4/61	Envelope_Cu2p-#4/61	Background_Cu2p-#4/61
962.25	4250	4250	4250	4250	4250	4250
962.1	4277.92	4277.92	4277.92	4277.92	4277.92	4277.92
961.95	4250	4250	4250	4250	4250	4250
961.8	4260.42	4260.42	4260.42	4260.42	4260.42	4260.42
961.65	4200.42	4200.42	4200.42	4200.42	4200.42	4200.42
961.5	4172.5	4172.5	4172.5	4172.5	4172.5	4172.5
961.35	4155.83	4155.83	4155.83	4155.83	4155.83	4155.83
961.2	4192.5	4192.5	4192.5	4192.5	4192.5	4192.5
961.05	4197.5	4197.5	4197.5	4197.5	4197.5	4197.5
960.9	4287.5	4287.5	4287.5	4287.5	4287.5	4287.5
960.75	4260.42	4260.42	4260.42	4260.42	4260.42	4260.42
960.6	4235.42	4235.42	4235.42	4235.42	4235.42	4235.42
960.45	4133.33	4133.33	4133.33	4133.33	4133.33	4133.33
960.3	4212.5	4212.5	4212.5	4212.5	4212.5	4212.5
960.15	4200.83	4200.83	4200.83	4200.83	4200.83	4200.83
960	4204.58	4204.58	4204.58	4204.58	4204.58	4204.58
959.85	4252.08	4252.08	4252.08	4252.08	4252.08	4252.08
959.7	4209.58	4209.58	4209.58	4209.58	4209.58	4209.58
959.55	4242.92	4242.92	4242.92	4242.92	4242.92	4242.92
959.4	4255.83	4255.83	4255.83	4255.83	4255.83	4255.83
959.25	4275	4275	4275	4275	4275	4275
959.1	4238.75	4238.75	4238.75	4238.75	4238.75	4238.75
958.95	4177.92	4177.92	4177.92	4177.92	4177.92	4177.92
958.8	4227.92	4227.92	4227.92	4227.92	4227.92	4227.92
958.65	4278.33	4278.33	4278.33	4278.33	4278.33	4278.33
958.5	4271.67	4271.67	4271.67	4271.67	4271.67	4271.67
958.35	4170.83	4170.83	4170.83	4170.83	4170.83	4170.83
958.2	4222.5	4222.5	4222.5	4222.5	4222.5	4222.5
958.05	4217.92	4217.92	4217.92	4217.92	4217.92	4217.92
957.9	4257.08	4257.08	4257.08	4257.08	4257.08	4257.08
957.75	4311.67	4311.67	4311.67	4311.67	4311.67	4311.67
957.6	4275	4275	4275	4275	4275	4275
957.45	4299.58	4299.58	4299.58	4299.58	4299.58	4299.58
957.3	4335	4335	4335	4335	4335	4335
957.15	4274.58	4274.58	4274.58	4274.58	4274.58	4274.58

957	4301.67	4301.67	4301.67	4301.67	4301.67	4301.67
956.85	4260	4260	4260	4260	4260	4260
956.7	4276.67	4276.67	4276.67	4276.67	4276.67	4276.67
956.55	4315.42	4315.42	4315.42	4315.42	4315.42	4315.42
956.4	4390	4390	4390	4390	4390	4390
956.25	4423.33	4423.33	4423.33	4423.33	4423.33	4423.33
956.1	4384.58	4384.58	4384.58	4384.58	4384.58	4384.58
955.95	4312.92	4312.92	4312.92	4312.92	4312.92	4312.92
955.8	4312.92	4312.92	4312.92	4312.92	4312.92	4312.92
955.65	4327.5	4327.5	4327.5	4327.5	4327.5	4327.5
955.5	4415.83	4415.83	4415.83	4415.83	4415.83	4415.83
955.35	4377.92	4377.92	4377.92	4377.92	4377.92	4377.92
955.2	4399.58	4399.58	4399.58	4399.58	4399.58	4399.58
955.05	4441.67	4441.67	4441.67	4441.67	4441.67	4441.67
954.9	4492.5	4492.5	4492.5	4492.5	4492.5	4492.5
954.75	4448.75	4448.75	4448.75	4448.75	4448.75	4448.75
954.6	4514.17	4514.17	4514.17	4514.17	4514.17	4514.17
954.45	4470.42	4470.42	4470.42	4470.42	4470.42	4470.42
954.3	4502.92	4502.92	4502.92	4502.92	4502.92	4502.92
954.15	4592.92	4592.92	4592.92	4592.92	4592.92	4592.92
954	4568.33	4568.33	4568.33	4568.33	4568.33	4568.33
953.85	4624.17	4624.17	4624.17	4624.17	4624.17	4624.17
953.7	4662.08	4662.08	4662.08	4662.08	4662.08	4662.08
953.55	4717.5	4717.5	4717.5	4717.5	4717.5	4717.5
953.4	4706.67	4706.67	4706.67	4706.67	4706.67	4706.67
953.25	4677.08	4677.08	4677.08	4677.08	4677.08	4677.08
953.1	4857.08	4857.08	4857.08	4857.08	4857.08	4857.08
952.95	4929.17	4929.17	4929.17	4929.17	4929.17	4929.17
952.8	5030	5030	5030	5030	5030	5030
952.65	5245	5245	5245	5245	5245	5245
952.5	5389.58	5389.58	5389.58	5389.58	5389.58	5389.58
952.35	5494.58	5494.58	5494.58	5494.58	5494.58	5494.58
952.2	5696.67	5696.67	5696.67	5696.67	5696.67	5696.67
952.05	5874.58	5874.58	5874.58	5874.58	5874.58	5874.58
951.9	5859.17	5859.17	5859.17	5859.17	5859.17	5859.17
951.75	5771.67	5771.67	5771.67	5771.67	5771.67	5771.67
951.6	5651.67	5651.67	5651.67	5651.67	5651.67	5651.67
951.45	5526.67	5526.67	5526.67	5526.67	5526.67	5526.67
951.3	5205.42	5205.42	5205.42	5205.42	5205.42	5205.42
951.15	5018.75	5018.75	5018.75	5018.75	5018.75	5018.75

951	4789.58	4789.58	4789.58	4789.58	4789.58	4789.58
950.85	4679.17	4679.17	4679.17	4679.17	4679.17	4679.17
950.7	4641.67	4641.67	4641.67	4641.67	4641.67	4641.67
950.55	4596.67	4596.67	4596.67	4596.67	4596.67	4596.67
950.4	4459.17	4459.17	4459.17	4459.17	4459.17	4459.17
950.25	4388.75	4388.75	4388.75	4388.75	4388.75	4388.75
950.1	4332.08	4332.08	4332.08	4332.08	4332.08	4332.08
949.95	4325.42	4325.42	4325.42	4325.42	4325.42	4325.42
949.8	4312.5	4312.5	4312.5	4312.5	4312.5	4312.5
949.65	4275.42	4275.42	4275.42	4275.42	4275.42	4275.42
949.5	4212.92	4212.92	4212.92	4212.92	4212.92	4212.92
949.35	4284.58	4284.58	4284.58	4284.58	4284.58	4284.58
949.2	4284.17	4284.17	4284.17	4284.17	4284.17	4284.17
949.05	4187.5	4187.5	4187.5	4187.5	4187.5	4187.5
948.9	4252.08	4252.08	4252.08	4252.08	4252.08	4252.08
948.75	4240	4240	4240	4240	4240	4240
948.6	4236.25	4236.25	4236.25	4236.25	4236.25	4236.25
948.45	4187.92	4187.92	4187.92	4187.92	4187.92	4187.92
948.3	4183.33	4183.33	4183.33	4183.33	4183.33	4183.33
948.15	4187.5	4187.5	4187.5	4187.5	4187.5	4187.5
948	4113.33	4113.33	4113.33	4113.33	4113.33	4113.33
947.85	4077.5	4077.5	4077.5	4077.5	4077.5	4077.5
947.7	4115.42	4115.42	4115.42	4115.42	4115.42	4115.42
947.55	4141.67	4141.67	4141.67	4141.67	4141.67	4141.67
947.4	4126.25	4126.25	4126.25	4126.25	4126.25	4126.25
947.25	4127.5	4127.5	4127.5	4127.5	4127.5	4127.5
947.1	4109.17	4109.17	4109.17	4109.17	4109.17	4109.17
946.95	4156.25	4156.25	4156.25	4156.25	4156.25	4156.25
946.8	4132.92	4132.92	4132.92	4132.92	4132.92	4132.92
946.65	4145.42	4145.42	4145.42	4145.42	4145.42	4145.42
946.5	4138.33	4138.33	4138.33	4138.33	4138.33	4138.33
946.35	4146.67	4146.67	4146.67	4146.67	4146.67	4146.67
946.2	4044.17	4044.17	4044.17	4044.17	4044.17	4044.17
946.05	4090	4090	4090	4090	4090	4090
945.9	4043.75	4043.75	4043.75	4043.75	4043.75	4043.75
945.75	4054.17	4054.17	4054.17	4054.17	4054.17	4054.17
945.6	4110	4110	4110	4110	4110	4110
945.45	4096.67	4096.67	4096.67	4096.67	4096.67	4096.67
945.3	4056.67	4056.67	4056.67	4056.67	4056.67	4056.67
945.15	4076.25	4076.25	4076.25	4076.25	4076.25	4076.25

945	4098.75	4098.75	4098.75	4098.75	4098.75	4098.75
944.85	4035.42	4035.42	4035.42	4035.42	4035.42	4035.42
944.7	4057.08	4057.08	4057.08	4057.08	4057.08	4057.08
944.55	4067.92	4067.92	4067.92	4067.92	4067.92	4067.92
944.4	4035.42	4035.42	4035.42	4035.42	4035.42	4035.42
944.25	3987.08	3987.08	3987.08	3987.08	3987.08	3987.08
944.1	4027.08	4027.08	4027.08	4027.08	4027.08	4027.08
943.95	4016.67	4016.67	4016.67	4016.67	4016.67	4016.67
943.8	3952.5	3952.5	3952.5	3952.5	3952.5	3952.5
943.65	3911.67	3911.67	3911.67	3911.67	3911.67	3911.67
943.5	3985.42	3985.42	3985.42	3985.42	3985.42	3985.42
943.35	4017.92	4017.92	4017.92	4017.92	4017.92	4017.92
943.2	3993.33	3993.33	3993.33	3993.33	3993.33	3993.33
943.05	4037.92	4037.92	4037.92	4037.92	4037.92	4037.92
942.9	4000.83	4000.83	4000.83	4000.83	4000.83	4000.83
942.75	3935.42	3935.42	3935.42	3935.42	3935.42	3935.42
942.6	3958.75	3958.75	3958.75	3958.75	3958.75	3958.75
942.45	3978.33	3978.33	3978.33	3978.33	3978.33	3978.33
942.3	3940.83	3940.83	3940.83	3940.83	3940.83	3940.83
942.15	3905.42	3905.42	3905.42	3905.42	3905.42	3905.42
942	3979.58	3979.58	3979.58	3979.58	3979.58	3979.58
941.85	3908.75	3908.75	3908.75	3908.75	3908.75	3908.75
941.7	3911.25	3911.25	3911.25	3911.25	3911.25	3911.25
941.55	3926.67	3926.67	3926.67	3926.67	3926.67	3926.67
941.4	3873.33	3873.33	3873.33	3873.33	3873.33	3873.33
941.25	3853.33	3853.33	3853.33	3853.33	3853.33	3853.33
941.1	3859.58	3859.58	3859.58	3859.58	3859.58	3859.58
940.95	3865.83	3865.83	3865.83	3865.83	3865.83	3865.83
940.8	3819.58	3819.58	3819.58	3819.58	3819.58	3819.58
940.65	3850.83	3850.83	3850.83	3850.83	3850.83	3850.83
940.5	3784.58	3784.58	3784.58	3784.58	3784.58	3784.58
940.35	3792.08	3792.08	3792.08	3792.08	3792.08	3792.08
940.2	3837.5	3837.5	3837.5	3837.5	3837.5	3837.5
940.05	3818.75	3818.75	3818.75	3818.75	3818.75	3818.75
939.9	3847.92	3847.92	3847.92	3847.92	3847.92	3847.92
939.75	3852.5	3852.5	3852.5	3852.5	3852.5	3852.5
939.6	3793.33	3793.33	3793.33	3793.33	3793.33	3793.33
939.45	3860.42	3860.42	3860.42	3860.42	3860.42	3860.42
939.3	3772.08	3772.08	3772.08	3772.08	3772.08	3772.08
939.15	3834.58	3834.58	3834.58	3834.58	3834.58	3834.58

939	3832.92	3832.92	3832.92	3832.92	3832.92	3832.92
938.85	3805.83	3805.83	3805.83	3805.83	3805.83	3805.83
938.7	3834.17	3834.17	3834.17	3834.17	3834.17	3834.17
938.55	3796.67	3796.67	3796.67	3796.67	3796.67	3796.67
938.4	3832.5	3832.5	3832.5	3832.5	3832.5	3832.5
938.25	3777.92	3777.92	3777.92	3777.92	3777.92	3777.92
938.1	3720	3720	3720	3720	3720	3720
937.95	3822.5	3822.5	3822.5	3822.5	3822.5	3822.5
937.8	3781.67	3781.67	3781.67	3781.67	3781.67	3781.67
937.65	3845.83	3845.83	3845.83	3845.83	3845.83	3845.83
937.5	3830.42	3843.28	3843.29	3843.28	3843.29	3843.28
937.35	3853.75	3843.24	3843.25	3843.24	3843.25	3843.24
937.2	3862.92	3843.17	3843.18	3843.17	3843.18	3843.17
937.05	3858.33	3843.11	3843.15	3843.11	3843.15	3843.11
936.9	3864.58	3843.03	3843.15	3843.03	3843.15	3843.03
936.75	3873.75	3842.91	3843.23	3842.91	3843.23	3842.91
936.6	3926.25	3842.6	3843.39	3842.6	3843.39	3842.6
936.45	3854.58	3842.55	3844.42	3842.55	3844.42	3842.55
936.3	3889.58	3842.37	3846.54	3842.37	3846.54	3842.37
936.15	3944.17	3841.99	3850.74	3841.99	3850.74	3841.99
936	3971.67	3841.49	3858.8	3841.5	3858.81	3841.49
935.85	3951.67	3841.07	3873.22	3841.1	3873.24	3841.07
935.7	3961.25	3840.62	3896.54	3840.68	3896.6	3840.62
935.55	4009.17	3839.98	3930.8	3840.17	3930.98	3839.98
935.4	3955	3839.54	3976.54	3840.05	3977.05	3839.54
935.25	4031.25	3838.81	4029.51	3840.11	4030.81	3838.81
935.1	4092.08	3837.85	4080.87	3840.98	4084	3837.85
934.95	4057.08	3837.02	4118.28	3844.09	4125.36	3837.02
934.8	4136.25	3835.89	4129.92	3850.94	4144.99	3835.88
934.65	4057.5	3835.09	4112.19	3865.21	4142.41	3835.04
934.5	4186.25	3833.86	4069.84	3890.58	4126.88	3833.7
934.35	4136.25	3833.04	4015.49	3933.16	4116.58	3832.55
934.2	4201.67	3832.55	3961.01	3997.39	4128.65	3831.15
934.05	4223.33	3833.45	3914.8	4085.12	4174.06	3829.66
933.9	4293.75	3837.59	3879.81	4190.69	4252.3	3827.89
933.75	4311.67	3849.45	3855.63	4298.67	4351.63	3826.06
933.6	4372.08	3877.1	3839.77	4384.34	4453.26	3823.98
933.45	4463.75	3935.1	3829.47	4422.15	4543.63	3821.55
933.3	4678.33	4046.66	3822.03	4398.64	4630.74	3818.29
933.15	4860	4245.96	3815.99	4320.73	4754.01	3814.33

933	5017.5	4574.95	3810.46	4210.92	4976.81	3809.76
932.85	5358.75	5073	3804.15	4094.55	5363.95	3803.87
932.7	5869.17	5754.35	3796.13	3990.15	5948.58	3796.02
932.55	6622.08	6578.4	3785.32	3905.61	6698.76	3785.28
932.4	7387.5	7426.69	3771.61	3841.25	7496.36	3771.59
932.25	8219.58	8109.31	3754.69	3792.47	8147.1	3754.69
932.1	8609.58	8429.34	3736.24	3755.48	8448.59	3736.24
931.95	8404.58	8279.11	3718.5	3727.72	8288.33	3718.5
931.8	7742.5	7702.3	3703.2	3707.36	7706.45	3703.2
931.65	6767.5	6874.37	3691.56	3693.32	6876.13	3691.56
931.5	5850.42	5999.72	3683.35	3684.06	6000.42	3683.35
931.35	5136.25	5231.37	3677.83	3678.1	5231.64	3677.83
931.2	4613.75	4641	3674.27	3674.37	4641.09	3674.27
931.05	4287.5	4233.02	3671.94	3671.97	4233.05	3671.94
930.9	4172.5	3975.12	3670.04	3670.05	3975.13	3670.04
930.75	4035.83	3824.6	3668.65	3668.65	3824.6	3668.65
930.6	3954.17	3742.56	3667.56	3667.56	3742.56	3667.56
930.45	3883.75	3700.69	3666.74	3666.74	3700.69	3666.74
930.3	3853.75	3680.5	3666.03	3666.03	3680.5	3666.03
930.15	3800.42	3671.33	3665.52	3665.52	3671.33	3665.52
930	3790	3667.24	3665.05	3665.05	3667.24	3665.05
929.85	3746.67	3665.52	3664.74	3664.74	3665.52	3664.74
929.7	3677.08	3664.95	3664.69	3664.69	3664.95	3664.69
929.55	3701.25	3664.63	3664.55	3664.55	3664.63	3664.55
929.4	3639.17	3664.48	3664.46	3664.46	3664.48	3664.46
929.25	3660	3664.45	3664.44	3664.44	3664.45	3664.44
929.1	3689.17	3664.35	3664.34	3664.34	3664.35	3664.34
928.95	3656.67	3664.32	3664.32	3664.32	3664.32	3664.32
928.8	3665.42	3664.31	3664.31	3664.31	3664.31	3664.31
928.65	3607.92	3664.1	3664.1	3664.1	3664.1	3664.1
928.5	3680.42	3664.04	3664.04	3664.04	3664.04	3664.04
928.35	3661.67	3664.03	3664.03	3664.03	3664.03	3664.03
928.2	3650	3650	3650	3650	3650	3650
928.05	3652.5	3652.5	3652.5	3652.5	3652.5	3652.5
927.9	3653.33	3653.33	3653.33	3653.33	3653.33	3653.33
927.75	3658.33	3658.33	3658.33	3658.33	3658.33	3658.33
927.6	3617.08	3617.08	3617.08	3617.08	3617.08	3617.08
927.45	3622.08	3622.08	3622.08	3622.08	3622.08	3622.08
927.3	3726.25	3726.25	3726.25	3726.25	3726.25	3726.25
927.15	3688.33	3688.33	3688.33	3688.33	3688.33	3688.33

2. Flotation Results (Unpublished)

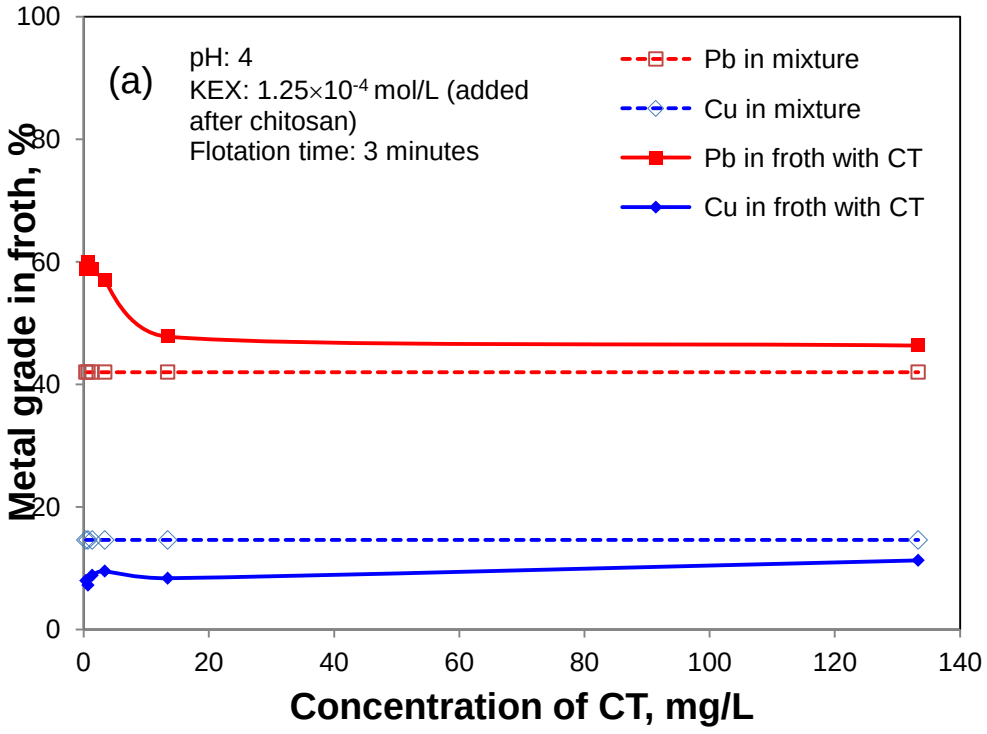

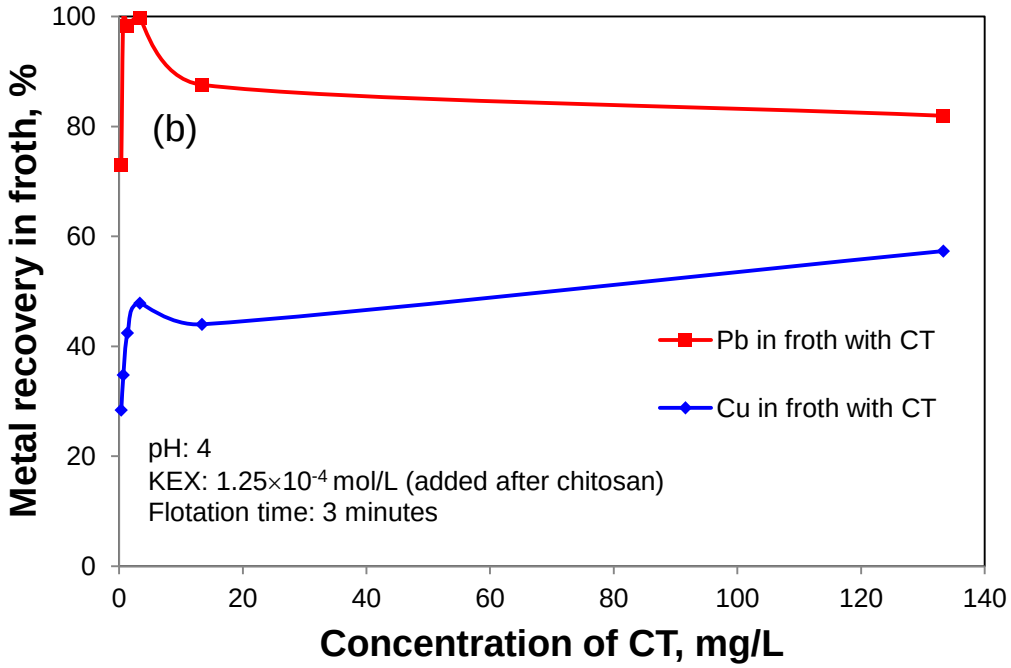

Figure 1. Effect of changing the concentration of CT (chitosan) on the flotation separation of mixtures of chalcopyrite and galena (1:1). pH was maintained at 4. (a). Metal grade in froth products; (b). Metal recovery in froth products. (KEX: 1.25×10^{-4} mol/L; Condition time: 3 min; Flotation time: 3 min)

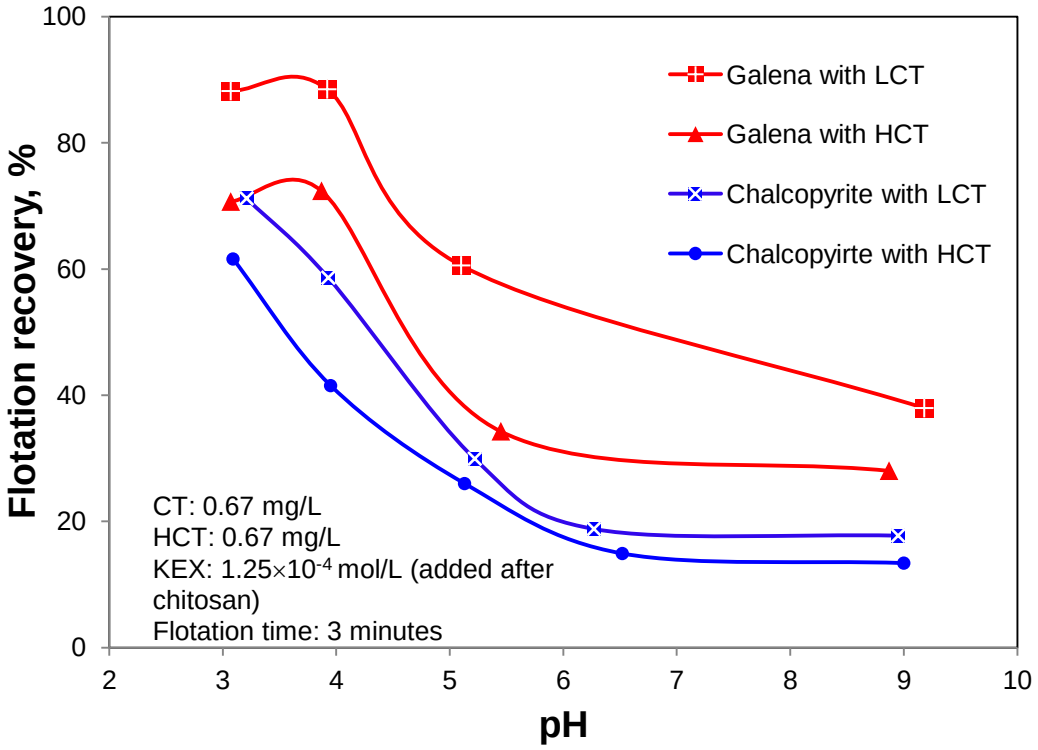

Figure 2. Flotation of single minerals of chalcopyrite and galena as a function of pH in the presence of chitosan with different molecular weight. (The low MW chitosan (LCT) had a MW ranging from 50 000 to 190 000 Da, while the medium MW chitosan (CT) had a MW ranging from 190 000 to 310 000 Da and the high MW chitosan (HCT) had a MW over 375 000 Da)

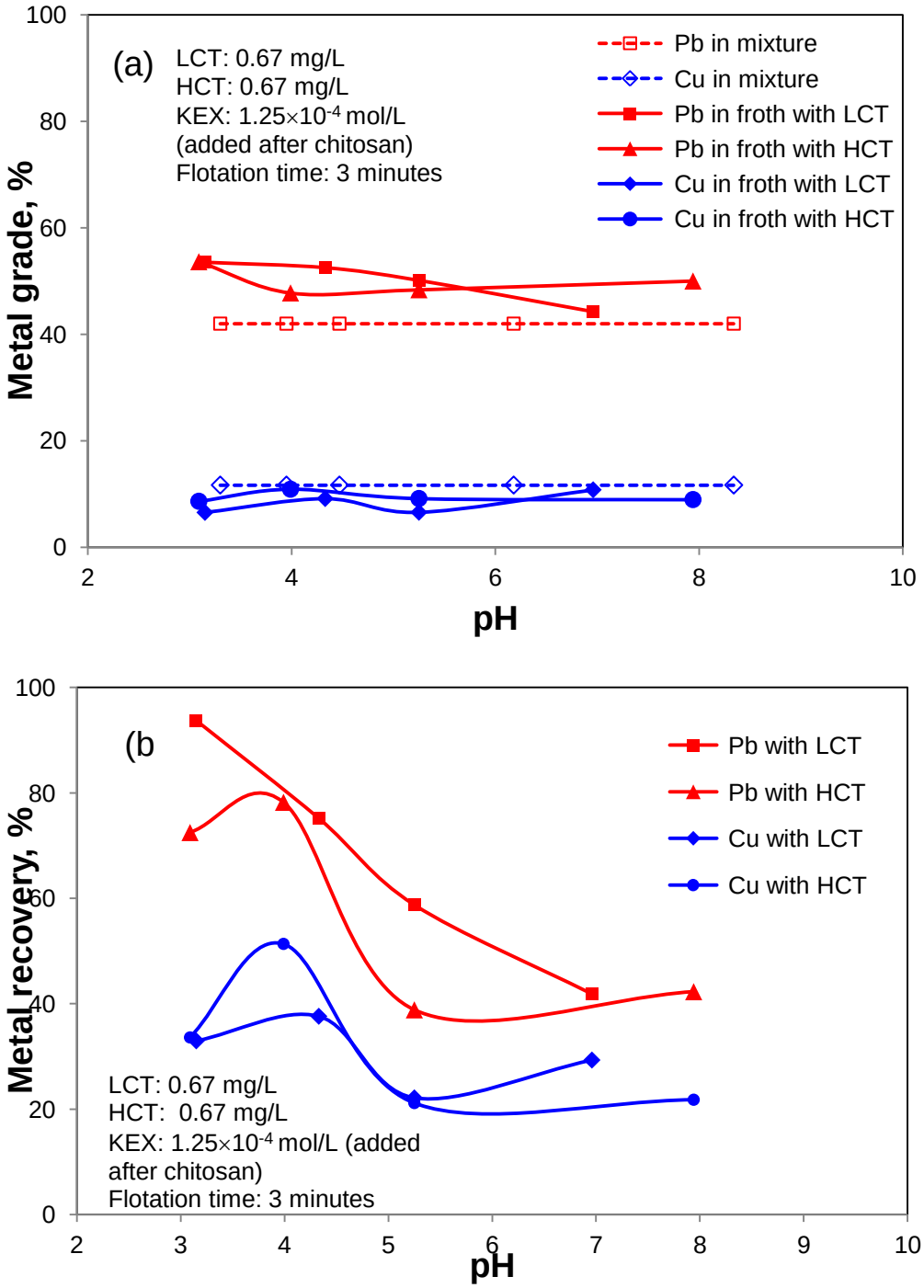

Figure 3. Flotation of mixtures of chalcopyrite and galena (1:1) as a function of pH. (a). Metal grade in froth products; (b). Metal recovery in froth products. (KEX: 1.25×10^{-4} mol/L; Chitosan: 0.67 mg/L; Condition time: 3 min; Flotation time: 3 min)